Fabricio Luchesi Forgerini

Interação de agentes e processos estocásticos em redes complexas

Interacting agents on complex networks and stochastic processes in them

Fabricio Luchesi Forgerini

Interação de agentes e processos estocásticos em redes complexas

Interacting agents on complex networks and stochastic processes in them

"All of physics is either impossible or trivial. It is impossible until you understand it, and then it becomes trivial."

— Ernest Rutherford

Fabricio Luchesi Forgerini

Interação de agentes e processos estocásticos em redes complexas

Interacting agents on complex networks and stochastic processes in them

Tese apresentada à Universidade de Aveiro para o cumprimento dos requesitos necessários à obtenção do grau de Doutor em Física (em conjunto com as Universidades do Minho, Aveiro e Porto), realizada sob a orientação científica de Sergey N. Dorogovtsev, Investigador Coordenador do Departamento de Física da Universidade de Aveiro e José Fernando Ferreira Mendes, Professor Catedrático do Departamento de Física da Universidade de Aveiro.

Apoio financeiro da Fundação para a Ciência e a Tecnologia e do Fundo Social Europeu no âmbito do POPH - QREN - (SFRH/BD/68813/2010).

the jury

president

Doutor Carlos Fernandes da Silva

Professor Catedrático do Departamento de Educação da Universidade de Aveiro

supervisor

Doutor Sergey Dorogovtsev

Investigador Coordenador do Departamento de Física da Universidade de Aveiro

co-supervisor

Doutor José Fernando Ferreira Mendes

Professor Catedrático do Departamento de Física da Universidade de Aveiro

examiners committee

Doutor Wagner Figueiredo

Professor Associado IV do Departamento de Física da Universidade Federal de Santa Catarina

Doutora Iveta Rombeiro do Rego Pimentel

Professora Associada da Faculdade de Ciências da Universidade de Lisboa

Doutora Maria Augusta Oliveira Pereira dos Santos

Professora Associada da Faculdade de Ciências da Universidade do Porto

acknowledgements

I would like to thank my advisor Professor Sergey Dorogovtsev and coadvisor Professor José Fernando Mendes for their guidance, support and ideas for my research. Thanks also go to the group I worked with in Aveiro: Alexander Goltsev, António Luis Ferreira, Fernão Abreu, Manuel Barroso, Gareth Baxter, Massimo Ostilli, Olivier Bertoncini, KyoungEun Lee, Sooyeon Yoon, Detlef Holstein, Rui Américo da Costa, João Gama Oliveira, Patrícia Silva. I would also like to thank Professor José Carmelo from University of Minho for the support before I came in Portugal. Special thanks go to brazilian friends I made in Aveiro, Nuno Crokidakis and Orahcio de Sousa, for enjoyable and fruitful collaborations.

I would like to thank my friends and colleagues in Brazil: Professor Wagner Figueiredo, Professor Nilton Branco, Professor Paulo Jacob São Thiago, Professor Bruno Rizzuti, Professor Adriano Guilherme, Professor Deniz Motta, Professor Hidembergue Ordozgoith, the Rector of UFAM - Professor Márcia Perales and all UFAM staff in Coari.

From the Department of Physics of Aveiro, I would also like to thank Francisco Reis, Fátima Bola, Cristina Rei, Emília Fonseca, Afonso de Carvalho and Gonçalo Ramalho, for their continued support during my PhD.

Thanks also go to my friends and colleagues Patrícia Lima, Sónia Pinho, Luis Cerca, Paulino Muteto, João Nuno, Fábio Figueiras, João Amaral, and all my family for the support.

Last but not least, I thank very much my dear wife Grasiely Borges for all her support, love and comprehension.

palavras-chave Redes complexas, física estatística, processos de ramificações, dinâmica de evoluções, modelos de opiniões, processos de optimização

resumo Nas últimas décadas, um grande número de processos têm sido descritos em termos de redes complexas. A teoria de redes complexas vem sendo utilizada com sucesso para descrever, modelar e caracterizar sistemas naturais, artificias e sociais, tais como ecossistemas, interações entre proteínas, a Internet, WWW, até mesmo as relações interpessoais na sociedade.

Nesta tese de doutoramento apresentamos alguns modelos de agentes interagentes em redes complexas. Inicialmente, apresentamos uma breve introdução histórica (Capítulo 1), seguida de algumas noções básicas sobre redes complexas (Capítulo 2) e de alguns trabalhos e modelos mais relevantes a esta tese de doutoramento (Capítulo 3).

Apresentamos, no Capítulo 4, o estudo de um modelo de dinâmica de opiniões, onde busca-se o consenso entre os agentes em uma população, seguido do estudo da evolução de agentes interagentes em um processo de ramificação espacialmente definido (Capítulo 5). No Capítulo 6 apresentamos um modelo de optimização de fluxos em rede e um estudo do surgimento de redes livres de escala à partir de um processo de optimização. Finalmente, no Capítulo 7, apresentamos nossas conclusões e perspectivas futuras.

keywords Complex networks, statistical physics, branching process, dynamics of evolution, opinion models, optimization process

abstract

During the last decades, a great number of processes has been described by complex networks. The complex network theory has been used successfully to describe and characterize natural, artificial and social systems, namely ecosystems, protein-protein interaction, the Internet and WWW and also social relationships.

In this thesis we present some models of interacting agents in complex networks. Initially, we present a brief historical introduction (Chapter 1), followed by some basic notions of networks (Chapter 2) and the background and related relevant work for this thesis (Chapter 3).

In Chapter 4 we present a study of an opinion model, in which agents reach an agreement. In Chapter 5 we investigated the evolution of branching trees embedded in Euclidean spaces and in Chapter 6 we study a model of current flow optimization and a simple optimization based model for growing networks with power-law degree distributions. Finally, in Chapter 7, we present our conclusions and perspectives.

Contents

List of Figures

List of Tables

Chapter 1

Introduction

1.1 Brief Historical Introduction

During the last decades the study of networks has attracted great interest of many researchers from different areas. This interest is due to the general impact of theories of networks and their numerous potential applications in many fields. Many problems in the fields like biology, social sciences and technological applications can be interpreted in terms of networks.

A network is a set of nodes (vertices) representing the fundamental units of the network, linked by a set of connections (called links or edges) characterizing any relationship between these units. Configurations of nodes and links occur in a great diversity of applications. Any object involving nodes and links between them may be called a network or a graph.

The pioneering work, which is regarded as the birth graph theory, (and, as well of the science of networks) namely the solution to the called the Königsberg bridge problem, was made by Leonhard Euler in 1735.

In the city of Königsberg (now Kaliningrad, Russia) the Pregel river flowed through the city such that in its center was an island, and after passing the island, the river broke into two parts, as shown in the left side of Fig. 1.1. Seven bridges were built across Pregel in the city. The problem, believed to be a challenge at that time, was: Can a pedestrian walk across Königsberg passing each bridge only once?

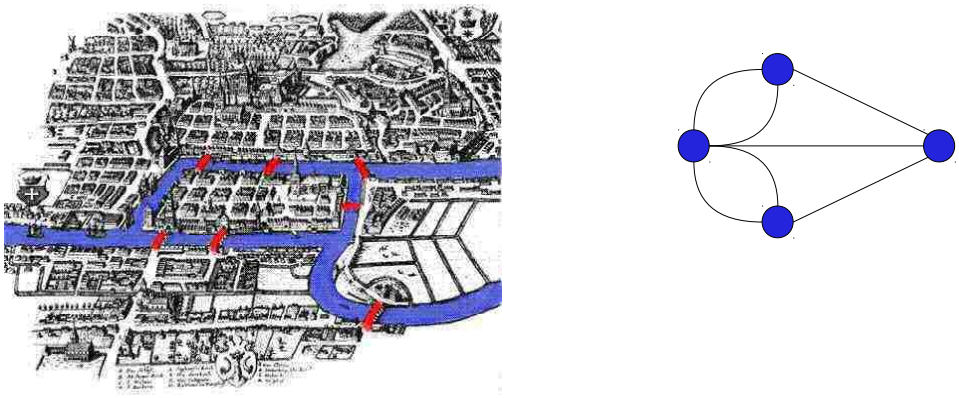

Figure 1.1: The map of Königsberg in Euler's time with layout of the seven bridges, highlighting the Pregel river and the bridges on left side. The corresponding graph is shown on right side.

The young Euler solved the problem in terms of a graph[1]. In the Königsberg bridge problem, the nodes represent the land masses and the links represent the bridges (see Fig. 1.1). Euler proved that when each of the nodes of a graph in the problem has an odd number of links there is no path passing each link only once.

In the beginning of the 1950s, a simple mathematical model of a random graph was considered by Ray Solomonoff and Anatol Rapoport but their initial ideas did not attracted much attention at that time. At the end of that decade, E. N. Gilbert rediscovered the Solomonoff-Rapoport (actually Bernoulli binomial random graph) model, and the $G_{N,p}$, as it is known, was introduced. The notation $G_{N,p}$ indicates a statistical ensemble of networks, G, with two fixed parameters: a given number of nodes N (in each ensemble member) and a given probability p that two nodes have an interconnecting link [1]. There is another random graph, introduced by Paul Erdős and Alfréd Rényi in the middle of the 1950s, called $G_{N,L}$ model [2, 3], that contributed to establish the random graph theory. The $G_{N,L}$ is a statistical ensemble graphs with two parameters: a fixed number of nodes N and a fixed number of links, L, for each member of the ensemble.

[1]The terms graph and network will be used interchangeably.

Another seminal work was done in the 1960s by social psychologist Stanley Milgram [4]. In this experiment, Milgram observed at first time the well-known *small-word* phenomenon. Milgram distributed letters to randomly selected people in Omaha (Nebraska) and Boston (Massachusetts), in USA. Each person received a letter with some instructions. The participants should try to develop the letters to the target person by passing it to someone they knew on first name basis and who they believed, knew the target or knew somebody who knew the target. These acquaintances were then asked to do the same, repeating the process until the document reached the designated target.

Among the results of this research, the most impressive is that the letters that came to be delivered to the target (about 1/3 of the total) after passing through only, on average, 5.5 people. From this surprisingly small number, emerges the idea that, "six handshakes separate us from everyone else". Other modern studies have been performed by modern ways such as e-mail and the result found is close to that found by Milgram.

Many other studies of networks involving relations between people have been exploited by the social sciences. Currently, new technologies like the Internet have facilitated the social networking. Other types of networks such as biological (e.g., the relationship between predator-prey or artificial electric power grids, for example) have been extensively studied [5, 6]. What makes the study of complex networks so exciting is its fundamental significance, as for many different problems, networks show similar behaviors. The search of the universal features of complex networks is the main trend in the network studies.

Back in the 1960s much progress has been achieved in the theories of random graphs. We indicate for example the work of Derek Price [7], which showed that the distribution of the degrees of some networks follows a power law, i.e., these networks are uncorrelated random graphs with a given degree sequence. In the 1980s other advances have been achieved, in particular, the *configuration model* proposed by Béla Bollobás [8] and other graph theory mathematicians but also the solution of the Ising model on a regular *Bethe lattice*, by Rodney Baxter [9]. After the work of Baxter physicists began to create interest in studies of networks, using the techniques of statistical physics.

At the end of the 1990s, high impact ideas were presented, including the model proposed by

Duncan Watts and Steven Strogatz [10] to explain the small-world phenomenon and the Lázló Barabási and Réka Albert model, who introduced the concept of preferential attachment [11]. The solution of this model was given later by Sergey Dorogovtsev, José F. Mendes and Alexander Samukhin [12]. A major development in the studies of complex networks has taken place since then, exploiting empirical data from various types of networks such as social networks, Internet, World Wide Web, biological and technological networks. The summary of the concepts and the state of the art in the area of complex networks can be found in the reviews[13, 14, 15].

One issue that has received much attention in complex networks studies is community structure formation. In large networks $(N \to \infty)$ with a finite mean degree, the network is, in average, sparse. The community structure means the appearance of densely connected groups of vertices, with sparser connections between different groups in the network. The detection and characterization of heterogeneity in real-world networks, including community structure, clustering and q-core structure is of significant importance, since most of real networks have far more complicated organization than uncorrelated networks[16, 17, 18, 19].

1.2 Networks in the real world

Researchers from many different areas investigated different types and models of networks. In many cases, the starting point is to obtain data from real systems. Mark E. J. Newman suggested a classification for different categories of networks: social networks, biological networks, information networks and technological networks. The intention here is to make a brief presentation of the most important features of well studied networks. This division into classes is useful since the networks in the same class can often be treated by using similar techniques [20].

1.2.1 Social Networks

Social networks are formed by individuals or groups of individuals with some relationship or interaction among its members. The nodes represent people or groups of people and the links are social interactions among them. One can study social networks with diverse interpersonal

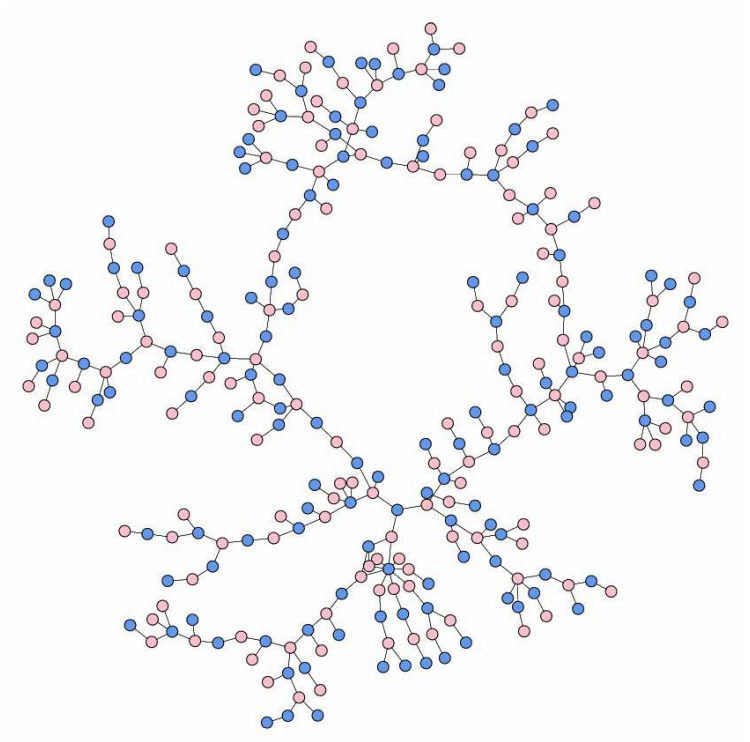

Figure 1.2: Network of sexual relationships in American high school, created by Bearman, Moody and Stovel [21].

interactions or relations among the social groups, such as friendship, emotional, communication patterns, professional and sexual relationships. An example of a social network is shown in Fig. 1.2, representing the network of sexual relationships in a large American high school [21].

Some of the social networks show the small-world phenomenon, as one can see in the Milgram's experiment. The average distance between two arbitrary individuals tends to have very short paths and it may have some effects in how fast the information (or a disease) can spread through the social networks. Some other properties such as high clustering coefficient, clique and community structures were usually reported [20].

Modeling social networks is a difficult task, given the subjectivity involved[2] and the limitation of network sizes. Various methods are used to obtain data of a social network. The most common

[2]Social relationships can be seen different from one person to another, i.e. an individual A can consider an individual B as a friend, but the opposite may not be true.

are questionnaires and interviews but direct observation, data collected from clubs, associations and even archival records were also used. Today the social networks hosted on the Internet such as *Orkut* [22], *Facebook* [23] and others [24] are valuable data sources for network researchers.

Collecting data from some social networks can be difficult, specially seeking for individuals engaged in illegal or illicit activities. Drug users, sex workers and criminals are examples of difficult to reach or hidden populations. In this case, a specific technique, *snowball sampling*, is applicable [25]. In this technique one can try identify an initial group of members, who provides information of other members. This process is repeated until a large sample of the target population is extracted.

Understanding this social dynamics one can anticipate and act in some situations, such as the spreading of a disease in a network of sexual relationships. In particular, one can more effectively, for instance, immunize a fraction of the population, making possible to stop the spread of a disease.

1.2.2 Biological Networks

Numerous biological systems have naturally a network organization. One can refer to the vascular system, the network of metabolic pathways, food web or the network of our nervous system, etc. Important classes of Biological Networks include, in particular, Biochemical, Neural and Ecological Networks.

Biochemical Networks

Many of the biochemical processes that occur in living beings can be interpreted in terms of chemical reaction networks. Among these networks that represent interactions and mechanisms at molecular level, there are protein-protein interaction [26] and genetic regulatory networks [27, 28].

The metabolic networks have universal features, such as the citric acid cycle, which is found in different types of cells. Similarly, genome forms a network of switchings between the proteins. Some properties such as scale-free topology have also been reported for protein interaction net-

works [26]. Recent developments in instrumental microbiology made possible the identification of relationships among genetic human diseases and their associated genes [29].

Ecological Networks

In ecological networks, the interactions between species are described. The nature of these interactions can be competition for resources, parasitism relationships or even an advantageous interaction such as pollination or seed dispersal. Generally, the interactions are represented by directed links and the species are represented by nodes. In particular, food webs between prey and predators interactions atracted significant interest of researchers [30, 31], even though only few habitats were completely documented. Some studies shows that the food webs are highly clustered, and the average path length between species is below 3 [32, 33].

One should note that, the experimental data for ecological networks is hard to obtain. As pointed by Dorogovtsev and Mendes, it is hard to separate an ecological system perfectly and it is hard to construct a food web uniquely [6]. One should add to this the fact that all known food webs are very small (the number of nodes is less than 200). An example of food web is shown in Fig. 1.3, where United Kingdom Grassland Trophic Web is shown. Red nodes represent basal species, such as plants, orange nodes represent intermediate species, and yellow nodes represent top species (primary predators). Links characterize the interaction between two nodes, and the link is thicker at the predator end and thinner at the prey end. Image produced with FoodWeb3D, written by R.J. Williams and provided by the Pacific Ecoinformatics and Computational Ecology Lab (`www.foodwebs.org`, Yoon *et al.* 2004) [34].

Neural Networks

The worm *C. elegans* is an example of organism with a neural network completely mapped. It has about 300 neurons and close to 2000 directed connections with a mean degree $\langle q \rangle = 14$ [35]. This neural network shows an exponential degree distribution, small average path lengths and a quite high clustering coefficient [10, 36, 37].

Much more complex is the neural network formed by the human brain. The number of

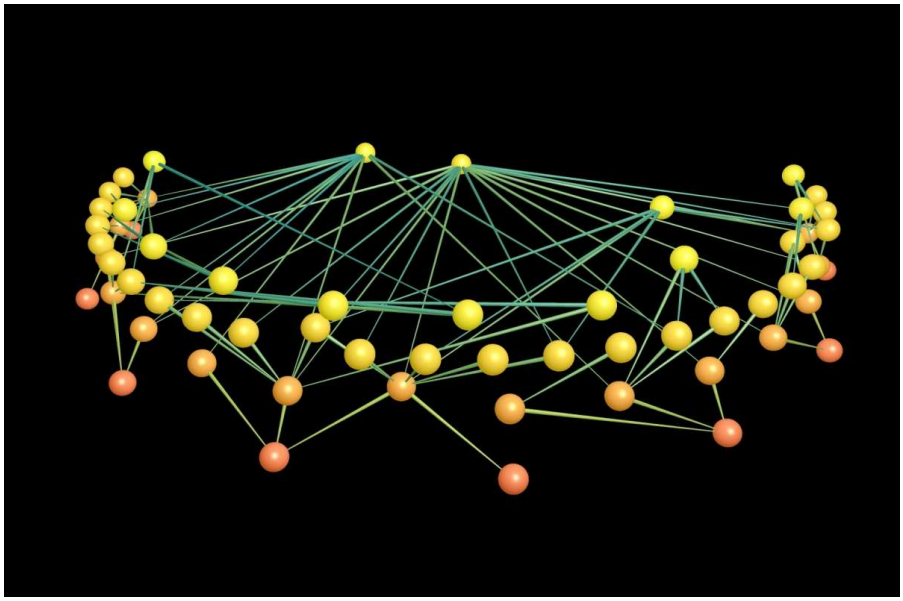

Figure 1.3: Food web of the United Kingdom Grassland based on data collected from 24 sites between 1980 and 1992. Image produced with FoodWeb3D (`www.foodwebs.org`).

neurons in the human brain is of the order of 10^{11} [6]. One can build a functional network of the human brain by using images from the functional magnetic ressonance technique. This technique measures brain activity by detecting changes of the blood flow, which is related to energy use by cells in different areas of the brain. It was observed that the distribution of functional connections is scale-free ($2 \leq \gamma \leq 2.2$) and the clustering coefficient is orders of magnitude larger than those of corresponding random networks [38].

1.2.3 Information Networks

Information networks represent relations between structures of knowledge content. Citations of scientific papers, the World Wide Web [3], the records of patents, the structure of languages and

[3] We should not confuse the Internet with the World Wide Web, two concepts commonly viewed as equal. The Internet basically is the physical network consisting of computers (routers, large scale computers which control the data flow, or "autonomous systems", collection of computers linked by a local data routing, e.g. the network domain of an University), interconnected by wires. Contrastingly, the WWW is a virtual network of information, built into the websites where the information is stored.

keyword indexes are examples of these information networks.

In particular, in these type of networks, the links are directed and can have weights, characterizing the strength of interaction between nodes.

The World Wide Web

The WWW is a virtual network in which the nodes are web pages (hypertext of documents containing the information) and the links are hyperlinks. The World Wide Web was created in the 1980s by Timothy Berners-Lee (the original conception of the Web) at the high-energy physics lab CERN, in Geneva. The aim of Tim Berners-Lee was to help CERN physicists to share research information in a single information network.

The WWW is directed, since a hyperlink is naturally directed. In this network, page A may have a link to page B but the page B may also have a link back to the page A. This structure forms a cycle, and we have reciprocal links. Unlike the World Wide Web, a citation network, for example, has no cycles. One can see this type of structure in Fig. 1.4, where examples of citation and WWW networks are shown.

The size of the WWW is huge: contains at least 8.8 billion pages[4]. In particular, a high clustering coefficient, small world phenomenon (average path length around 16) and the distribution of the links (incoming and outgoing) as power laws were usually reported in the WWW studies [20].

Citation Networks

A network of citations between scientific papers is an information network in which the papers are nodes and links are references from one paper to another. A seminal work in this type of networks was published in the 1960s by Derek Price [7]. In this paper Price reported a power law degree distribution of the citations. Today this kind of citations study is refered to "information science" in the branch called bibliometrics.

In a network of citations of scientific papers, the network is acyclic, since an article can only

[4]Measured on Monday, 01 October, 2012 in http://www.worldwidewebsize.com/

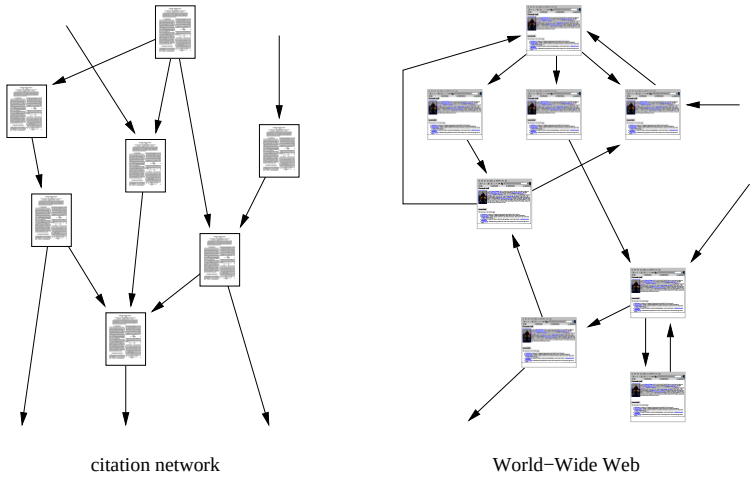

Figure 1.4: Citation and WWW networks. One can see that on the left side, the citation network is acyclic while on the right side the WWW has a cyclic structure, adapted from [13].

mention (have a link) earlier articles. You can not cite future articles. [5]. The distribution of the in-degrees in the citation networks follow a power law while the out-degrees has an exponential tail [20].

Language Networks

The structure of a language can be represented in terms of a network. Ferrer i Cancho and Solé studied a network of words constructed as follows: each word is a node; two words have a link connecting them if they appear next to each other (no more than two words apart) in English sentences [39].

This language network has a small average path length ($\overline{\ell} = 2.67$), high clustering coefficient ($C = 0.437$) and a power-law degree distribution with two different exponents, $\gamma = 1.5$ for $q \leq 10^3$ and $\gamma \simeq 2.7$ for $q > 10^3$. One can create a different language network, connecting words based on their meanings [40]. The results are not so different from the previous study, with average path length ($\overline{\ell} = 4.5$), clustering coefficient ($C = 0.7$) and a power-law degree distribution.

[5] An exception to this are the articles published online into the electronic archive database (`http://arXiv.org`) in which one can update and change their papers' references [1]

1.2.4 Technological Networks

Technological Networks are usually created for the distribution of resources. Distribution networks for electricity, water, telephone and data, distribution of services as mail and delivery goods, railway, road and the Internet are some examples of technological networks. These networks are in constant expansion, in particular, improving for faster and cheaper way to distribute goods and services.

Internet

The Internet is the best documented and studied technological network. Researchers can study the Internet structure by following large samples of data routes. The path the information takes from one computer to another can be found by a traceroute tool [41]. One can treat the Internet as a network in which the nodes are computers (routers and other devices) and the links are connections (physical connections such as wires and optical fiber lines) between them. This representation of the Internet is shown in Fig. 1.5.

When any information is sent from one computer, this information is divided into "small packets" and each data packet is sent separately over the Internet. After reaching its destination the packets are reassembled and the original information is reconstructed. By following a specific data packet one can trace the route from our computer (source) to the target (destination). By sending a large number of packets, one can reconstruct the topology of the Internet from traceroute tool. Computers of end-users can appear and disappear from the network as they are turned on and off. Therefore most studies of the Internet topology disregard end-user computers and look only at the domain-level or the router-level of Internet [42, 43].

Another branch of the Internet studies are related to the resilience of a network, i.e. its ability to stay connected after a failure or an intentional attack. The removal of some nodes in may cause a fragmentation of the network, limiting the communication. Some failures may trigger a cascade of subsequent failures, switching off or disconnect most of the nodes of the network [44, 45, 46].

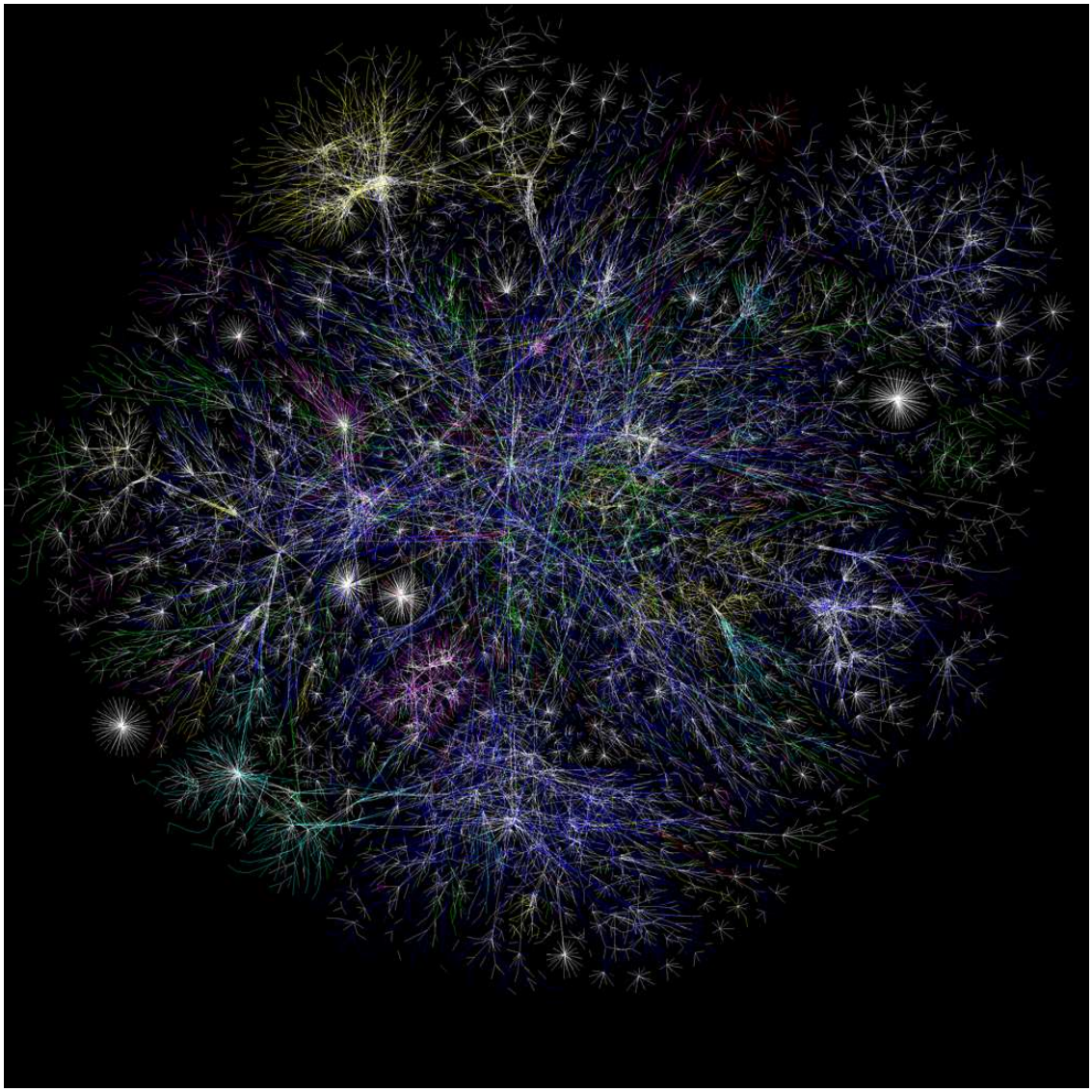

Figure 1.5: Graphic representation of the Internet in 2005. This picture was created by the Opte Project (`www.opte.org`) aiming a visual representation of the Internet. The colors indicate the following areas: net, ca, us (blue); com, org (green); mil, gov, edu, (red); jp, cn, tw, au (yellow); uk, it, pl, fr (pink); br, kr, nl (light blue); unknown (white).

Power Grids

Power grids are networks providing the transportation of electric power from the generators to the high(or mid)-voltage substations. In this case, the nodes are the generators, transformers and substations and the links are the high-voltage power lines. Local low-voltage substations and local power delivery are normally neglected [10, 47]. Typically power grids are small networks with an exponential degree distribution.

Recent interest in the study of these networks have been motivated by the devastating effects of power grids failures [46, 48]. Sometimes a failure can affect a large region of a country, where a cascade failure may cause extensive electricity blackouts.

Telephone Networks

In a telephone network the nodes are telephone numbers and the links (directed) are the calls from one number to another. The topological structure of the telephone network is relatively simple: end user's subscribers are connected to the local offices which are connected among themselves and also connected to the long distance offices. The long distance offices are also connected among each other by trunk lines. It was found that this long distance calls' network have a power law degree distribution for incoming and outgoing calls [49].

Transportation, distribution and delivery

Road, rail, air, river, and sea routes can form networks of the transport lines, transportation not only people but also distribution of goods, package and letters delivery [47, 50, 51, 52, 53]. Oil, gas and water pipelines are also examples of this type of technological networks, usually shaped by geographical boundaries [54].

Interestingly, there is no consensus among researchers about what is represented by nodes and links. For some authors, the distance between two nodes on the network (rail in this case) is not the number of links among the train stations, but simply the number of trains needed to travel between two different locations [50]. In the road network studies, the geografic locations are usually the nodes and the links are formed by the routes between them [55].

Chapter 2

Basic Notions of Networks

The aim of this Chapter is to describe some basic notions of complex networks, such as degree, adjacency matrix, degree distribution, clustering and also mean distance, measurements needed to reveal the structure of networks.

2.1 Basic Features

In simple words, a Network is a set of points (which we call nodes or vertices) with connecting lines between them (which we call links or edges). In principle, networks can have different types of nodes (see Fig. 1.2), links can have weight and can be directed (Fig. 1.4). In Fig. 2.1 one can see three different types of networks: (a) undirected, (b) weighted and (c) directed.

One can consider temporal evolution of networks. Some networks, e.g., the WWW, citation and friendship networks, internet, etc. can have nodes added or removed and the weights of the links can change in time. These networks are non-equilibrium and they will be discussed in Chapter 5.

Next Sections will describe some of mathematical tools to analyze, describe and measure networks.

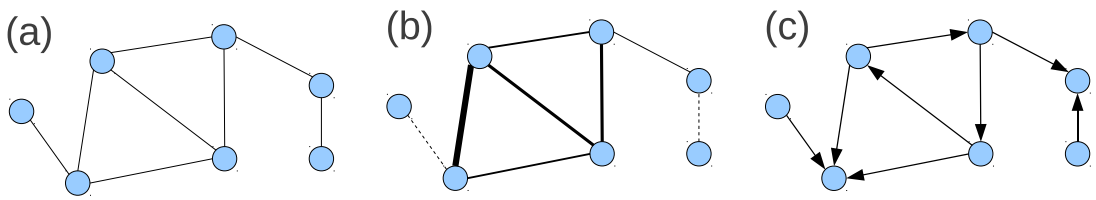

Figure 2.1: Examples of three different types of networks: (a) an undirected network with a single type of nodes and links; (b) weighted network with different types of links; (c) network with directed links.

2.2 Adjacency Matrix

The Adjacency Matrix provides a complete mathematical representation of a network. In a network with N nodes, the adjacency matrix A_{ij} has size $N \times N$. Each element in the matrix is related to one of L links between the nodes: $A_{ij} = 1$ if there is a link between nodes i and j; $A_{ij} = 0$ otherwise. The adjacency matrix of a simple tree with $N = 8$ and $L = 7$ shown in Fig. 2.2 is

$$A = \begin{pmatrix} 0 & 1 & 0 & 0 & 0 & 0 & 0 & 0 \\ 1 & 0 & 1 & 0 & 0 & 1 & 0 & 0 \\ 0 & 1 & 0 & 1 & 1 & 0 & 0 & 0 \\ 0 & 0 & 1 & 0 & 0 & 0 & 0 & 0 \\ 0 & 0 & 1 & 0 & 0 & 0 & 0 & 0 \\ 0 & 1 & 0 & 0 & 0 & 0 & 1 & 1 \\ 0 & 0 & 0 & 0 & 1 & 0 & 0 & 0 \\ 0 & 0 & 0 & 0 & 1 & 0 & 0 & 0 \end{pmatrix}. \tag{2.1}$$

All properties of a network can be extracted from the adjacency matrix. The degree of a node, for instance can be obtained by

$$q_i = \sum_{j=1}^{N} A_{ij}. \tag{2.2}$$

For a random network, an adjacency matrix corresponds to a single realization, only one member of the statistical ensemble.

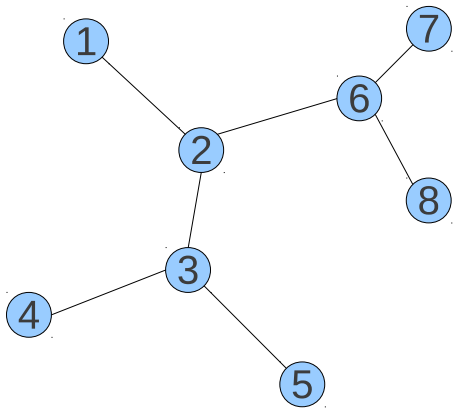

Figure 2.2: Example of a simple tree with labeled nodes. The corresponding adjacency matrix is shown in Eq. 2.1.

The main diagonal of the adjacency matrix has all zeros if the network has no loops. In the case of loops, an element A_{ii} is equal twice the number of links connecting the node i to itself. The adjacency matrix is symmetric if its represent an undirected network. Otherwise the matrix is not symmetric as one can see in the Fig. 2.3, which also shows a network with multiple links (sometimes called *multigraph*) and self-links.

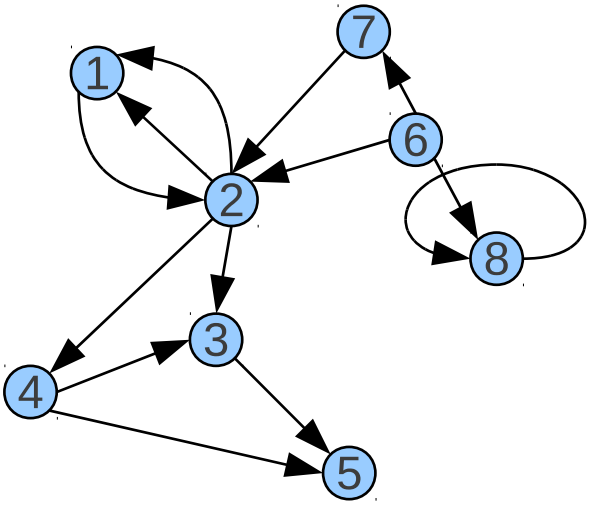

$$A^d = \begin{pmatrix} 0 & 1 & 0 & 0 & 0 & 0 & 0 & 0 \\ 2 & 0 & 0 & 0 & 0 & 1 & 1 & 0 \\ 0 & 1 & 0 & 1 & 0 & 0 & 0 & 0 \\ 0 & 1 & 0 & 0 & 0 & 0 & 0 & 0 \\ 0 & 0 & 1 & 1 & 0 & 0 & 0 & 0 \\ 0 & 0 & 0 & 0 & 0 & 0 & 0 & 0 \\ 0 & 0 & 0 & 0 & 0 & 1 & 0 & 0 \\ 0 & 0 & 0 & 0 & 0 & 1 & 0 & 1 \end{pmatrix}$$

Figure 2.3: Directed network with multiple links and its adjacency matrix.

For directed networks, the adjacency matrix A^d_{ij} is defined by $A^d_{ij} = 1$ if $j \to i$; $A^d_{ij} = 0$ otherwise. In a multigraph, A^d_{ij} is equal to the number of links from node j to node i.

A more compact way to store and sometimes treat a structure of a network is by using the *link list* (or *edge list*) [1]. This representation is given by a list of all links between nodes. The network shown in Fig. 2.2 can be represented by the corresponding link list: (1,2), (2,3), (2,6), (3,4), (3,5), (6,7), (6,8). Due to the usually large number of zeros in the adjacency matrix, this representation is usefull for saving memory on computers when the network is large.

A weighted network have their links with weights. If the weights are all integer, a weighted network is actually a multigraph, where multiple links correspond to the weights of the links.

2.3 Connectivity Measures

The basic characteristic of a node, degree is the total number of its connections. The basic characteristic of a random network is its degree distribution. Much information about a network is related to degree distribution. A network with a power-law degree distribution, $P(q) \sim q^{-\gamma}$ with $2 \leq \gamma \leq 3$, for instance, is expected to be resilient to a random removal of links [56]. Measurements related to connectivity will be discussed in the next sections.

2.3.1 Degree

The degree q_i, is the number of links attached to a node i. It is a local measure given by equation 2.2 while the mean degree of the network is

$$\langle q_i \rangle = \frac{1}{N} \sum_{i=1}^{N} q_i. \tag{2.3}$$

Most real-world networks are directed, such as World Wide Web, Citation networks and Food Webs. For directed networks two types of degree are assigned: in-degree, q_i^{in} is the number of incoming links and out-degree, q_i^{out} is the number of outgoing links of a node i.

[1] In this representation, for a directed network, (1,2) means that there is a link from node 2 to node 1.

2.3.2 Degree Distribution

The degree distribution $P(q)$ is the probability that a node chosen uniformly at random within the network has a degree q:

$$P(q) = \frac{\langle N(q) \rangle}{N}, \tag{2.4}$$

where N is the total number of nodes in the network and $\langle N(q) \rangle$ is the average number of nodes of degree q in the network, where the averaging is over the entire statistical ensemble [2]. In other words, this is the fraction of nodes in the network, which have degree q. For directed networks one needs to take into account the degree distribution for incoming and outgoing degree for a node i, $P(q_i^{in})$ and $P(q_i^{out})$.

Once the distribution is known, much information can be obtained by the calculation of moments of this distribution. The n-th moment of the distribution is

$$\langle q^n \rangle = \sum_{q=0}^{\infty} q^n P(q). \tag{2.5}$$

The first moment $\langle q \rangle$ is the mean degree while the second moment is a mesure of the degree fluctuations of the distribution. If $\langle q^2 \rangle$ diverges, structure and function dramatically changes in the network, in contrast to those for finite $\langle q \rangle$ [57].

A degree distribution usually have one of these distributions forms: Exponential, Poisson, Power-law, Multifractal or Discrete distributions. Examples of the most common types of degree distributions are shown in Fig. 2.4.

An exponential degree distribution has the form

$$P(q) = Ce^{-\alpha q}. \tag{2.6}$$

Exponential degree distributions were reported in some real-world networks such as the Worldwide Marine Transportation Network [58], Email Network [59] and Power Grid Network [60].

[2] Many empirical studies of networks measure one single realization while computer simulations usually take average among a finite number of different realizations [6].

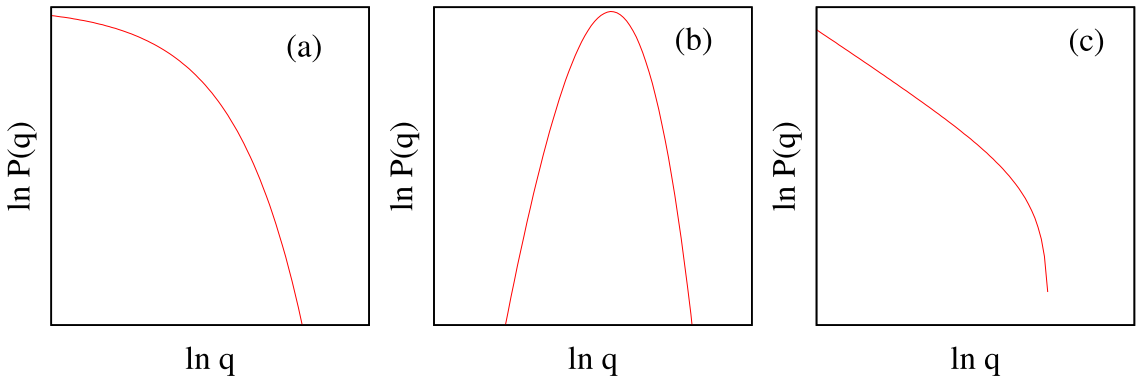

Figure 2.4: Examples of the most common types of degree distributions: (a) exponential, (b) poisson and (c) power-law (with a cut-off) degree distributions.

A classical random network such as the Erdős-Rényi model, have a Poisson degree distribution

$$P(q) = e^{-\langle q \rangle} \frac{\langle q \rangle^q}{q!} \tag{2.7}$$

when the number of nodes $N \to \infty$. Both Exponential and Poisson degree distributions have all their moments finite. These distributions have a natural scale, namely, an average degree.

One of the most common, power-law degree distribution is observed in many real networks,

$$P(q) \sim C q^{-\gamma}, \tag{2.8}$$

where C and γ are constants. The power-law distributions are also called scale-free or fractal, and networks with these distributions are called scale-free networks, since has no any natural scale. This type of distribution is often referred to a Zipf's law or Pareto distribution [61]. The cut-off shown in the Fig. 2.4 (c) is due to the finite size effects common in all real networks.

Multifractal and Discrete degree distributions are less studied than those discussed above. A multifractal distribution has no specific exponent and combines a continuum spectrum of power laws, with different exponents.

2.3.3 Degree Correlations

In uncorrelated networks, the degrees of the nearest neighbors are uncorrelated. The Erdős-Rényi model is an example of uncorrelated network. Real-world networks are typically correlated. This means that the degree q of a node depends on the degree of its nearest neighbors q'.

By using the joint probability $P(q'|q)$ one can describe the correlation of a network, a probability of a node with degree q being connected to another node with degree q'. [3] If $P(q'|q)$ does not depend on q as in uncorrelated networks, the joint probability is a function of only q':

$$P(q'|q) = \frac{q'P(q')}{\langle q \rangle}. \tag{2.9}$$

The mean degree of the nearest-neighbors of a node of degree q can be written as

$$\overline{q}_{nn}(q) = \sum_{q'} q'P(q'|q). \tag{2.10}$$

If a network is uncorrelated, one can insert Eq. 2.9 in Eq. 2.10, namely

$$\overline{q}_{nn} = \sum_{q'} q' \frac{q'P(q')}{\langle q \rangle} = \frac{\langle q^2 \rangle}{\langle q \rangle}, \tag{2.11}$$

where $\overline{q}_{nn}$ do not depends on q.

Correlated networks can be assortatives, or disassortatives. In an assortative network $\overline{q}_{nn}(q)$ is a growing function of q and highly connected nodes mostly have the nearest neighbors of high degrees. In a disassortative network, $\overline{q}_{nn}(q)$ decreases with q and a node of a high degree mostly have low degree nodes as nearest neighbors. The assortativity of a network can be determined by using the Pearson coefficient [65]. In this case, for $r > 0$ the network is assortative; for $r < 0$, the network is disassortative and for $r = 0$, the network is uncorrelated.

[3] The joint probability should be normalized, $\sum_{q'} P(q'|q) = 1$ and obey the detailed balance, $qP(q'|q)P(q) = q'P(q|q')P(q')$ [64].

2.3.4 Hubs

Hubs (highly connected nodes) play an important role in the network dynamics. A removal nodes from the network can cause a fragmentation of the network, destroying the connected component. In this case, the network will be a set of disconnected clusters. Removal of hubs destroys a network specially rapidly.

The difficulty in destroying the giant component by removal of vertices is used as a criterium of resilience of the network against failures [48]. There are two kinds of resilience: against a random removal of nodes and against a targeted removal of nodes. The Internet, for instance, is resilient against random failures: it still working if some routers are disconected at random [66, 46]. A different situation emerges in the case of an intentional removal of hubs. Networks with $\gamma \leq 3$, known to be resilient to random failues, are sensitive in the case of an intentional attack [44, 45].

2.3.5 q-core Structures

The q-core of a network is the largest subgraph in which all nodes have at least q interconnections [17]. The q-core indicates the best interconnected parts in a network and may be obtained by the "pruning algorithm". Remove from a network all nodes of degree less than q. Some of the resting nodes may remain with less than q links. Then remove these nodes, and so on, until no further removal is possible. The result, if it exists, is the q-core. Fig. 2.5 shows q-cores in a small network and the pruning algorithm to find a q-core.

The 2-core differ a slightly from the original network. The 3- and higher q-cores, on the other hand, show a great contrast to the connected component. Networks without loops, i.e. trees, have no ($q \geq 2$)-cores. If a network is tree-like (i.e. it has no finite loops), it can only have an infinite ($q \geq 2$)-core. In a loopy network, a single giant and numerous finite q-cores can coexist, while in tree-like networks there can only be a single giant q-core.

The birth of this giant q-core, for $q \geq 3$ is an unusual phase transition, different from both continuous and first-order transitions, the two classes of phase transitions normally used by physicists. In a continuous phase transition, the order parameter emerges continuously without

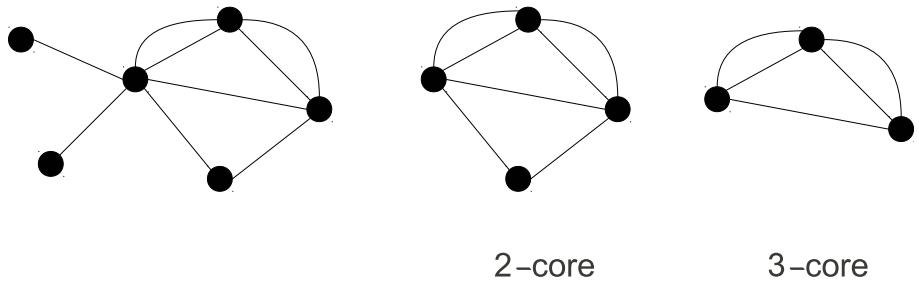

Figure 2.5: A small network on the left and the corresponding 2- and 3-cores on the right side. To find a q-core, one can remove all nodes with degree less than q. After that, one can check if the remaining nodes has degree grater than q. If not, one may prune these nodes with degree less than q.

---

a jump, in contrast to a first-order transition, where the order parameter emerges abruptly. The transition associated with the birth of the q-core combines the characteristics of both transitions. This phase transition is called a *hybrid transition*.

Another problem closely related to the q-core of random graphs is the bootstrap percolation on complex networks. Goltsev *et. al* described the properties of the q-core and explained the meaning of the order parameter for the q-core percolation and the origin of the specific critical phenomena [18]. G. J. Baxter *et. al* studied bootstrap percolation on an arbitrary sparse undirected, uncorrelated complex network of infinite size using the configuration model (a random graph with a given degree sequence) [67]. In their study they also found a hybrid phase transition and described how this behavior changes when the network is damaged.

2.4 Loops in a Network

The presence of loops is a common feature in real-world networks. In a social network for instance, there is a high probability that two people with a common friend are also friends themselves. This characteristic was highlighted by A. Rapoport in the 1950's [68]. A useful

measurement of loops in a network is their *clustering coefficient*.

2.4.1 Clustering

The concept of clustering reflects how the first neighbors of a node are connected to each other, so it is a non-local feature. The clustering coefficient of a given node quantifies the density of connections around this node. If node A is directly connected to nodes B and C, then there is a probability that the node B is also directly connected to the node C. This probability is the clustering coefficient.

The local clustering coefficient of a node i with q_i nearest neighbors, and with t_i links between them is defined as:

$$C_i(q_i) = \frac{2t_i}{q_i(q_i - 1)}, \tag{2.12}$$

and may vary between 0 and 1. When all the nearest neighbors of a node i are interconnected, $C_i = 1$. The same result is obtained for a fully connected network.

The clustering coefficient of the entire network, the *mean clustering coefficient*, is the average of the local clustering coefficient over all nodes:

$$\overline{C} = \left\langle \frac{2t_i}{q_i(q_i - 1)} \right\rangle = \sum_q P(q)\overline{C}(q). \tag{2.13}$$

Clustering refers to the statistics of the number of triangles (loops of length 3) in the network, which is common in the real networks, specially in social ones.

2.5 Distance Measures

Statistics of node separation essentially determines dynamic processes on networks. Here, the separation of nodes is related not to Euclidean distance but rather to the length of the shortest path between nodes measured as the number of links connecting them [4].

[4] In Cap. 5 we will investigate the role of Euclidean distance related to a branching process in a biological network.

2.5.1 Shortest Path Length

One can define the distance ℓ_{ij} between two vertices i and j as the shortest path length, sometimes called a *geodesic distance*, as the minimum number of links connecting one node to another[5]. A well-known algorithm to find the shortest path length in a network is the *breadth-first search* [20]. A single run of this algorithm finds the distance between a node i and all other nodes in the same connected component.

One can naturally introduce for a network, the mean path length, $\overline{\ell}$ where the average path ℓ_{ij} is taken over all those pairs of nodes i and j which have at least one connecting path,

$$\overline{\ell} = \frac{2}{N(N-1)} \sum_{i=1}^{N} \sum_{j=i+1}^{N} \ell_{ij}. \tag{2.14}$$

2.5.2 Diameter of a Network

The diameter of a network ℓ_D, is the length of the longest geodesic distance (shortest path) between any two nodes in the network for which there exists an interconnecting path. In many networks when $N \to \infty$, $\overline{\ell}$ is of the order of ℓ_D. For small worlds, typically

$$\ell_D \sim \frac{lnN}{ln\langle q \rangle}. \tag{2.15}$$

In the case of a network with several disconnected clusters, one can define the diameters of its isolated clusters [40].

2.5.3 Small-world phenomenon

The term small-word express the surprisingly smallness of the mean shortest path in networks. Milgram's experiment described in Sec. 1.1 is the famous demonstration of this phenomenon. A modern version of this experiment was performed by Dodds *et. al* using e-mail in 2003 [69] and were found very similar results.

[5] In directed networks, the shortest path runs in only one direction, following the direction of the links.

In more strict terms, the small-word effect means that the mean separation of nodes grows slower than the any positive network size. We will discuss details of small-world effect in Sec. 3.1.3 devoted to the model proposed by Duncan Watts and Steven Strogatz with the small-world feature.

In some networks the separation distance of nodes grows even slower than $\ln N$. For uncorrelated scale free networks, with $2 \leq \gamma \leq 3$ the mean separation distance of nodes grows with N as $\ln N / \ln(\ln N)$, and this effect is known as the "ultra small-world" phenomenon [70, 71].

2.6 Centrality Measures

Centrality measures characterize the position and the properties of a node within entire network, the "global" importance of a given node. In a social network, for instance, the person with more connections usually have higher influence or prestige than others. In a network of scientific papers, a large number of citations that a paper receives usually indicates its relevance and influence in the scientific community.

2.6.1 Betweenness Centrality

The key measure of centrality is the *betweenness centrality* proposed by L. C. Freeman [72] in the 1970's. For a given node m, it is the number of shortest paths between other (than m) nodes that run through the node m. The betweenness centrality is defined as

$$b(m) = NF \sum_{i \neq m \neq j} \frac{B(i,m,j)}{B(i,j)}, \tag{2.16}$$

where $B(i,j) > 0$ is the number of shortest paths between vertices i and j and $B(i,m,j)$ is the number of the shortest paths passing through node m. The NF is a normalization factor proposed by Freeman, $NF = 2/[(N-1)(N-2)]$ in order to obtain $0 \leq b(m) \leq 1$. N is the total number of nodes in the network. The betweenness centrality indicates the importance of a node, showing the fraction of the network traffic which passes this node.

2.6.2 PageRank

The PageRank is an algorithm used by Google Inc. for ranking web pages [6]. It was developed by Larry Page and Sergey Brin for characterization of the importance of a web page [73]. PageRank assigns a numerical weight to each node i of a network and the result is shown as the PageRank of i, $PR(i)$. The result of a query is shown in a list from highest to lowest PageRank.

The idea of PageRank is that the popularity is proportional to the number of times this page is visited by randomly surfing. The PageRank essentially depends on the number of incoming links of a node, and usually a higher number of incoming links results in a high PR.

The PageRank of a web page i is defined as

$$PR(i) = \frac{d}{N} + (1-d) \sum_{j:j\to i} \frac{PR(j)}{q_{out,j}}, \tag{2.17}$$

where N is the size of a network, $q_{out,j}$ is the outgoing degree of a node j, and the sum is over all pages that link to i. If $d = 0$, and a node has no outlinks, the node can capture the random walker and terminates the process. To avoid this event, the process should be restarted from a random with some probability. The parameter d is the probability that one jumps to a randomly chosed webpage instead to one of the nearest neighbors of a node. This parameter usually is chosen as $d = 0.15$.

[6] This method is registered in the United States Patent and Trademark Office with the name: Method for node ranking in a linked database, and can be accessed on http://patft.uspto.gov/netacgi/nph-Parser?patentnumber=6285999.

Chapter 3

Background and Related Work

The aim of this Chapter is to describe the background and some related works to this study. In order to understand how the heterogeneity of a network can influence stochastic processes, games, epidemics and opinion models on a complex network, some characteristics need to be introduced. In particular, next sections will be devoted to these characteristics, and we will present some basic definitions and results.

3.1 Models of Networks

In the last decade many network models have been proposed to mimic features usually observed in real-world networks such as the small world effect, scale-free degree distribution, community structures and high clustering. We will describe most influential network models: the Erdős-Rényi model, the Gilbert model, Configuration model, the Watts-Strogatz model and the Preferential attachment model.

3.1.1 Erdős-Rényi and Gilbert models

The models known as the Erdős-Rényi model (ER) and the Gilbert model are the two main versions of the so-called classical random graphs. These models actually are random networks under some constraint. A random graph is not a single generated network, but an ensemble

of networks. The Erdős-Rényi random graph, also called $G_{N,L}$, is a statistical ensemble of all possible graphs with two given parameters: a fixed number of nodes N and a fixed number of links, L, for each member of the ensemble [2, 3, 74].

The Gilbert model, $G_{N,p}$, is a statistical ensemble of networks, with two fixed parameters: a given number of nodes N (in each ensemble member) and a given probability p that two nodes have a interconnecting link [75].

In the limit of large sparse networks ($N \to \infty$), these two models are equivalent, and $\langle q \rangle = 2L/N = p(N-1)$. The degree distribution of this has a Poisson form and all their moments converge:

$$P(q) = \frac{e^{-\langle q \rangle} \langle q \rangle^q}{q!} \, . \tag{3.1}$$

The classic random graphs have the clustering coefficient $\langle C \rangle = \langle q \rangle / (N-1)$ since all nodes are connected with the same probability p. When $\langle q \rangle$ is constant as $N \to \infty$, the network is sparse. In the classical random graphs, for $\langle q \rangle \gg 1$, a giant connected component is present in the network. $\langle q \rangle = 1$ is the point of a phase transition in which a giant connected component emerges. This phase transition is similar to that one observed in percolation theory for infinite dimensional lattices.

3.1.2 Configuration model

In order to generalize the classical random graphs, Bender and Canfield introduced a new model of a random graph with a given degree sequence [76]. Béla Bollobás mathematically completed this generalization and named it the *Configuration Model* [8]. The model generates uncorrelated random graphs with an arbitrary degree. The idea of the configuration model is to build a maximally random graph with a given degree distribution.

By choosing a certain degree sequence q_i for the nodes $i \ldots N$, we can obtain a desired degree distribution $P(q)$ for the network for a sufficiently large network. In numerical simulations we can simply choose the degree sequence from a desired degree distribution. After that we set for each node i the number of stubs q_i from the degree sequence. At random we choose a

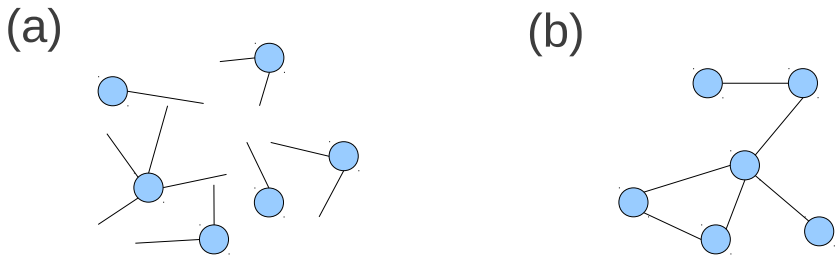

Figure 3.1: An example of a network constructed by the configuration model. One can see the set of stubs (a) and one possible member of the statistical ensemble of the configuration model after make the connections (b).

pair of nodes and make the connections. Once all the nodes are connected, we will have one member of the ensemble of networks with the given $P(q)$. The network produced by this model is uncorrelated. Fig. 3.1 explains the configuration model construction.

3.1.3 Watts-Strogatz model

A large number of real-networks has a high clustering coefficient and demonstrate the small world phenomenon. Classical random graphs (Erdős-Rényi and Gilbert models) and the configuration model generate networks with typically small clustering. In 1998 Watts and Strogatz proposed a new model of complex networks (WS) which combines the small-world effect and high clustering, the *small-world model* [10].

The model is constructed based on a regular lattice, by moving or rewiring randomly chosen links from the original positions, connecting distant nodes by long-range shortcuts. Starting with a one-dimensional network with periodic boundary conditions (e.g. a circle with links between first and second neighbors), by rewiring the links from the original nodes to random selected ones we create long distance shortcuts. The links are moved with some probability p. Self-connections and double links are not allowed in this model. One can see this process in Fig. 3.2 where the original network ($p = 0$) and the WS network with rewiring probability $p = 0.1875$ are shown.

In this model, for $p = 0$ the network shows high clustering but no small-world effect. On the

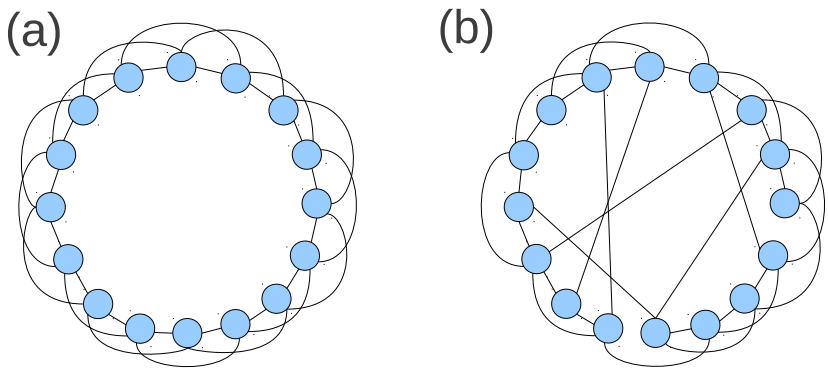

Figure 3.2: Example of a small-world network generated by WS model with probability of rewiring $p = 0$ (a) and $p = 0.1875$ (b), in this case 6 of 32 links are rewired.

other hand, for $p = 1$ the network shows the opposite. For a long range of intermediate values p, this model shows both features simultaneously [20]: even for a small, but finite p, these networks demonstrate high clustering and short $\overline{\ell}$.

3.1.4 Preferential attachment model

Numerous networks are observed to have scale-free degree distributions, approximately following power laws. The first work in this direction was made by Price, who presented a model for growing network with power law degree distribution [7]. The most famous and well studied model of growth networks with power law degree distribution is the *Preferential attachment model*, developed by Barabási and Albert [11]. In simple words, in this model, nodes with high degree attract new links with higher probability. The probability that a new node becomes attached to a previous existent node with degree q is proportional to a function of this degree, $f(q)$. For networks with scale-free degree distribution, the preference function is

$$f(q) = \frac{C + q}{N(C + \langle q \rangle)}, \tag{3.2}$$

where C is a constant. These networks follow a power law with exponent $2 \leq \gamma < \infty$.

Barabási and Albert reproduced two aspects usually seen in real-world networks that are absents in ER and WS models. First, both these networks have a fixed number of nodes N

connected at random (ER model) or rewired (WS model). But many real networks are growing networks. Second, in both models, nodes are interlinked uniformly at random. In real networks a new connection is often made by linking a new node to most connected nodes in the network. For instance, a well cited paper is more likely to be cited than an unknown paper.

In the BA model, the probability $\wp_i$ that a new node is attached to node i is

$$\wp_i = \frac{q_i}{\sum_j q_j}, \tag{3.3}$$

where q_i is the degree of the node i and the sum in the denominator is over all nodes in the network.

The network is generated by the following rule:

1. The network starts from some initial configuration (e.g. a connecting cluster).

2. At each step a new node is attached to $m \geq 1$ of the previous nodes selected with probability $\wp$ proportional to their degrees.

3. Repeate 2 until the network reaches the desired size N.

After t time steps the network generated has $N = t$ nodes and $L \cong mt$ links, which gives the sum in denominator of the Eq. 3.3

$$\sum_{j=1}^{N} q_j \cong 2mt. \tag{3.4}$$

The degree distribution can be found from the evolution of the mean degree of node i,

$$\frac{\partial \langle q_i \rangle}{\partial t} = m\wp_i = m\frac{\langle q_i \rangle}{\sum_j q_j} = \frac{\langle q_i \rangle}{2t}. \tag{3.5}$$

The rate of the grows of $\langle q_i \rangle$ is the probability that the node receives a link multiplied by the number of conections n.

Solving this equation, we have $\langle q_i \rangle(t) = Ct^{1/2}$. Thus $q_i(t_i) = m$, so $C = m/t^{1/2}$. The evolution of the mean degree $\langle q_i \rangle$ is described by,

$$\langle q_i \rangle(t) = m \left(\frac{t}{t_i} \right)^{\frac{1}{2}}. \tag{3.6}$$

From these, one can get for large q an estimate

$$P(q) \sim \frac{2m^2}{q^3}, \tag{3.7}$$

following a power law $P(q) \sim q^{-\gamma}$ with $\gamma = 3$.

This result was independently found by Dorogovtsev, Mendes and Samukhin [12], in which was found the exact form of the stationary degree distribution for large sizes of growing networks.

Other extensions and generalizations of the preferential attachment model have been suggested, connecting already existent nodes by new links [77], removal of links [78] or a non-linear preferential attachment function [79, 80].

3.2 Epidemics in networks

The models that are discussed focus in spreading infectious diseases in populations. The mathematical modeling of epidemics is much older than the study of complex networks. It started by the works of MacKendrick in the 1920s [81, 82]. In this traditional approach every individual through network has the same chance per unit of time to have contact with every other. This assumption doesn't take into account the topology of the network.

The theories of epidemiology describe epidemic within fully connected graphs, classical random graphs and lattices, where each of the individuals can be in two or more states: S - susceptible, I - infected, R - removed or recovered (but not susceptible), E - exposed and M - births with temporary immunity. Different models can be based on the individual states and they are usually named by their acronyms. SI, SIS, SEIS, SIR, SEIR, SEIRS, MSEIR and MSEIRS are some examples of epidemic models.

These models can be defined on substrates or lattices but also on complex topologies. In this thesis the SI, SIS and SIR models will be briefly presented and discussed. For more detailed

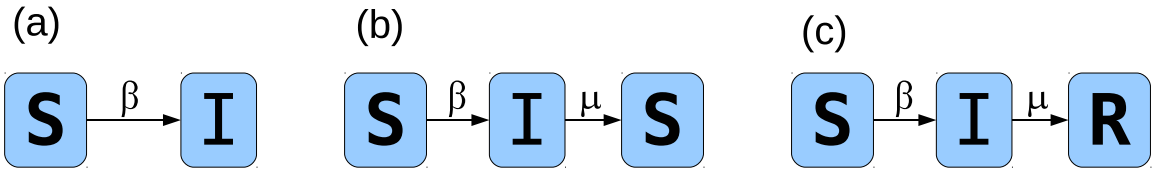

Figure 3.3: General diagram for states of the nodes in three epidemic models. The models SI (a), SIS (b) and SIR (c) as well the infection rates (β), and the recovery rates (μ) are represented.

discussion of spreading infectious disease, the review by Herbert W. Hethcote can be consulted [83].

3.2.1 SI model

In this simple epidemic model, an individual in the population is in one of the two possible states: susceptible (S) or infected (I). A susceptible individual becomes infected if has contact with an infected neighbor. It is important to find out if the disease spreads through the population or becomes extinct after some time, or in other words, if there exists a critical infection rate β_c above which the disease survives.

In the SI model, the two possible states of an individual are represented in the Fig. 3.3 (a). Initially, a network of N individuals have a small number I of infected nodes. At each step, a susceptible individual becomes infected with rate β if one of its nearest neighbors are infected.

The notation for the SI model is shown in the table 3.1. The total population is constant, $N = S + I$ and $s + i = 1$.

For a fully connected graph, the probability to meet a susceptible person at random is S/N, so the evolution equation for infection spreading in the population is

$$\frac{di}{dt} = \beta \frac{SI}{N} = \beta si \tag{3.8}$$

and for the susceptible individuals

$$\frac{ds}{dt} = -\beta \frac{SI}{N} = -\beta si. \tag{3.9}$$

N	Total population
S	Number of susceptible individuals
I	Number of infected individuals
β	Infection rate
s	Fraction of susceptible individuals
i	Fraction of infected individuals

Table 3.1: Summary of notation for the SI model.

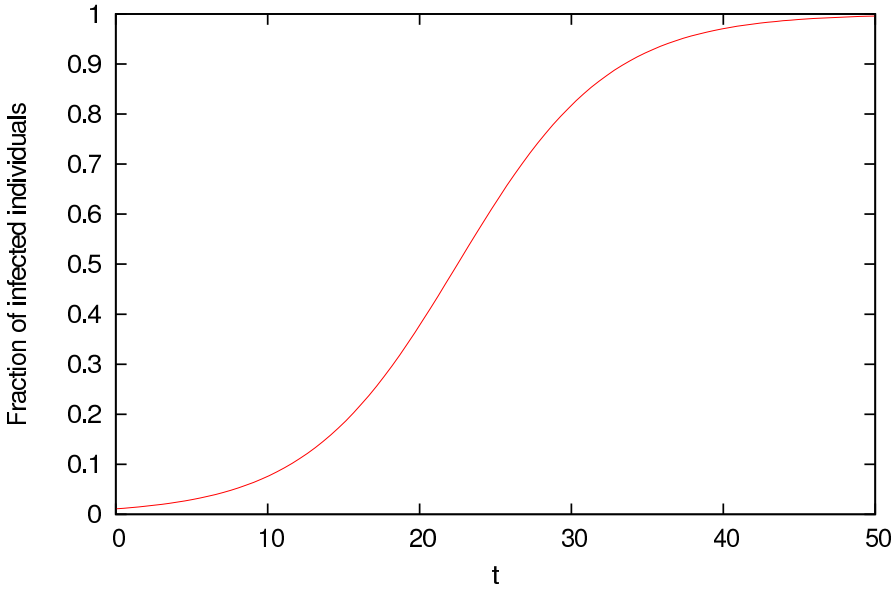

Figure 3.4: Evolution of the fraction of infected nodes in the SI model, called the logistic growth curve. For this picture, the initial fraction of infected $i_0 = 0.02$ and the infection rate $\beta = 0.01$.

Using $s = 1 - i$, we can rewrite the equation 3.8 as

$$\frac{di}{dt} = \beta(1 - i)i. \tag{3.10}$$

This equation is called the logistic growth equation, and the solution is

$$i(t) = \frac{i_0 e^{\beta t}}{1 - i_0 + i_0 e^{\beta t}}, \tag{3.11}$$

where i_0 is the fraction of infected individuals at $t = 0$. This solution is shown in Fig. 3.4. As one can see, in the SI model the disease spreads and eventually reaches the entire population.

3.2.2 SIS model

In the SIS model, an individual can be susceptible (S), infected (I) or can recovery and become susceptible (S) again, as is shown in Fig. 3.3 (b). The rate of recovery of an infected node $(I \to S)$ is μ and a susceptible node becomes infected $(S \to I)$ with rate β if it has at least one infected nearest neighbor. This model allows reinfection, as influenza and many other diseases that do not confer immunity. The summary of notations for the SIS model is shown in table 3.2.

N	Total population
S	Number of susceptible individuals
I	Number of infected individuals
β	Infection rate
μ	Recovery rate
λ	Reproductive number
s	Fraction of susceptible individuals
i	Fraction of infected individuals

Table 3.2: Summary of notation for the SIS model.

The control parameter of the SIS model is the so-called reproductive number, $\lambda = \beta/\mu$. If a few nodes are infected, the disease will quickly die out if the reproductive number is below some value, *an epidemic threshold*, λ_c. In homogeneous situations (nodes with a narrow distribution of connections) in networks, the epidemic threshold is determined by the mean degree of a node, $\lambda_c \sim 1/\langle q \rangle$. If the reproductive number is above the epidemic threshold, an epidemic spreads throughout the network.

For the SIS model defined on uncorrelated networks, the epidemic threshold is

$$\lambda_c = \frac{\langle q \rangle}{\langle q^2 \rangle}. \tag{3.12}$$

An important quantity is the *prevalence*, which is the fraction of infected individuals. Above the epidemic threshold, the prevalence approaches a nonzero value, similar to the logistic growth curve in the SI model.

The evolution equations for the SIS model on a fully connected graph are

$$\frac{ds}{dt} = \mu i - \beta s i, \tag{3.13}$$

for the fraction of susceptible and

$$\frac{di}{dt} = \beta s i - \mu i, \tag{3.14}$$

for the fraction of infected individuals.

Using $s = 1 - i$ (constant population) in the equation 3.14,

$$\frac{di}{dt} = (\beta - \mu - \beta i)i, \tag{3.15}$$

which has the solution

$$i(t) = (1 - 1/\lambda)\frac{Ce^{(\beta-\mu)t}}{1 + Ce^{(\beta-\mu)t}}, \tag{3.16}$$

where the constant C is

$$C = \frac{\beta i_0}{\beta - \mu - \beta i_0}. \tag{3.17}$$

When $\beta > \mu$ the solution produces a curve formally similar to the SI model, as one can see in Fig. 3.2.2. The principal difference is that only a fraction of the population is finally infected.

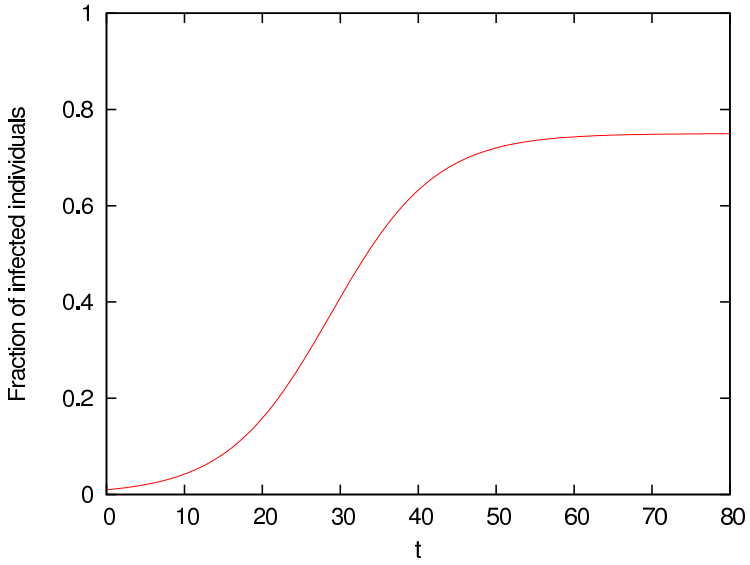

Figure 3.5: Evolution of the fraction of infected nodes in the SIS model with $i_0 = 0.02$, $\beta = 0.2$, $\mu = 0.1$.

3.2.3 SIR model

In the SIR model an individual can be in one of the three states, infected, susceptible or recovered. The recovery rate for an infected individual $(I \rightarrow R)$ is μ. This model does not allow reinfection: recovered individuals have permanent infection immunity. A susceptible individual becomes infected $(S \rightarrow I)$ with rate β if he or she has an infected nearest neighbor, as are represented in Fig. 3.3 (c). The reproductive number for the SIR model is $\lambda = \beta/\mu$. The summary of notations for the SIR model is shown in table 3.3.

N	Total population
S	Number of susceptible individuals
I	Number of infected individuals
R	Number of recovered individuals
B	Number of births
D	Number of deaths
β	Infection rate
μ	Recovery rate
λ	Reproductive number
s	Fraction of susceptible individuals
i	Fraction of infected individuals
r	Fraction of recovered individuals

Table 3.3: Summary of notation for the SIR model.

We can analize the evolution of the epidemic outbreak for a fully connected graph. The equations for the SIR model are

$$\frac{ds}{dt} = -\beta si, \tag{3.18}$$

$$\frac{di}{dt} = \beta si - \mu i, \tag{3.19}$$

$$\frac{dr}{dt} = \mu i. \tag{3.20}$$

Evaluating these equations numerically, one can see the evolution of the fractions of the population in each of the three states. In contrast to the SIS model, the SIR model shows an

epidemic outbreak at initial times but approaches zero in the limit of infinite time. One can see this typical behavior in Fig. 3.6 for the case of constant N.

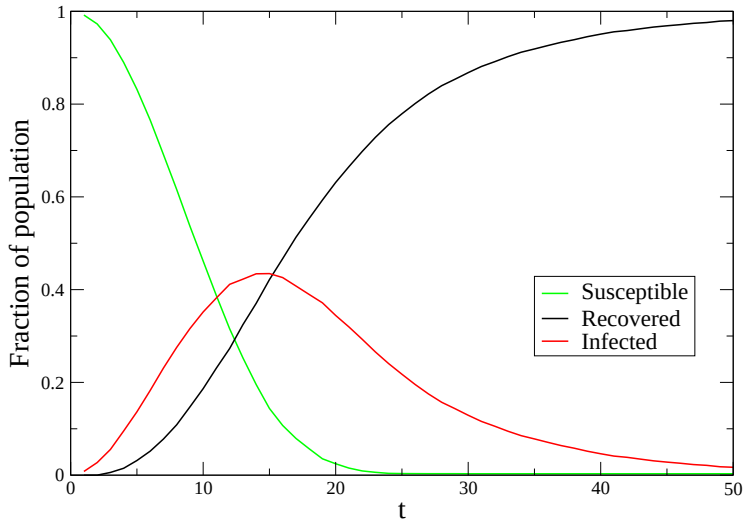

Figure 3.6: Evolution of the population in the SIR model. The initial fraction of infected $i_0 = 0.01$, $\beta = 0.4$, $\mu = 0.15$ and $N = 10000$ nodes.

In 2001 Pastor-Satorras and Vespignani [16] considered the spread of infectious disease within an uncorellated network with an arbitrary degree distribution, extending the traditional epidemic in homogeneous media. The most important result was the absence of an epidemic threshold. For the SIR model, the epidemic threshold,

$$\lambda_c = \frac{\langle q \rangle}{\langle q^2 \rangle - \langle q \rangle} = \frac{1}{\overline{b}} \tag{3.21}$$

where $\overline{b} = (\langle q^2 \rangle / \langle q \rangle) - 1$, coincides with the percolation threshold, because in many aspects, the SIR model is equivalent to the percolation problem [84].

In the networks with a heavy-tailed degree distribution, the epidemic threshold is low, dramatically smaller than $1/\langle q \rangle$ the value of the classical random graph. This may indicates that for some real-world networks (e.g. the Internet), an infection can spreads independently of their infection rates.

Disease spreading was studied in numerous network models. For example, for small-world networks, we can cite [85, 86]. For epidemics in networks with high clustering, it was found that

the high clustering can affect the epidemic threshold and the size and the resilience of the giant connected component [87, 88]. A popular topic is various immunization strategies [84, 89, 90]. The usual approach is a targeted immunization of the HUBs, since they are connected with high number of nodes, are easily infected. Pastor-Satorras and Vespignani show that, for scale-free networks with $\gamma \leq 3$, the epidemic threshold is absent. By immunization of the most connected nodes, one can restore a finite epidemic threshold and eradicate a virus [89]. This approach requires global information of the network. It can also be used local information to choose the nodes immunized [90] and prevent epidemics.

In the real world, the spread of infectious diseases is rather due the high population mobility, in contrast to the models where the individuals stay permanently in their nodes.

In the case in which the population is not constant, at each time step B individuals are added to the population and D are removed. The fraction $b = B/N$ are added into the susceptible group and the fraction of diseased $d = D/N$ are removed from entire population. The new equations are:

$$\frac{ds}{dt} = -\beta si + b - ds, \tag{3.22}$$

$$\frac{di}{dt} = \beta si - \mu i - di, \tag{3.23}$$

$$\frac{dr}{dt} = \mu i - dr. \tag{3.24}$$

Evaluating numerically these equations, in Fig. 3.7 we show the evolution of the Susceptible, Infected and Recovered populations for the case where deaths and births are taken into account. One can see that in this case the nonzero steady steady can be reached.

In constrast to the case of the constant population, in which infection always disappears in the long run, here it reaches a nonzero steady state level of the infected population, even if $b = d$.

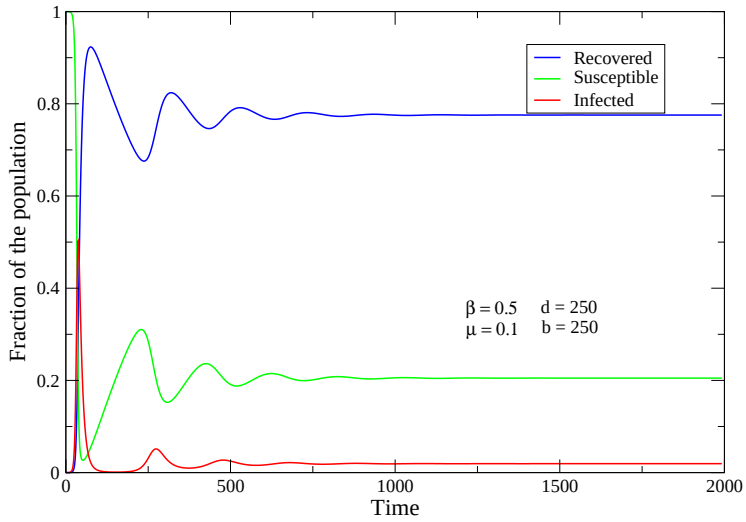

Figure 3.7: Fractions of the population in the SIR model for a non-constant population. The parameters used for the numerical solutions are shown in the figure.

3.3 Community Structures

In networks with community structures, connections are denser within communities and sparser between them. Many networks show clustering or transitivity, the presence of numerous triangles of connections in a network. In a social network of friendships between individuals, there is a high probability that two friends of a given individual will also be friends of one another and most social networks show community structures [13, 91].

Many methods have been proposed for the problem of identifying community structures [5, 92, 93, 94]. These methods seek for natural divisions of large networks into communities, usually by grouping nodes according to their similarities. Another method to identify communities in a network is by using the so called divisive method. By using this technique, one can identify links connecting different communities and remove them, dividing the network into small components.

In a seminal paper, M. Newman and M. Girvan proposed a divisive algorithm for discovering communities [95]. This algorithm calculates the betweenness centrality for the network and removes the link with largest centrality. After the removal, the betweenness centrality is calculated for the remaining network and the link with largest centrality is again removed. This process is repeated until no links remain and the number of links decreases from L to zero, while the

network is divided into communities. This algorithm correctly shows community structures of various real-world networks [1].

Networks with high clustering and loops are particularly difficult for mathematical analysis. Newman proposed a model [19] that generalizes the standard "configuration model", which is a model of random graph with clustering and arbitrary degree distribution. Recently, geographical properties of social networks have attracted much attention. Some empirical studies have analyzed the distribution of distances between friends in real social networks and found that the probability density function (PDF), $P(r)$, of an individual to have a friend at a geographic distance r is about $P(r) \propto r^{-1}$ [96].

Yanqing Hu *et. al* [97] suggested that the origin of this dependence comes from a general perspective based on the concept of entropy. They showed that the $P(r) \sim 1/r$ law can be seen as a result from maximization of entropy, what means that an individual seeks to maximize the diversity of its friendships in the social network.

3.4 Information Spreading

How information, ideas, gossips and influence spreads through a social network is a topic often studied [98, 99]. The information about the pathways in which the information spreads can be used to optimize communications, for example. In social spreading models, the information flows in one direction, from people who have the information to those who do not have.

In a recent work, J. Kleinberg and K. Ligett proposed a model for reasoning about the way information is shared in a social network [100] taking into account social conventions issues. Maksim Kitsak *et. al* proposed a way to identify most efficient "spreaders" in a network [101]. As a result they show that, in contrast to common belief, the most influential spreaders in a social network do not correspond to the best connected people or to the most central nodes.

Information spreading through a population have some similarities with the spreading of an infectious disease. In this case, informed people play the role of an infected agent, while the uninformed ones correspondent to susceptible agents. Recovered agents are represented by stiflers, i.e., agents who lost interest in diffusing information. Differently from the epidemic

models in which an infected node spontaneously becomes recovered, in information spreading an informed agent becomes stifler when its neighbors are already informed.

Similar to the epidemic models, one can study if a finite fraction of the population is reached by the information or if there is an *epidemic threshold* for the rate of spreading, in which an *endemic state* is reached. The model introduced by Daley and Kendall [102] accounts for spreader, ignorant and stifler agents. For this model in the case of homogeneous mixing, for any rate of spreading information, a finite fraction of the population is reached by the information. This model of information spreading was studied also in complex networks. For scale-free networks, the fraction of population reached is smaller than the case in which homogeneous networks are considered [103]. For small-world networks, there is an epidemic threshold dependent on the rewiring parameter p. If p is greater than certain value p_c, the information reaches a finite fraction of the population. For $p < p_c$, the information remains around its origin [104].

3.5 Opinion Models

The dynamics of opinion sharing and competing attracted attention from physicists and numerous different models have been proposed to investigate how competing opinions among agents evolve in populations. The dynamics opinion models are about how a group of people reaches an agreement. The dynamics of agreement and disagreement is treated in terms of the variation of the number of different opinion states in population, where each agent (individual) can have a few opinions[1].

It is clear that these models are reductive since we have a few variables representing opinions about an issue. On the other hand, as pointed by Castellano *et al.* [102], "in everyday life(...) people are sometimes confronted with a limited number of positions on a specific issue, which often are as few as two: right/left, Windows/Linux, buying/selling...". The main problem is how to describe the interaction among people by rules and study this evolution.

The first physicist who created an opinion model, based on a probabilistic framework of

[1]In this thesis we will only discuss the cases where the opinion is a discrete variable. For some models of continuous opinions, see the review of Castellano *et al.* [102]

sociodynamics was Weidlich in 1971 [105]. After that, S. Galam *et al.* used the Ising model to describe opinion dynamics [106, 107]. In these models, the coupling of the spins represents the interaction between agents. The magnetic field plays a role of mass media acting as an external field. Depending on the field, the system may reach total consensus (all agents with the same opinion) or a state where both opinions are present (in the case of only two opinions are allowed).

In the past few years new models have been proposed [102, 108, 109]. Here we will discuss the models that have been received more attention such as the Voter model 3.5.1, the Majority rule model 3.5.2 and the Sznajd model 3.5.3.

3.5.1 Voter model

The voter model was first considered by Cliford and Sudburry [110] as a model for competition of species. The name "voter model" was gived by Holley and Liggett [111] in 1975. It is a type of contact process which is one of the few non-equilibrium processes that can be exactly solved in any dimension [102]. The voter model became popular by being a model with simple non-equilibrium dynamics with a nontrivial behavior.

This model is a simple model of opinion in which an agent i (or in this case, voter) is located at a node of a network. Each agent has a binary opinion ($s_i = \pm 1$), and at each time step a randomly chosen agent assumes the opinion of one of its neighbors j, $s_i = s_j$.

The average opinion (magnetization) is calculated summing over all the agent's opinions in the network:

$$m = \frac{1}{N} \sum_{i=0}^{N} s_i. \tag{3.25}$$

The system evolves until reaches a consensus state with all agents with the same opinion, -1 or $+1$, and stays there forever. So, these two states are absorbing states. One can see that this model also shown the up-down symmetry. Starting the process with a random configuration of opinions, the dynamics of the voter model will increase order in the system.

In Fig. 3.8 one can see the evolution of the agent's opinion in the voter model defined on a square lattice with 250000 agents. The simulation starts with opinions randomly distributed

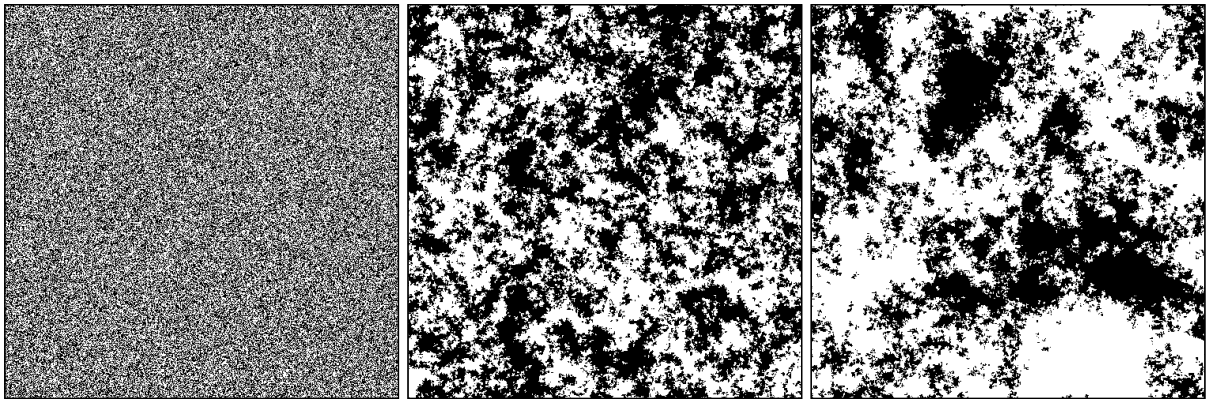

Figure 3.8: Evolution of the Voter Model on a square lattice. 250000 agents start with opinions randomly distributed (left panel) and, at each time step, an agent assumes the opinion of one of its neighbors. Each opinion (± 1) is represented by a black (-1) or white ($+1$) region in the picture. From left to the right we can see three different time steps, $t = 0$, $t = 2500$ and $t = 5000$.

among the agents and three different time steps are shown.

The steady state is reached when $m = 1$ or $m = -1$, solutions corresponding to the absorbing states [112]. For the voter model in one- or two-dimensions, these are the only possibilities for the steady state. For higher dimensions no consensus is reached and domains of different opinions can coexist. According to Castellano *et al.*, the lack of consensus is related to the nature of random walks in $d > 2$: diffusing active interfaces have a finite probability to meet and annihilate each other [102].

3.5.2 Majority rule model

The majority rule model is a sociophysics model proposed by Serge Galam in 2002 [113]. In this model the network is a complete graph (where each agent can communicate with each other) composed by N agents with opinions $+1$ or -1. At each instant of time r agents are selected at random and all agents in this group (called discussion group) follow the majority opinion inside the group as one can see in Fig. 3.9. The unity of time is measured in number of updates per spin for the majority rule model.

The discussion group r does not have a fixed size and it is, at each time step, selected from a

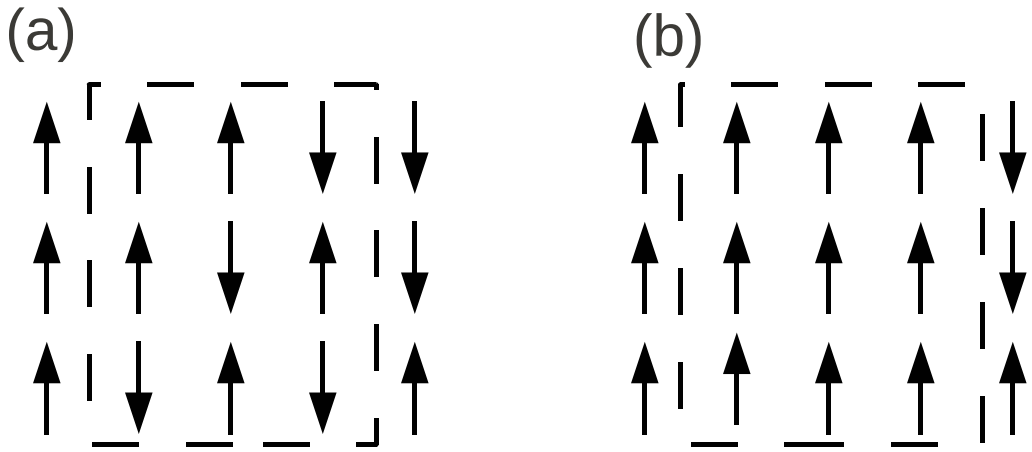

Figure 3.9: Majority rule model: the majority opinion inside a discussion group (inside the box) (a) is taken by all agents at the next time step (b).

given distribution. If the number of agents in the group is odd, there is always a majority opinion. On the other hand, if r is an even number there is a possibility of a tie, and in this case, a bias is introduced in favor of some opinion. The introduction of this bias is inspired in the principle of social inertia, where people are reluctant to accept a reform in the case where the majority is not clear [102, 108].

One can see the evolution of the Majority Rule model in Fig. 3.10. The agent's opinion, starting from ρ_{ini}, evolves until the steady state. The simulations were performed with the discussion group r selected from a gaussian distribution (mean zero and $\sigma = 1$). In our simulations, in case of a tie among agents, the opinion -1 is favored.

The steady state is reached when all the agents have the same opinion. If the initial density of agents ρ_{+1} (ρ_{-1}) with opinion $+1$ (-1) is higher than a critical value ρ_c, all agents will finally reach consensus. The time to reach the consensus scales as the logarithm of the number of agents in the systems. If r if odd, $\rho_c = \frac{1}{2}$ due to the symmetry of opinions. If r is even, $\rho_c < \frac{1}{2}$ favoring the biased opinion.

This model was solved analytically by Krapivsky and Redner in 2003 by mean field analysis [114]. In their solution the authors have considered an odd number of agents in the discussion group r.

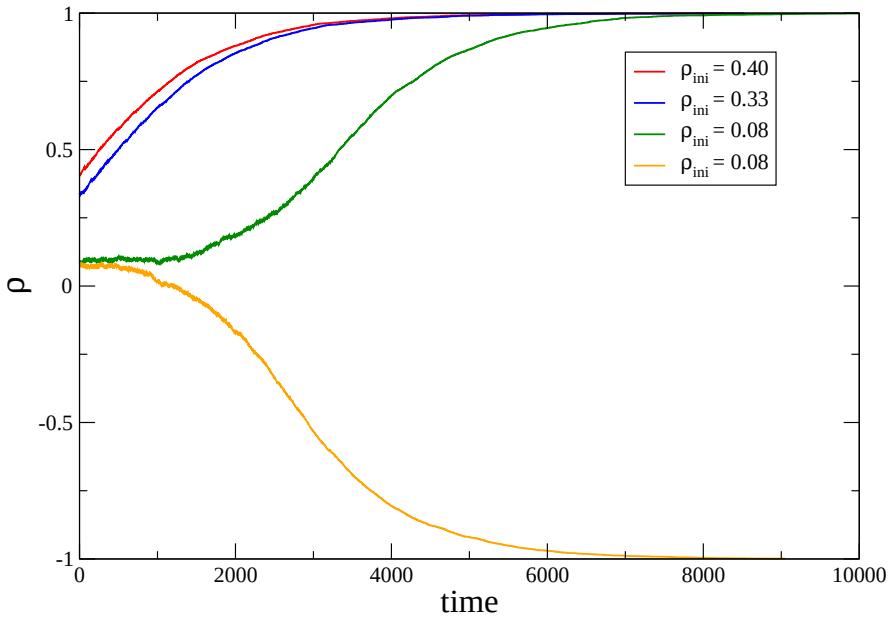

Figure 3.10: Evolution of the agent's opinion in the Majority Rule Model for different values of the initial fraction ρ_{ini}. In case of a tie, the opinion -1 is favored. Each curve corresponds to a single realization.

The average magnetization is

$$m = \frac{1}{N}\sum_i s_i = \rho_{+1} - \rho_{-1}, \tag{3.26}$$

where s_i is the opinion of the agent i. The size of r is 3 and at each time step, the number of agents with some opinion increases or decreases by one. The variation of the number of agents with same opinion can be written as

$$dN_{+1} = 3(\rho_{+1}^2\rho_{-1} - \rho_{+1}\rho_{-1}^2) = -6\rho_{+1}(\rho_{+1} - \frac{1}{2})(\rho_{+1} - 1) \tag{3.27}$$

and so

$$\frac{dN_{+1}}{N}\frac{N}{3} = \dot{\rho}_{+1} = -2\rho_{+1}(\rho_{+1} - \frac{1}{2})(\rho_{+1} - 1), \tag{3.28}$$

where the time step is $dt = 3/N$. Equation 3.28 has 3 fixed points: $\rho_{+1} = 0, 1/2, 1$. The point $\rho_{+1} = 1/2$ is unstable and the points $\rho_{+1} = 0, 1$ are stable, so all agents will have the same opinion as the initial majority, as was found by Galam.

The average time until the system reaches consensus is proportional to the logarithm of the number of agents N in the mean-field limit. Computer simulations suggested that the consensus time grows as N^2, for the bidimensional case. For higher dimensions, the system may be trapped into metastable states evolving even slower. Numerical simulations of the critical properties of the majority voter model on $d-$dimensional hypercubic lattices show that the upper critical dimension is 6, reproducing the mean-field results [115].

3.5.3 The Sznajd model

The rationale behind the Sznajd model is the emergence of social collective behavior due to interactions between individuals, constituting the microscopic level of a social system. Two agents having the same opinion can convince other agents in the network. In the original one-dimensional version of the model, each individual can have one of two opinions represented by Ising spins ('yes' or 'no', 'up' or 'down'). A pair of parallel spins on sites i and $i+1$ forces its two neighbors, $i-1$ and $i+2$, to have the same opinion (orientation), while for an antiparallel pair (i, $i+1$), the left-hand neighbor ($i-1$) takes the opinion of spin $i+1$, while the right-hand neighbor ($i+2$) takes the opinion of spin i [116].

In this simplest formulation of the Sznajd model, two types of steady states are reached: either complete consensus (ferromagnetic-state) or stalemate, in which every agent has an opinion which is different from that of its neighbors (antiferro-magnetic state). The Sznajd rule for the antiparallel pair is unrealistic and it is usually replaced in the extensions of Sznajd models, so if a pair of agents are in disagreement, the neighbors maintain their opinions [102]. The original model in one dimension has no phase transition due to the coexistence of two (ferro- and antiferromagnetic) stationary states.

Considering the Sznajd model defined on a square lattice and not a pair of neighbors, but a 2×2 plaquette with four neighbors, Stauffer *et al.* [117] made each fully polarized plaquette convince its eight neighbors. For this model, they found a phase transition for an initial density of up spins $d = 1/2$. In the most common version of the Sznajd model, a pair of agents convince all their neighbors, as shown in Fig. 3.11.

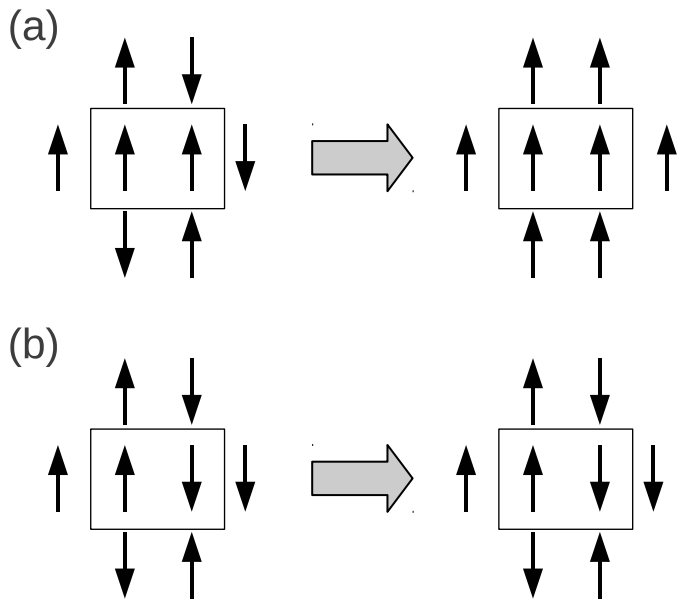

Figure 3.11: The standard version of the Sznajd model defined on the square lattice: a pair of agents with same opinion (inside the box) convince all their neighbors (a), while in the case of disagreement the neighborhood keep their opinions (b).

This model has been extensively studied, and numerous modifications have been proposed, e.g., square [117], triangular [118], and cubic lattices [119]; increased interaction range [120] and number of states of the variable [121, 122, 123]; and diffusion of the agents [123, 124]. The model was also applied to areas such as politics, marketing, spread of opinions among traders and finance [125, 126].

An exact solution for a Sznajd-like dynamics on a complete graph was given by Slanina and Lavička [127]. In their model two agents i and j interact with a third agent k, all taken at random. If the opinions of the first two agents are the same, the third follows the previous agents, otherwise nothing happens.

Other studies focused on the Hamiltonian formulation of the model. In this approach an equivalent dynamics is considered, based on minimization of *disagreement function*, essentially a spin-spin interaction function [128, 129, 130].

Chapter 4

Consensus Model

In this Chapter we study numerically a modified version of the Sznajd Opinions model, introduced in the last Chapter. We include in our model reputation, a mechanism which limits the capacity of persuasion of the agents. The reputation is introduced as a time-dependent score, which can be positive or negative. The introduction of this mechanism avoids dictatorship (full consensus, all spins parallel) for a wide range of parameters of the model. Two different situations were considered in this study: the case where the reputation of the agents increases for each persuaded neighbor (case 1) and the case where the reputation of an agent can increase for each persuasion but can also decrease when a neighbor keeps his opinion (case 2).

Our results show that the introduction of the reputation destroys full consensus even for initial densities of up spins greater than $1/2$. The relaxation times follow a log-normal-like distribution in both situations, but they are greater in case 2 due to the competition of reputations. In addition, we show that the usual phase transition occurs and depends on the initial concentration of individuals with same opinion d, but the critical points d_c are different in the two cases considered.

4.1 Reputation in the Sznajd Model

The explanation of the emergence of consensus in a population with interaction agents was the great success of the Sznajd model. Since the model was introduced in 2000, many different modifications were proposed and successfully applied to many different areas. The Sznajd model is robust against the following situation: if one convinces the neighbors only with some probability p, and leaves them unchanged with probability $1 - p$, the consensus will be still reached after a long time.

Unfortunately the dynamics of social relationships in real world shows a large number of details which are commonly neglected in many models, such as the influence of mass media in the opinions formation or the authoritarianism forcing the agents to follow some standardized opinion or a persuasion of an agent to follow a group's opinion.

In order to formulate a more realistic model, we introduce in this work a reputation mechanism. We believe that the inclusion of reputation in our model turns it closer to a real system, where not only the number of individuals with same opinion matters. We believe that the reputation of the agents who holds an opinion is an important factor in persuasion the agents across the community. In other words, an individual more easily changes their opinion if he or she is influenced by people with good reputation.

On the other hand, people with bad reputation are usually ignored. The reputation limits the capacity of persuasion of the agents, compared to the standard model. In fact, our results considering the simple microscopic rules of the model show that not only a full consensus situation occurs, but a democracy-like situation is possible.

As was pointed by *Castellano et al.*, we probably would not pay much attention to a single guy staring at the sky, but instead, if a group of people stares at the sky at same time, we probably may be tempted to do the same [102]. Convincing somebody is easier for a group of people than for a single individual. Moreover, convincing somebody is even easier for a group with very good reputation.

4.2 Description of the Model

We consider the generalization of the Sznajd model defined on the square lattice with $L \times L$ agents [131]. Our model is based on the rules explained in Fig. 4.1. According to these rules a plaquette of agents with same opinion convince all their eight neighbors. This differs from the one-dimensional original model where a pair of neighboring agents i and $i+1$ determines the opinions of their two nearest neighbors $i-1$ and $i+2$. In addition, an integer number (R_i) labels each player, i, and represents its reputation across the community, in analogy to the Naming game model considered by Brigatti [132].

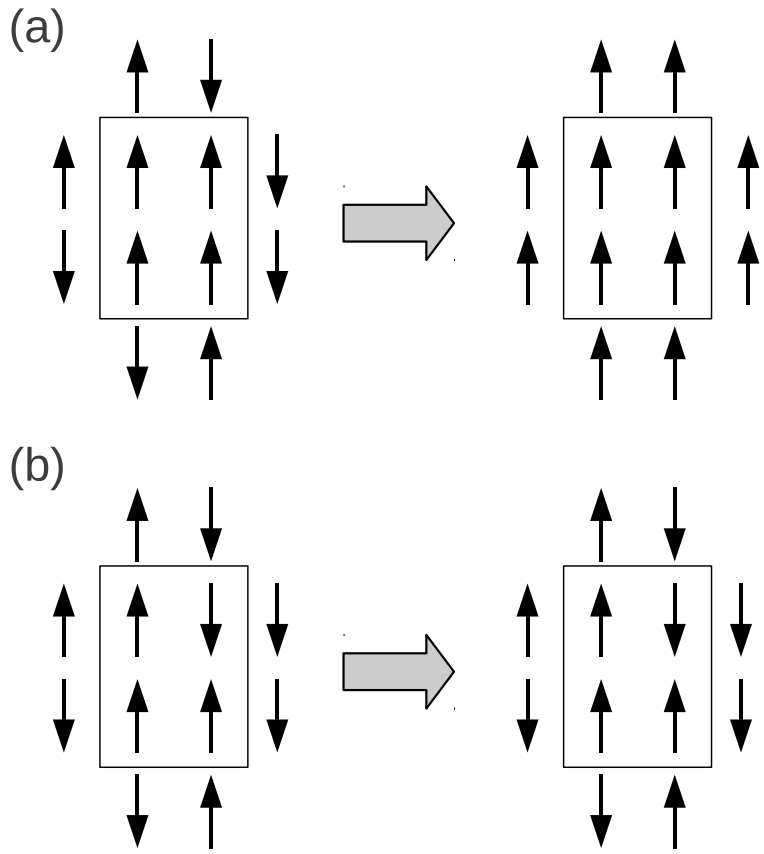

Figure 4.1: Generalization of the Sznajd model defined on the square lattice by Stauffer *et al.*: a plaquette of agents with same opinion (inside the box) convince all their eight neighbors (a), while in the case of any disagreement the neighbors keep their opinions (b).

The reputation (agent's score) $R_i(t)$ is time dependent. The agents start the dynamics with a Gaussian distribution of R, and during the time evolution, the reputation of each agent changes according to its capacity of persuasion, following the rules explained in this section. The initial state of the system is a population of $L \times L$ agents with randomly assigned opinions (± 1 Ising spins) and a Gaussian distribution of R, centered at 0 with standard deviation σ. As will be shown, the model displays the same results for various standard deviations of the distribution of reputation.

At each time step, the following microscopic rules control our model:

1. Randomly choose a 2×2 plaquette of four neighbors on the lattice.

2. If not all four spins in the plaquette are parallel, leave its neighbors unchanged and return to step 1.

3. Otherwise we calculate the average reputation of this plaquette:

$$\bar{R} = \frac{1}{4} \sum_{i=1}^{4} R_i \ ,$$

   where $R_i, i = 1, 2, 3, 4$ is the reputation of each plaquette's agent.

4. Compare the reputations of each neighbor with the average reputation of the plaquette. If the reputation of a neighbor is less than the average one, this neighbor follow the plaquette orientation. On the other hand, if the neighbor reputation is greater than $\bar{R}$, nothing occurs.

5. For each persuasion, the plaquette agents' increase their reputation by 1. If the plaquette fails to convince its neighbors, then the reputations do not change[1].

If an agent convinces many others, his reputation increases. On the other hand, as will be shown in subsection 4.4.2, the persuasion abilities may decrease if fails to convince other individuals.

[1] If the plaquette and their neighbors have all parallel spins, neighbors and reputation are kept unchanged.

4.3 Reputation Dynamics

We considered two distinct situations: in the first situation, the reputation of each agent increases in the case of successful convincing other agents, whereas in the second situation the reputation may increase and decrease according with the agent's success convincing their neighborhood.

Case 1

In the first situation, if the plaquette convince their neighbors, then the reputation of each of the agents in this plaquette increases by 1. Otherwise the reputation do not change, as was explained before.

We will show that the introduction of the reputation destroys the final ferromagnetic (dictatorship) state on the standard Sznajd model. In our model, the final state (the end of evolution) is characterized by not all agents holding the same opinion - "democratic consensus".

Case 2

In the second situation which we consider, the agent's reputation decreases if the plaquette does not convince a neighbor. Our rules for this situation keep unchanged for the previous steps 1 - 4. The only difference is in the step 5 which changes in the following way:

5. For each persuasion, the plaquette agents' increase their reputation by 1. If the plaquette fails to convince their neighbors, the reputation of the agents inside the plaquette decrease by 1.

4.4 Numerical Results

Our results will be presented separately for the two cases. In case 1 we will show the phase transition occurring at an initial density of up spins, d, greater than 1/2. Differently, in case 2, this transition only occurs for $d \to 1$.

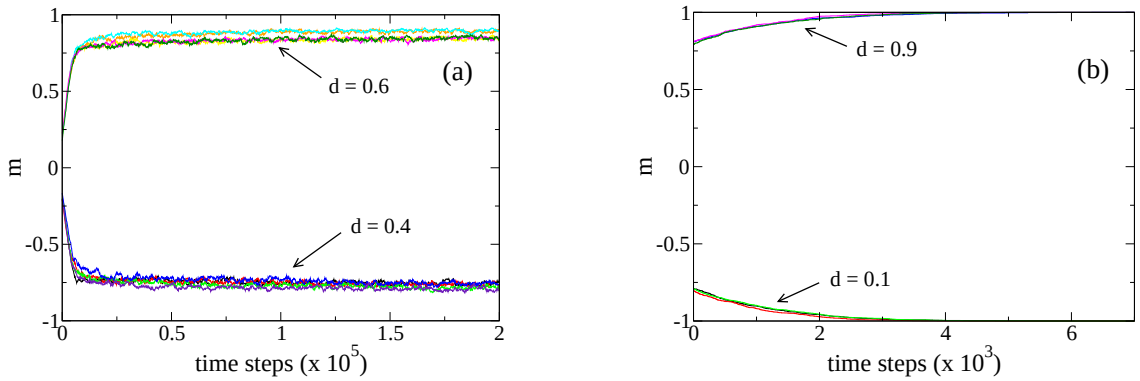

Figure 4.2: Time evolution of the magnetization (case 1) for $L = 53$, initial densities of up spins $d = 0.4$ and $d = 0.6$ and different samples (a). The system approaches steady state in which the total consensus is not reached, in contrast of the standard Sznajd model defined on the square lattice [117]. In figure (b) we show the results for $d = 0.1$ and $d = 0.9$. In these cases the system reaches consensus.

4.4.1 Case 1

In the simulations, we used the agent's initial reputations following a Gaussian distribution with standard deviation $\sigma = 5$. Following the previous works on the Sznajd model, we can start studying the time evolution of the magnetization per site,

$$m = \frac{1}{N}\sum_{i=1}^{N} s_i \ , \tag{4.1}$$

where $N = L^2$ is the total number of agents and $s_i = \pm 1$. In the standard Sznajd model defined on the square lattice, for $d < 1/2$ ($> 1/2$) the system goes to a ferromagnetic state with all spins down (up) in all samples, characterizing a phase transition at $d = 1/2$ in the limit of large L.

We show in Fig. 4.2 the evolution of the magnetization as a function of the simulation time in our model, for the case 1. Figure 4.2 (a) the evolution starts from the initial density of spins $d = 0.6$ (which is equivalent to the case of $d = 0.4$). One can see that the total consensus with all spins up (down) will not be achieved in any sample, indicating that a democracy-like situation is possible in the model without introduction of some kind of special agents (like contrarians and opportunists) [133]. In Fig. 4.2 (b), the evolution of the magnetization show situations where the

consensus is obtained starting from $d = 0.9$ and $d = 0.1$. In this situation the total consensus is finally reached, so one could expect the transition at $0.6 < d_c < 0.9$ (or, equivalently, $0.4 < d_c < 0.1$).

We have also studied the relaxation times of the model, i.e., the time needed to find all the agents at the end having the same opinion (a dictatorship state), in the original Sznajd model. In our model, the relaxation time is the time needed to reach a fixed point. In the case where full consensus is reached, the dynamics stops and the magnetization of the steady state is always $m = \pm 1$. On the other hand, in the cases where democratic states are reached, the magnetization of these steady state fluctuates around a mean value but the dynamics evolves continuously. In addition, the times to reach democratic steady states are normally larger than the times to reach full consensus.

The distribution of the times needed to reach the fixed point, averaged over 10^4 samples, is shown in Fig. 4.3 (a). We can see that the distribution of this time is compatible with a log-normal one for all values of the standard deviation σ, which corresponds to a parabola in the log-log plot of Fig. 4.3 (a). The same behavior was observed in other studies of the Sznajd model [117, 133, 134]. In Fig. 4.3 (b) we show the average relaxation time τ (also averaged over 10^4 samples) versus latice size L in the log-log scale. We can verify a power-law relation between these quantities, $\tau \sim L^{5/2}$, for all values of the standard deviation, σ. A power-law relation between τ and L was also found in a previous work on the Sznajd model, with exponent 2.6 [134].

Let us analyze the phase transition of the model. In simulations, a phase transition is never sharp, but it is indicated numerically by the change of the slope as L is becoming larger, as one can see in Fig. 4.4 (a). Only in an infinite lattice one can expect a sharp transition (step function) for f versus d. For this purpose, we simulated the system for different lattice sizes L and measured the fraction of samples having final states with all spins up when the initial density of up spins d is varied in the range $0.4 \leq d \leq 1.0$. In other words, this quantity f gives us the probability that the population reaches the total consensus, for a given value of d.

We have considered 1000 samples for $L = 31$ and 53, 500 samples for $L = 73$ and 101 and 200 samples for $L = 121$, all samples using $\sigma = 5$. The results are shown in Fig. 4.4 (a). One

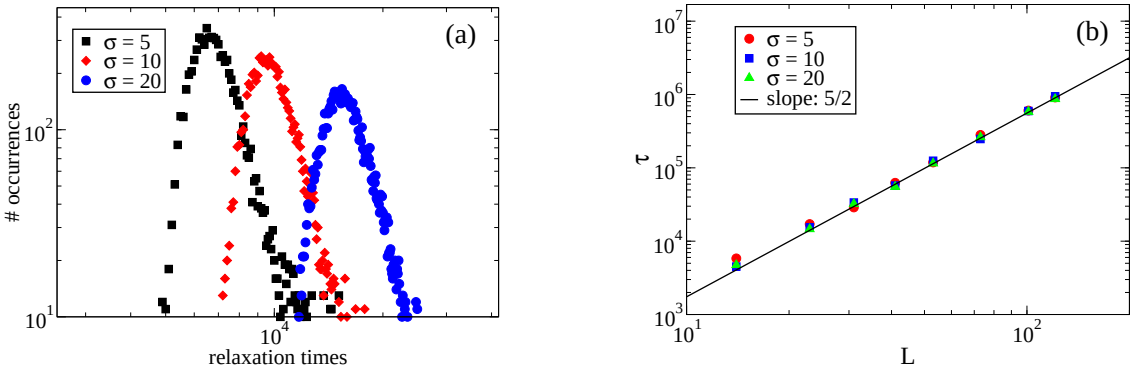

Figure 4.3: Log-log plot of the histogram of relaxation times (case 1) for $L = 53$ and $d = 0.8$, obtained from 10^4 samples, with agents' initial reputations following a Gaussian distribution with different standard deviations σ (a). The distribution is compatible with a log-normal one for all values of σ, which corresponds to the observed parabola in the log-log plot. The relaxation time τ, averaged over 10^4 samples, versus latice size L in the log-log scale (b). The straight line has slope 5/2. The result is robust with respect to σ.

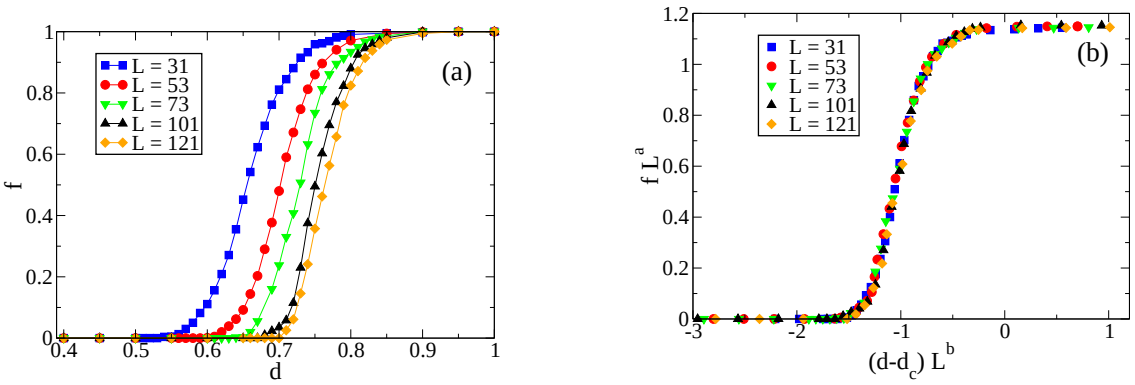

Figure 4.4: Fraction f of samples (case 1) which show all spins up when the initial density of up spins d is varied in the range $0.4 \leq d \leq 1.0$, for a set of lattice sizes L and $\sigma = 5$ (a). The total number of samples are 1000 (for $L = 31$ and 53), 500 (for $L = 73$ and 101) and 200 (for $L = 121$). It is also shown the corresponding scaling plot of f (b). The best collapse of data was obtained for $a = 0.035$, $b = 0.444$ and $d_c = 0.88$.

can see that the transition point is precisely in the region $d > 1/2$. In order to locate the critical point, we performed a finite-size scaling (FSS) analysis, based on the standard FSS equations [134, 135],

$$f(d, L) = L^{-a}\ \tilde{f}((d - d_c)\ L^b)\ , \tag{4.2}$$

$$d_c(L) = d_c + c\ L^{-b}\ , \tag{4.3}$$

where c is a constant and $\tilde{f}$ is a scaling function. The result found is

$$d_c = 0.88 \pm 0.01\ . \tag{4.4}$$

in the limit of large L, as shown in Fig. 4.4 (b). In addition, the best collapse of data was obtained for $a = 0.035$ and $b = 0.444$.

In the original Sznajd model on a square lattice, the system starts with half of the spins up and half down. Varying the initial density, the system finally has all spins down (if $d < 1/2$) or all spins up (if $d > 1/2$). For $d_c = 0.5$, half of the samples reaches steady state with spins up and half with spins down.

This difference of the critical point may be easily understood: at each time step, the randomly chosen 2×2 plaquette that may convince 8, 7, 6, ..., 1 or 0 neighbors, even if the plaquettes' spins are parallel. That will depend on the reputation of an agent and the average reputation of the plaquette. In the standard model, if the plaquettes spins' orientations are the same, then all the 8 plaquette's neighbors are convinced immediately. Thus, the usual phase transition of the SM also occurs in our model, for the case 1, but for a larger value of d. This transition is the same for different values of σ as one can see in Fig. 4.5.

4.4.2 Case 2

As was discussed in Section 4.2, in the second case the agent's reputations may also decrease, which introduces a competition of reputations in the game. The resulting evolution of the magnetization per site is shown in Fig. 4.6.

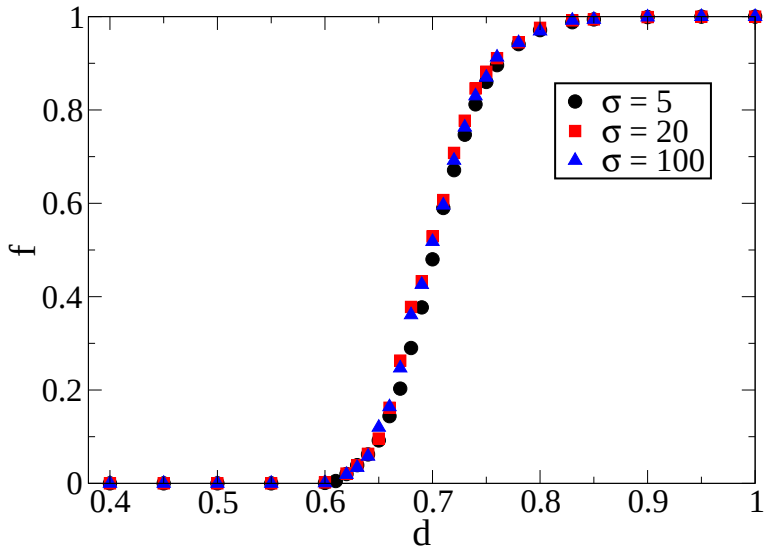

Figure 4.5: Fraction f of samples (case 1) which show finally spins up when the initial density d is varied in the range $0.4 \leq d \leq 1.0$, for $L = 53$, 1000 samples and various values of σ. The behavior of f does not change with σ.

At intermediate initial densities d (around $d = 0.5$) the system reaches steady states with $m < 1$, i.e., we have a democracy-like situation. The results nonetheless show a variety of steady states, differently from the results of the case 1, Fig 4.2 (a), reaching different steady states for the same d. We believe this is due to the evolution of the reputation, which for this case, may increase or decrease depending on the evolution of the average reputation of the plaquettes [136].

Another characteristic observed in case 2 of our model is that the magnetization evolves slowly to the steady state, even for large and small initial densities, $d = 0.9$ and $d = 0.1$. This fact can be observed in the inset of Fig. 4.6 (b), in which the system evolves until 7×10^5 time steps (observation time). The dashed line is $m = 1$ and we observe that one of the three realizations reaches consensus before the observation time. Thus, for the case 2 of our model, the full consensus is harder to reach and the emergence of democratic steady states is favored.

We have also studied the statistics of relaxation times in our model for case 2. The distribution of the number of sweeps through the lattice is shown in Fig. 4.7 (a) for different σ. One can see that, as in case 1, the relaxation time distribution is compatible with a log-normal one for all σ.

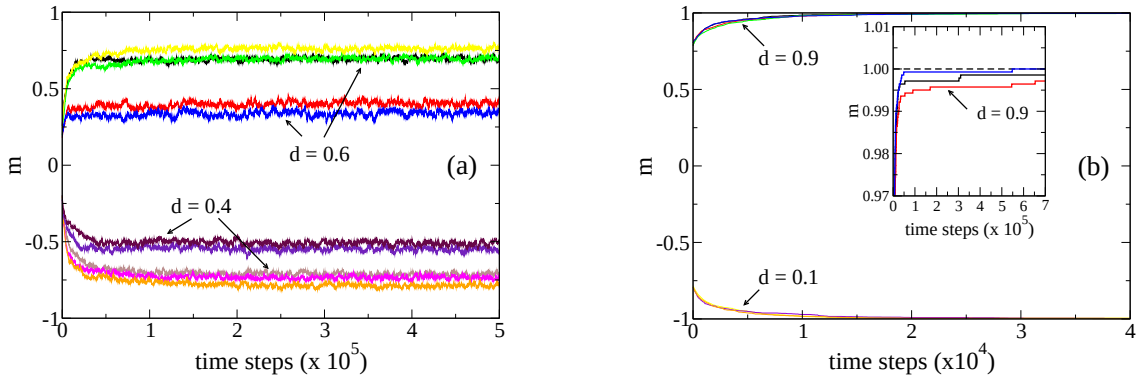

Figure 4.6: Time evolution of the magnetization (case 2) for $L = 53$, $\sigma = 5$ and initial densities of up spins $d = 0.4$ and $d = 0.6$. Different samples reach different democracy-like steady states for the same d. The results for $d = 0.1$ and $d = 0.9$ are shown in (b). Observe in the inset the system reaches full consensus in only one of the three samples during the observation time, 7×10^5 time steps. The dashed line in the inset is $m = 1$ (full consensus).

However, as one can expect, due to competition of reputations, the relaxation times in case 2 are greater than the corresponding relaxation times in case 1. In Fig. 4.7 (b) we show the relaxation time τ (averaged over 10^4 samples) versus latice size L in the log-log scale. In this case, we verify the same power-law behavior observed in case 1, $\tau \sim L^{5/2}$, for large L and any σ.

Following the approach described in the last subsection (case 1), we simulated the system for different lattice sizes L and measured the fraction of samples which show all spins up when the initial density of up spins d is within the range $0.5 \leq d \leq 1.0$. We considered the same number of samples as in the last subsection, and the results are shown in Fig. 4.8. One can see that the transition point $d_c > 0.88$, i.e., the critical density in case 2 is greater than in case 1, as expected due to the competition of reputations. In other words, when the reputation of an agent can increase for each successful persuasion and decrease for each unsuccessful persuasion, a higher initial density d is needed to reach a full consensus state.

One can observe in Fig. 4.8 that, for $L = 31$, the curve $f(d)$ is qualitatively distinct from those for larger sizes, mostly due to finite size effects. Our simulations show that, differently from the case 1, $f(d) = 1$ is only obtained for $d = 1$. This result may indicate that the phase

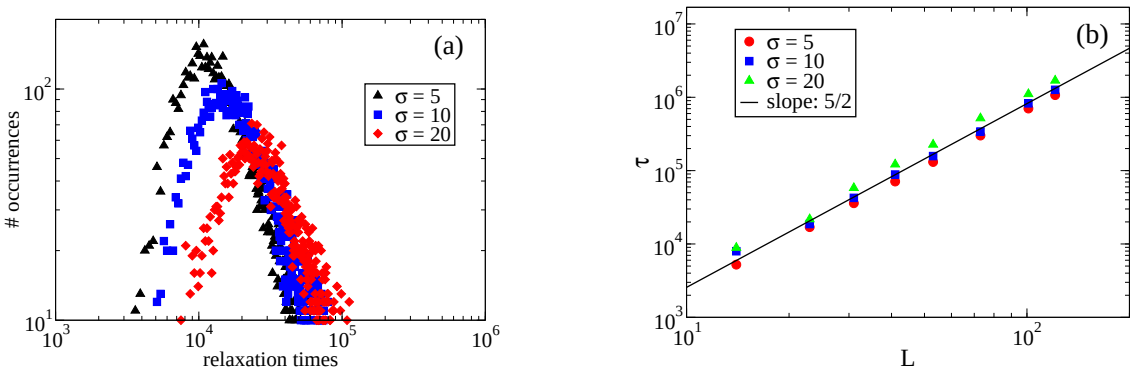

Figure 4.7: Log-log plot of the histogram of relaxation times (case 2) for $L = 53$ and $d = 0.98$, obtained from 10^4 samples, with agents' initial reputations following a Gaussian distribution with different standard deviations σ (a). The distribution is compatible with a log-normal one for all values of σ, which corresponds to the observed parabola in the log-log plot. It is also shown the relaxation time τ, averaged over 10^4 samples, versus latice size L in the log-log scale (b). The power-law behavior for large L is $\tau \sim L^{5/2}$, for all values of σ.

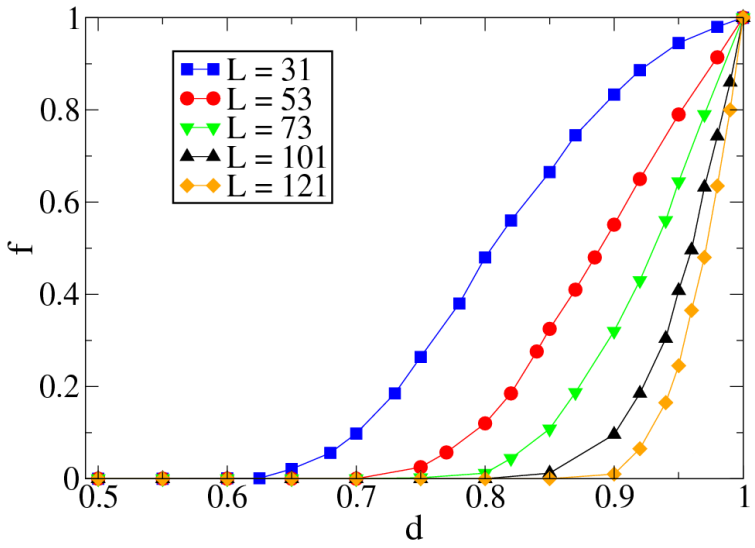

Figure 4.8: Fraction f of samples (case 2) which have finally all spins up versus initial fraction of up spins, for different lattice sizes L. The total number of samples is 1000 (for $L = 31$ and 53), 500 (for $L = 73$ and 101) and 200 (for $L = 121$). The simulations were performed for a maximum observation time 2×10^5 time steps.

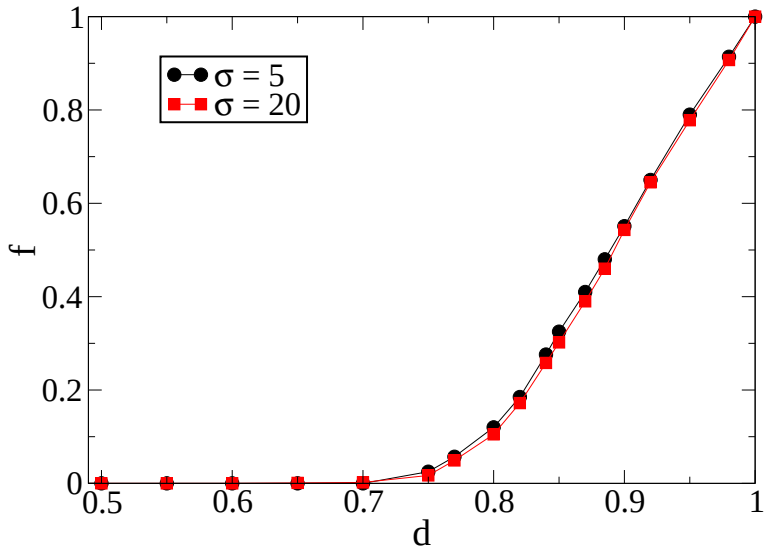

Figure 4.9: Fraction f of samples (case 2) which show all spins up for the observation time 2×10^5 time steps. The initial density d is within the range $0.5 \leq d \leq 1.0$, for $L = 53$, 1000 samples and two different values of σ. The behavior of $f(d)$ is independent of σ.

---

transition found in our model for the case 1 is absent for the case 2. However, we can not draw this conclusion, since the resuls are dependent on the observation time and, in our simulations, the largest observation time was 7×10^5 time steps. In Fig. 4.9 one can see that the behavior of $f(d)$ is independent of σ.

4.5 Remarks and Chapter Conclusions

We studied a modified version of the Sznajd sociophysics model. In particular we considered reputation, a mechanism that limits the capacity of persuasion of the agents. The reputation is introduced as a score for each player and is time dependent, varying due to the model's rules. The agents start with a random distribution of reputation values, and during the time evolution, the reputation of each agent changes according to its capacity of persuasion. We assumed that the initial values of the agents' reputation follow a Gaussian distribution centered at 0 with standard deviation σ. We studied two different situations: (i) the situation in which the reputations increase

due to each persuaded individual, and (ii) where the reputations increase for persuasion and decrease if a group of agents fail to convince one of its neighbors.

In the first case, we observed a log-normal-like distribution of the relaxation times, i.e., the time needed to reach a state with all the agents having the same opinion. In addition, the average relaxation times grow with the linear size of the lattice, as $\tau \sim L^{5/2}$. The system undergoes a phase transition, which was identified by measurement of the fraction f of samples which show all spins up when the initial density of up spins d is varied. f is the probability that the population reaches the full consensus for a given value of d. We localized the transition point by finite-size scaling analysis, and found $d_c = 0.88$. This critical density is greater than $1/2$, the value found by Stauffer *et al.* [117] in the standard formulation of the Sznajd model. The simulations indicate that the observed phase transition is independent of σ.

In the second case, we also found that the relaxation times are log-normally distributed, but they are greater than the relaxation times in case 1. We have observed the same power-law behavior $\tau \sim L^{5/2}$, for large L. The competition of reputations in case 2 increases the relaxation times and we cannot draw conclusions about the phase transition in this case.

Chapter 5

Evolution of Spatially Embedded Branching Trees with Interacting Nodes

In this Chapter we study the evolution of branching trees embedded in Euclidean spaces, which have suppressed branching of spatially close nodes. This cooperative branching process accounts for the effect of overcrowding of nodes in the embedding space and mimics the evolution of life processes (the so-called "tree of life") in which a new level of complexity emerges as a short transition followed by a long period of gradual evolution or even complete extinction. We consider the models of branching trees in which each new node can produce up to two twigs within a unit distance from the node in the Euclidean space, but this branching is suppressed if the newborn node is closer than at distance a from one of the previous generation nodes. This results in an explosive (exponential) growth in the initial period, and, after some crossover time $t_x \sim \ln(1/a)$ for small a, in a slow (power-law) growth. This special point is also a transition from "small" to "large worlds" in terms of network science. We show that if the space is restricted, then this evolution can end by extinction.

5.1 Introduction

A growing tree-like network can model different processes such as a technological or biological systems represented by a set of nodes, where each element in the network can create new elements. Innovation and discovery [137], artistic expression and culture [138], language structures [139, 140] and the evolution of life [141, 142] can be represented by a branching process in a tree [143]. Growing trees naturally represent a wide range of real-life processes and phenomena [6, 14, 142, 144, 145, 146]

"The evolution of life is, obviously, a nonuniform process" [141]. For biological evolution, this means that new types of biological objects emerge abruptly with subsequent gradual evolution. This evolutionary process can be schematically depicted as a tree ("the tree of life" [141, 142]), where branches, are, for example, different species. Importantly, the growth of this tree is complicated by interaction and competition between species. In this Chapter we discuss one of the simplest models of growing trees which can mimic this process.

The Galton-Watson branching process [147] provides a simple example of a growing tree with non-interacting nodes and so uncorrelated branching. A root node generates a number of daughter nodes distributed according to a Poisson function with mean μ. In that case, the whole network goes to extinction only if each of the root's daughters dies. In this case, the survival probability $\mathcal{Z}$ satisfies $1 - \mathcal{Z} = e^{-\mu\mathcal{Z}}$, which has a non-zero solution only when $\mu > 1$. The phase transition in the GW model that occurs at $\mu = 1$ is a general property of models with independent branching.

Interacting branching processes are much more interesting and difficult for analysis [137]. In this work we study evolving trees whose evolution is influenced by interaction between some of the existing nodes, for example, nodes of the previous generation, representing a competition of species for resources in a limited space. We assume that the growing tree is embedded in some metric space and assume that spatially close nodes of the previous generation suppress mutually their ability to born new nodes. In other words, overcrowding of nodes in the embedding space suppresses their "fertility". We also consider the evolving trees embedded in restricted areas of metric spaces, and investigate the possibility of complete extinction under certain model's

parameters.

This kind of interaction (competition), leading to suppression of branching, emerges if there is no sufficient space, no niches for the new nodes and branches (species). Due to the embedding space, we can introduce distance between two nodes other then the shortest path internode distance for this tree. For the sake of simplicity, we consider a D-dimensional Euclidean space, although the results do not depend qualitatively on D. Networks embedded in metric spaces and their evolution already attracted much attention [148, 149, 150, 151, 152, 153]. We are particularly interested in a transition (actually, crossover) between different regimes of the network growth, namely, explosive (exponential) evolution and gradual (power-law) one. Here the evolution of the network is characterized by the variation of the number of its nodes (which corresponds to biological diversity, for example). We find the position of this transition and express it in terms of a single model parameter. This transition coincides with crossover from a "small world" to "large world" network architectures [154], where small worlds show a logarithmic dependence of network diameters on their sizes (total numbers of nodes) and large words show a power-law dependence [13, 40].

One should emphasize a principal difference from the previous studies of this crossover. In Ref. [154], the crossover was controlled by a model parameter, while in the present study the small-world and large-world architectures are realized on different stages of the network evolution. In addition we find how the spatial distribution of nodes evolves and the possibility of complete extinction.

5.2 The Model

The model of interacting nodes, which we use, is schematically represented in Fig. 5.1, showing the grow of the tree embedded in a two-dimensional space. The growth of the tree starts from a root node (dark black circle in Fig. 5.1). At each time step, each of the nodes of the tree attempts to emit two leaves (leaf is a link with a new node, lighter circles), so at each time step a new generation of nodes is given birth. The network is embedded in a D-dimensional Euclidean space, and the root has zero coordinates.

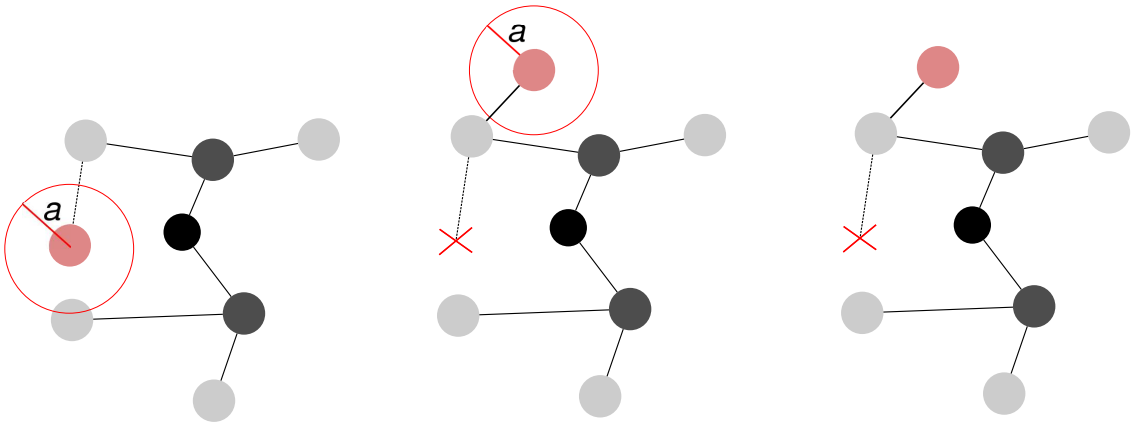

Figure 5.1: The scheme of the network growth on a plane. The black node shows the root, the nodes of the first and the second generations are dark and light grey, respectively. The furthermost left node attempts to born two children. The first attempt (left) is abandoned because of the nearby second generation node. The second attempt (center) is successful since the new node has no second generation node within radius a from it. This results in the network (right).

At each time step, we make the following:

1. Choose uniformly at random a node i (coordinates $\mathbf{x}_i$) from the previous generation and make an attempt to create its leaf with a new node at the point $\mathbf{x}_i + \mathbf{\Delta}_i$. Here the random vector $\mathbf{\Delta}_i$ is uniformly distributed within $-1 \leq \Delta_{x,i} \leq 1$, $-1 \leq \Delta_{y,i} \leq 1$, $\ldots$, $-1 \leq \Delta_{D,i} \leq 1$.

2. If among the nodes of the previous generation (excluding the parent node i) and among the nodes already created at this time step, no nodes are closer than at distance a from the point, $\mathbf{x}_i + \mathbf{\Delta}_i$, then create the leaf. If such nodes exist, abandon this attempt. Make the next attempt to create the second leaf from this node using the same rules.

3. From the rest nodes of the previous generation, choose uniformly at random nodes one by one and repeat the steps (1) and (2) until all the nodes of the previous generation will be updated.

We will also consider a variation of this model, in which for each attempted node birth, closeness to all existing nodes should be checked and not only to the previous generation nodes.

In this case, we are taking into account the possibility that more than one generation can coexist. These two variations of our model are related with the SIS and SIR epidemic models, which will be discussed in the next Section.

5.3 Connection between our model and epidemic models

In the first situation considered in our model (Case 1), only the previous generation nodes are take into account when testing node closeness from a potential newborn node. In the second situation (Case 2), all existing nodes are checked before the birth of a new node. Case 1 has some similarities with the SIS model, while the case 2 is related with SIR epidemic model.

5.3.1 SIS

In the SIS model, described in Sec. 3.2.2, a susceptible node becomes infected if it has contact with an infected neighbor, but it also can recover and become susceptible again. One can describe case 1 of our model as a version of the SIS model. The metric space is filled with susceptible nodes and the root is the infected one. At each time step, new attempts to infect are made by each node. The number of new nodes can be seen as the number of infected nodes in the epidemic outbreak.

5.3.2 SIR

In the SIR model, described in Sec. 3.2.3, the nodes can be in one of the three states, infected, susceptible or recovered. Similarly, one can describe case 2 of our model, as a version of the SIR model. The only difference is that, in previous case, the nodes can recover and get infected again, while in case 2 reinfections are not allowed. There is also a connection with SIR model and the percolation problem. John Cardy and Peter Grassberger show that the SIR model is in the same universality class as percolation [155].

Considering these connections between our branching model and the SIS and SIR models, it is possible to indicate some differences: i) in our model the total population is not constant and

ii) the spreading process is spatially localized.

5.4 Network size evolution

Figure 5.2 shows the result of simulation of this model for $D = 1$ and sufficiently small a, namely, the evolution of the number of nodes $N(t)$ of generation t which plays the role of time. Initially, N grows exponentially, $N = 2^t$. One can see that after certain crossover time t_x, the network growth is slower than exponential. For an arbitrary dimension D, one can easily estimate $N \cong \text{const}\,(t/a)^D$ at large t. To obtain this estimate, we assume that nodes of generation t are within a hypersphere which radius grows with a constant rate of the order of 1 (the rate is actually smaller than 1). This average rate of expansion is explained by the fact that children in this tree are born within unit distance from their parent nodes. Since the neighboring nodes cannot be closer than a distance a, we obtain $N \sim t^D/a^D$.

Note that if the parameter a is sufficiently large, N does not grow at all. If a is, say 2, $N = 1$ for any t, and our tree is a chain of nodes.

From $N(t \lesssim t_x) = 2^t$ and $N(t \gtrsim t_x) \sim \left(\frac{t}{a}\right)^D$, we have very roughly

$$2^{t_x} \sim \left(\frac{t_x}{a}\right)^D, \tag{5.1}$$

which leads to the estimate

$$t_x \sim \frac{D}{\ln 2} \ln\Big(\frac{1}{a}\Big), \tag{5.2}$$

at small a. In Sec. 5.6, we will demonstrate that this simple estimate is consistent with the results of our simulations.

Data similar to Fig. 5.2 are shown on the normal-log plot, Fig. 5.3 (a), for a few values of a ($D = 1$). The straight line in the figure is the dependence 2^t, and the crossover from the exponential to a slower growth is clearly seen. Figure 5.3 (a) was obtained from the model formulated in Sec. 5.2, in which the previous generation nodes affect the branching process. We performed similar simulations for the model, in which newborn nodes cannot be closer than at

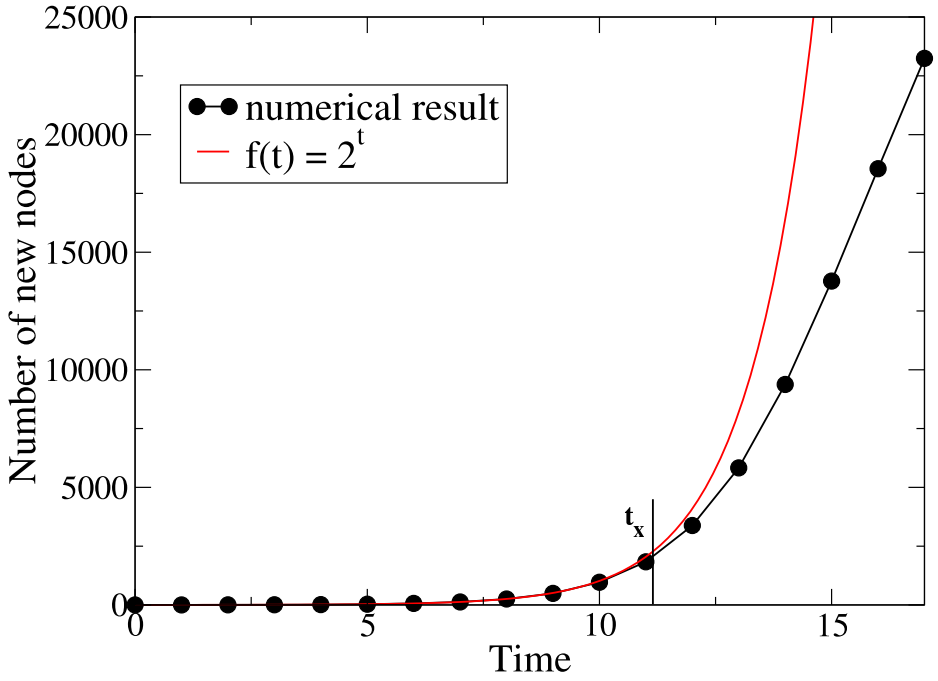

Figure 5.2: General picture of the number of new nodes as a function of time, for initial time steps of case 1, $D = 1$ and $a = 0.1$.

distance a from any of existing nodes (apart of their parents). The results of the simulations (the evolution of the number of nodes of generation t) are shown in Fig. 5.3 (b). In contrast to Fig. 5.3 (a), in the network in which all nodes influence branching, the number of nodes of generation t approaches a constant value $\overline{N}_{max}(a)$ at large t.

In the Fig. 5.3 (c) we have the same situation as in Fig. 5.3 (a), except in this case much larger values of a and time are considered. One can see that for larger values of the parameter a the branching process can stop for all samples considered, as shown in the inset. Fig. 5.3 (d) shows the same situation as shown in Fig. 5.3 (b) but for longer times. For this case of the model, when we take into account all the interactions with all existing nodes, the branching process always stops for sufficient long times.

One can easily obtain the plateau in Fig. 5.3 (b) using an estimate similar to that from the

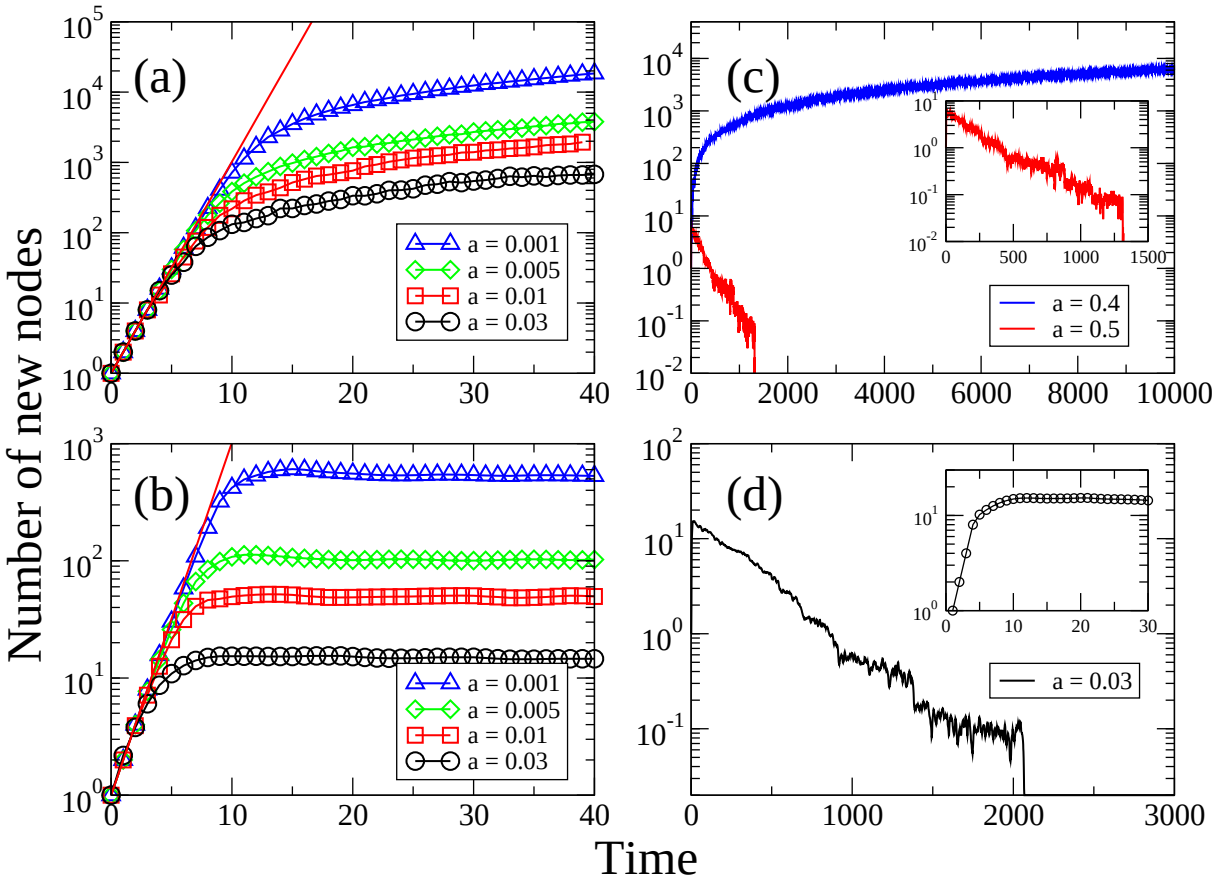

Figure 5.3: Evolution of the number of new nodes in the networks for different values of the parameter a ($D = 1$). The data were obtained after averaging over 100 samples. (a) The trees evolve according to the rules introduced in Sec. 4.2, i.e., only the previous generation nodes influence the branching process. (b) The trees in which newborns cannot be closer than at distance a from any of existing nodes (apart of their parents), i.e. the branching process is influenced by all existing nodes. (c) Same situation as seen in (a) but for long times and larger a. (d) Same data as shown in (b) but for long times. One can see that for (c) the branching process stops for for larger values of a while in (d), the number of new nodes always vanish, independent of a, for suficient long times.

previous section, $N_{tot} \cong \text{const}\,(t/a)^D$. The only difference is that now N_{tot} in that estimate is the total number of nodes in the network, and so for the number of nodes of generation t, we have

$$N_t = \frac{dN_{tot}(t)}{dt} \sim \frac{Dt^{D-1}}{a^D}, \tag{5.3}$$

and, in particular,

$$N_t \sim \frac{1}{a} \text{ at } D = 1. \tag{5.4}$$

The results of simulations for this model, which give $\overline{N}_{max} \approx 0.4/a$, see Fig. 5.4, agree with this simple estimate.

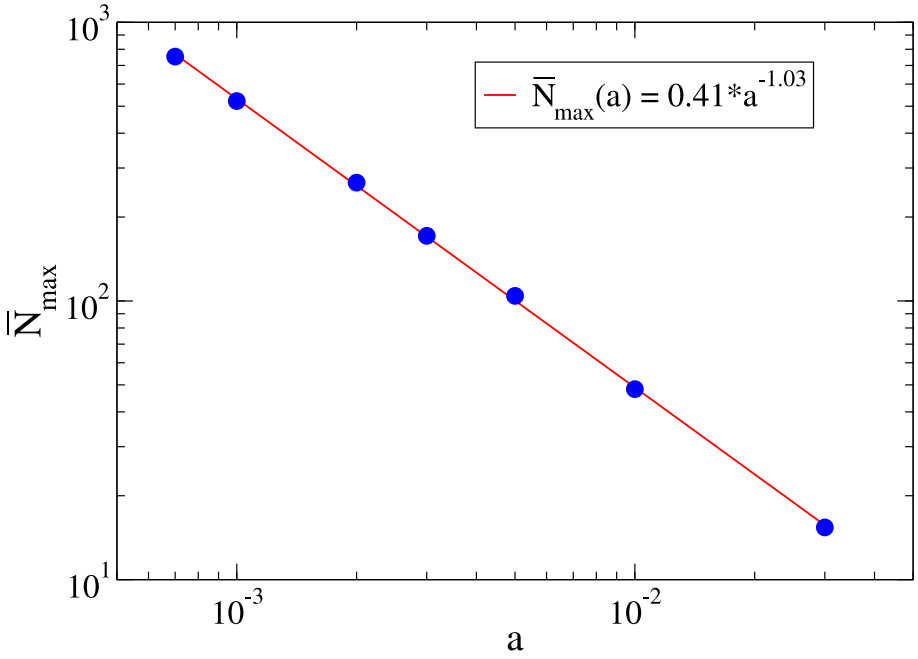

Figure 5.4: Log-log plot of $\overline{N}_{max}$ versus a obtained by simulating the model of trees in which newborn nodes cannot be closer than at distance a from any of existing nodes (apart of their parents). The straight line has slope -1.

The crossover time between two regimes of the network evolution is obtained in Fig. 5.5 for the growing tree model ($D = 1$) from the previous section. Note that the result, $t_x(a) =$

$-0.34 + 1.46\ln(1/a)$, agrees well with Eq. (6.9), $t_x \approx (D/\ln 2)\ln(1/a)$, since $1/\ln 2 \simeq 1.44$.

Clearly, the time t is of the order of the diameter d of this tree (the maximum separation between two nodes in a network). So we have the logarithmic dependence of the diameter d on the total number N_{tot} of nodes in these trees for $t \ll t_x$, and the power-law dependence $d(N_{tot})$ for $t \gg t_x$, which corresponds, respectively, to the small-world and large-world network architectures.

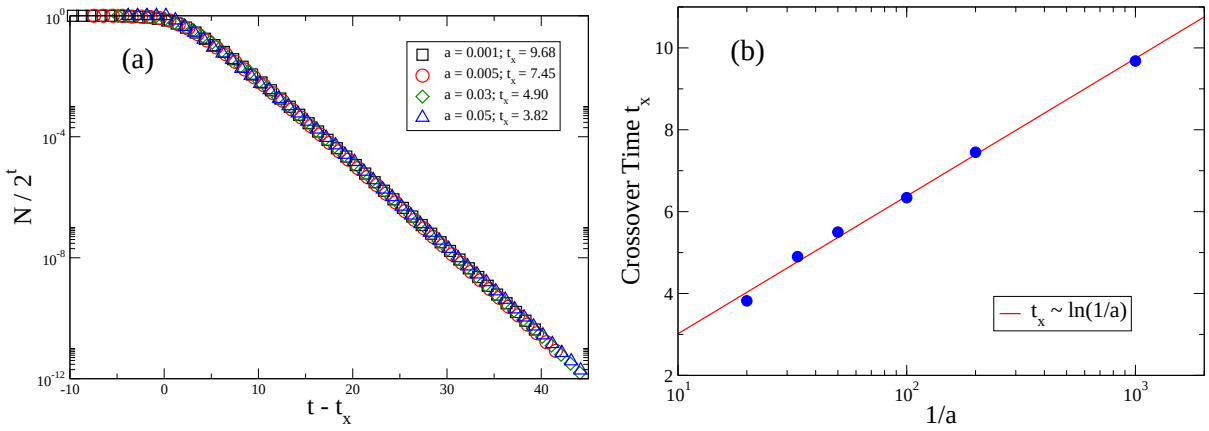

Figure 5.5: Finding of the crossover time t_x from simulation data for the model from the previous section. $N \equiv N_t$ is the number of the t-generation nodes. The dependencies $N/2^t$ versus $t - t_x$ for different values of a and $D = 1$ (a) collapse into a single curve for the crossover times $t_x(a)$ shown on panel (b). Fitting gives $t_x(a) = -0.34 + 1.46\ln(1/a)$, which is consistent with Eq. (6.9).

5.5 Spatial restriction

The majority of populations are restricted by geographical boundaries. It is natural to introduce a spatial restriction into the model. If our network is embedded in an infinite Euclidean space, the evolution is actually determined by the only parameter a (recall that we set the scale of displacements of children nodes from their parents to 1, i.e., this is the unit distance in this

problem). If the area of the space, in which the network is embedded, is restricted, then the model has an extra parameter, namely the linear size of the area, L. For simplicity, we assume that this area does not change with time.

Let the Euclidean coordinates $\mathbf{x}_i$ of all nodes in the network be within the area $-L < x_i < L$, $-L < y_i < L, \ldots, -L < D_i < L$. In our simulations we use periodical boundary conditions, but, in principle, this is not necessary. If L is finite, then one may expect that the size of the tree will finally approach some limiting value. The network has even a chance to extinct if at some moment all its nodes occur in one small area. It is well known that in, e.g., population biology, the smaller a population, the more susceptible it is to extinction by various causes [156].

Figure 5.6 demonstrates an example of the evolution of the network, for $a = 0.1$ and $L = 1$. The network rapidly enters the fluctuation regime, in which N_t fluctuates around a mean value $\overline{N}_{max}$, and extincts before 900 time steps. After that we again introduced a new root node and restarted the process.

The picture that we observe agrees with traditional views on extinction processes which show, as pointed by (D. M. Raup) "relatively long periods of stability alternating with short-lived extinction events" [157]. This kind of extinction may occur in random branching annihilating and other related processes studied in Refs. [158, 159]. In other models of biological evolution, extinction may require external factors or an environmental stress [160] or an internal mechanism, such as a mutation may lead to evolutionary events that, in some cases, cause extinction [161].

For the same model, we investigated the state of the branching process after $t_{\text{observation}} = 10^5$ generations (i.e., time steps) for various $L > 1$ and $a < 2$ (for $a > 2$, the network turns out to be a chain). In other words, we analyzed if the extinction time for given L and a is smaller than 10^5 generations or not. On the $(a/2, L/2)$ diagram, Fig. 5.7, the boundary separating the extinction and non-extinction regions is a monotonously growing curve $L(a)$. Note that with increasing observation time, the area of extinction should increase.

We suggest that if $t_{\text{observation}}$ tends to infinity, than for any finite L and non-zero a, the network may finally extinct, though it was impossible to verify this suggestion in our simulations. We investigated the probability of extinction for different samples of our model. Figure 5.8 shows the probability of extinction Π_{ext}, i.e., the fraction of samples in which the branching process

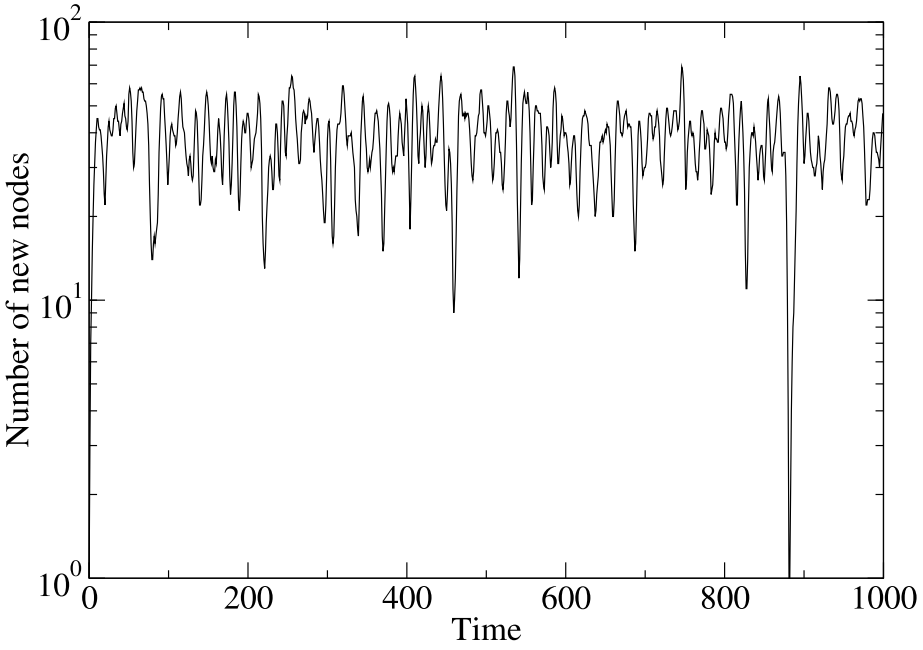

Figure 5.6: Evolution of the number of new nodes (number of nodes in the generation t) for a single realization of the network of Sec. 5.2 defined on a one-dimensional interval $-L < x < L$, where $L = 1$, $a = 0.1$.

stops before 10^{6th} generation of the process, for different L. One can see that this picture is a different representation of the phase diagram in the Fig. 5.7.

Figure 5.9 (a) shows the evolution of N_t for a few different values of a. The averaged N_t (averaged over times before extinction), $\overline{N}_{max}$, decreases with a as Fig. 5.9 (b) demonstrates. The simplest estimation gives $\overline{N}_{max}(a, L) \sim L/a$. Figure 5.9 (b) confirms that this estimate is reasonable, $\overline{N}_{max}$ is indeed inversely proportional to a, although these simulations indicate deviation from proportionality on L for sufficiently large L.

Since new nodes are born uniformly random in the interval $(-1, 1)$ from their parents, the case of $L = 1$ is special. In this situation, new nodes are actually born at any point of the ring with equal probability independently of the positions of their parents, and so a network structure here

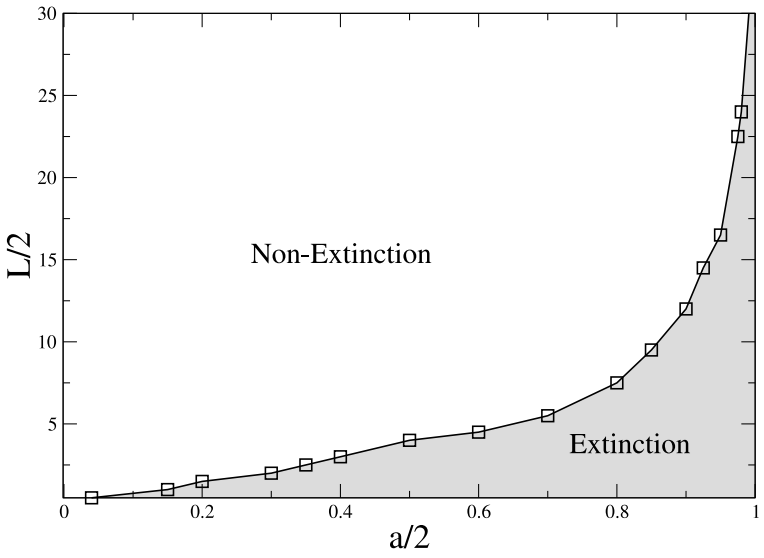

Figure 5.7: Extinction of the network embedded in the $(-L, L)$ during 10^5 generations. The extinction and non-extinction regions are present on the $L/2$ vs. $a/2$ diagram.

is not essential. One can consider this specific model with new nodes born at arbitrary points with equal probability at arbitrary L and find $\overline{N}_{max}(a, L) \approx 0.5L/a$. Figure 5.9 (b) for our original model shows a functionally faster growth of $\overline{N}_{max}(a, L)$ with L than this proportional dependence. Note finally that the deviations of fluctuating N_t from the mean values $\overline{N}_{max}$ in Fig. 5.9 (a) are of the order of $\sqrt{\overline{N}_{max}}$ for each L and a.

5.6 Node spatial distribution

In general, the nodes of the growing trees under consideration are non-uniformly distributed in the embedding spaces. Only if the embedding area is restricted, the spatial distribution finally becomes uniform, see Fig. 5.10 (a). For infinite embedding space, the evolution of the node spatial distributions is shown in Figs. 5.10 (b) and (c) for the trees in which the birth of new nodes is determined only by a previous generation and by all existing nodes, respectively. The distri-

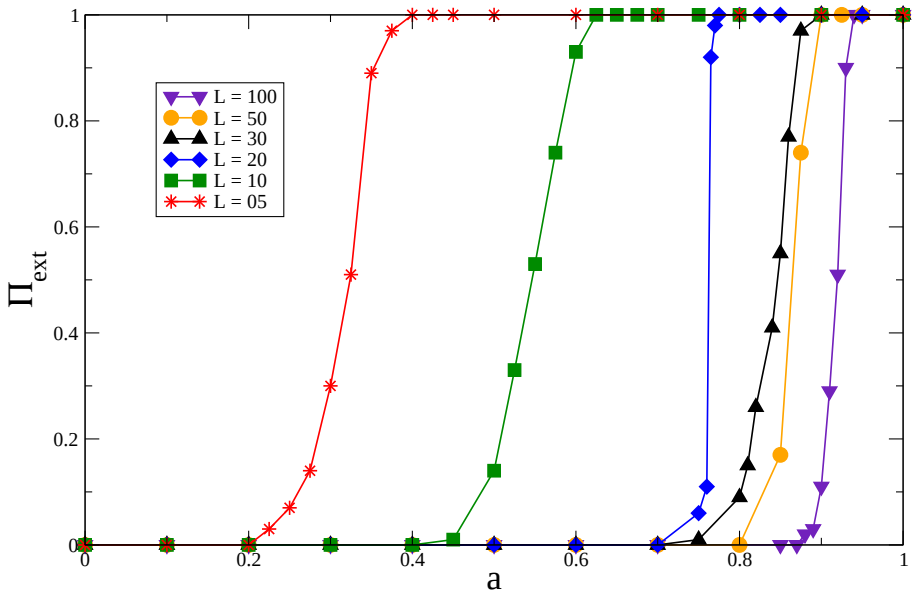

Figure 5.8: Probability of extinction versus a for 100 different samples and various values of L during 10^6 generations.

butions in three instances are shown. The triangular shape of these distributions in Fig. 5.10 (b) indicate that the spatial distribution of nodes of generation t has a symmetric step-function form with boarders moving away from the center (root) with constant velocity equal approximately to 0.5, so that their coordinates increase proportionally to t. The density of nodes between the borders is a constant equal approximately to $0.2/a$. In the second case, Fig. 5.10 (c), this expanding step-function form describes the evolution of the spatial distribution of all nodes in the tree. The border speed is approximately 0.6, and the density of nodes between borders is a constant equal approximately to $0.45/a$. (Note that, as it should be, this value is close to the number $\overline{N}_{max} \approx 0.4/a$ of new nodes found for this tree in Sec. 5.4, see Fig. 5.4.) These observations explain the high quality of simple estimates obtained in Sec. 4.2.

Finally, for the networks embedded in a restricted area, in which the birth of new nodes is determined by a previous generation, we also measured the distribution of the number of nodes in one generation. We observed that this distribution is centered at $\overline{N}_{max}$ and is close to the normal distribution.

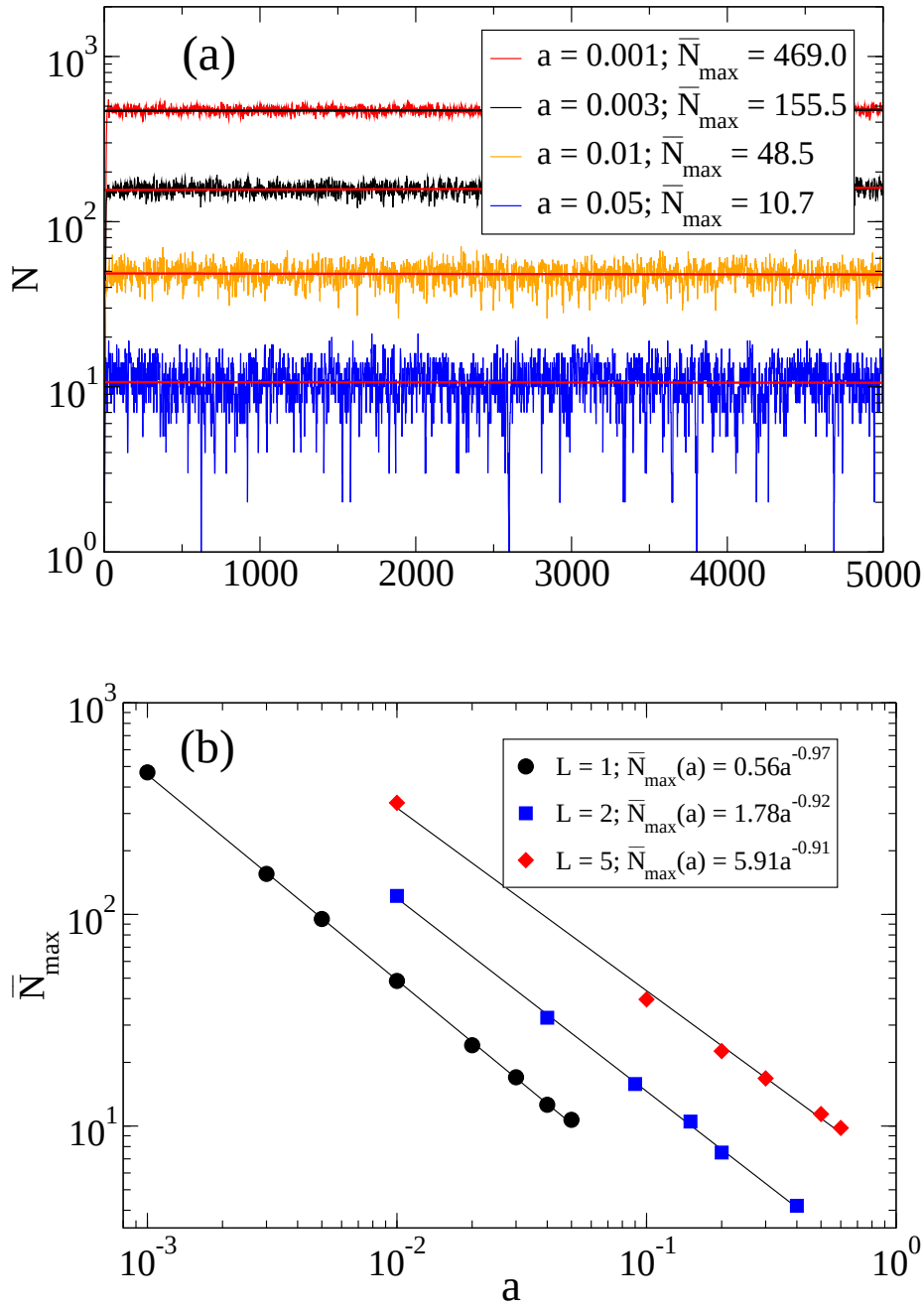

Figure 5.9: (a) Variation of the number of nodes N_t in the current generation with time, for different values of a. The network is embedded in the interval $-L \leq x \leq L$, where $L = 1$, and only the previous generation influences the branching process. The average value of N_t at large t, $\overline{N}_{max}$, is represented by a solid straight line. (b) $\overline{N}_{max}$ versus a for different L.

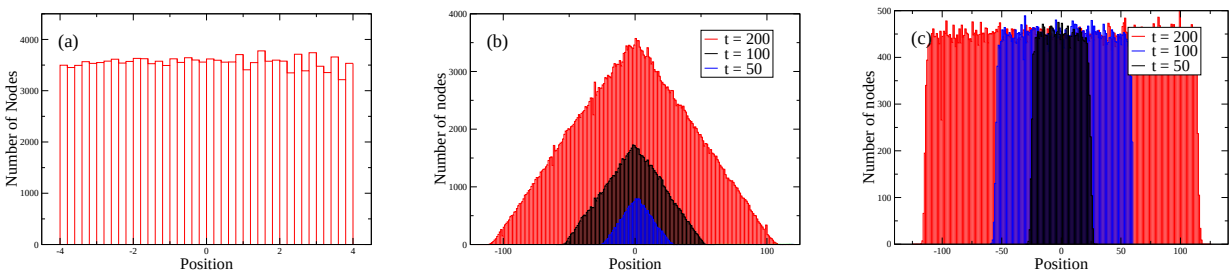

Figure 5.10: Distribution of nodes of the growing trees in space. (a) The node spatial distribution of the tree embedded in the interval $-1 \leq x \leq +1$ after 1000 time steps. The birth of new nodes in the tree is influenced only by a previous generation, $a = 0.01$. The vertical columns of the histogram show the numbers of nodes within bins of width 0.2. (b) The node spatial distributions for the tree embedded in a one-dimensional space at different instants of the growth. The birth of new nodes in the tree is influenced only by a previous generation, $a = 0.01$. The vertical columns of the histogram show the numbers of nodes within bins of width 1. (c) The same as for (b), but the birth of new nodes in the tree is influenced by all existing nodes, $a = 0.001$. Each of the results was obtained from a single realization.

5.7 Conclusions

In this Chapter we have studied an evolving tree network model with interacting nodes embedded into a Euclidean space, in which the branching process is determined by the relative position of nodes in space. The branching process starts from a single root node and, at each time step, each existent node in the network can branch to produce up to two new daughter nodes at the next generation. The new nodes are not allowed to emerge closer than a certain distance of a pre-existent node, defined by a parameter a, i.e., overcrowding suppresses the "fertility" of nodes. Thus, our model generates a competition between species or individuals (represented by the nodes) for resources, which can limit the density of nodes in the network and therefore the total population.

We have investigated two regimes of the evolution of these trees and crossover between them. In the initial stage of evolution, the network growth is exponentially fast, and the network is a small world. After some crossover time, this network becomes to grow much slower, and, in

this regime, the network has a large world architecture in terms of network science. We have demonstrated that the embedding of the network into a restricted area, which is natural for general evolution, set limits to growth and can result in complete extinction. The simplest models which we analyzed can only schematically describe real evolution processes in biology.

Chapter 6

Optimization in Networks

Numerous networks, such as transportation, distribution and delivery networks, have optimal design aimed at increasing efficiency, lowering costs, improving stability of function, etc. The optimal design fixes a network architecture, including clustering, degree distribution, hierarchicity, community structures and other structural metrics.

We have mentioned in Sec. 3.1.4, the preferential attachment mechanism in generating complex network architectures. An alternative mechanism generating complex networks is the optimization based process. In this Chapter we will consider (a) optimization of flows running on a network with a given architecture and (b) specific optimization driven network evolution, generating scale-free networks. In the first part, we discuss a transportation network model in which we optimize (minimize) some cost function, for the flux or current at each channel (link) of the network. In the second part of this Chapter we study a basic optimization based model generating networks with power-law degree distribution.

6.1 Flow optimization process

In this section we will consider a transportation network and specifically optimization of flows running on it. Networks that distribute goods, such as electricity, water, gas, telephone and data (Internet), or services as mail, railway, road are examples of transportation networks.

These networks are specifically designed for efficient transportation, minimizing transit times and costs.

All sort of transportation networks are faced with the same issue: traffic congestion among their channels. The traffic and its dynamics has been extensively considered by physicists [162, 163, 164, 165]. The study of optimization in transport networks is a topic of growing interest for theoretical researchers in the last years [166, 167, 168, 169, 170].

Let us consider a transportation network with N channels. The current j flows on the network channels (links, bonds), between the intersections in the network (nodes), satisfying the flow conservation rule at each intersection, taking into account that $j_i \geq 0$. The cost associated with transport through the channels is usually related to the time required to transport goods to their destination. Considering that, one can write the total transportation cost C as

$$C = \sum_i e_i \left(A j_i + B j_i^2 \right), \tag{6.1}$$

where e_i is a positive coefficient associated with each channel of the network and A and B are coefficients. Here we have neglected the higher order terms in the Eq. 6.1 and, for convenience, we considered $A = 1$ and $B = 1/2$.

When input current is small, apparently the optimal flow runs through a single chain of links with lower costs. When the input current increases, the optimal flow splits and the channels with higher costs become used. The resulting distribution of flows over links has the minimal value of C. One can determine the optimal current configuration among the channels by minimizing the cost function.

Considering the simplest case, a single node with an input current J is connected with two outgoing channels, j_1 and j_2, see Fig. 6.1. Here, we consider a local optimization, with independent nodes, and the current flows in just one direction. For this simple case, one can write the cost function as

$$C = e_1(j_1 + \frac{1}{2} j_1^2) + e_2(j_2 + \frac{1}{2} j_2^2). \tag{6.2}$$

By using the current flow conservation rule, $j_1 + j_2 = J$, one can minimizing the cost

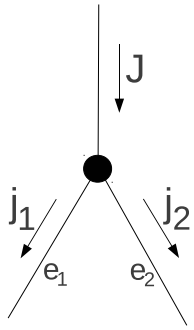

Figure 6.1: Distribution of currents within two outgoing channels of a node. The input current J is divided in two, j_1 and j_2, associated with costs e_1 and e_2.

function, $\frac{\partial C}{\partial j_i} = 0$. The current flow is

$$j_1 = \frac{e_2(J+1) - e_1}{e_1 + e_2} \tag{6.3}$$

and

$$j_2 = \frac{e_1(J+1) - e_2}{e_1 + e_2}. \tag{6.4}$$

These solutions allow negative current flows, which is an invalid situation, since we consider only positive currents. Thus, we can write the minimum input current I_c as $I_c = e_2/e_1 - 1$. One can see that for small input currents, $J < I_c$, only one outgoing channel will be used (that one with minimal cost). On the other hand, for $J > I_c$, both outgoing channels will be used, minimizing the cost function.

6.1.1 Simulations

Depending on the input flow, smaller or greater fraction of a network is used, so the quantity of interest on this problem is the number of used (with current running through them) channels. One can perform computer simulations on this transportation network and measure the number of empty channels B. We consider a directed network, with four channels (two incoming and two outgoing) for each node. In our simulations we considered three different situations: two-dimensional lattice, three-dimensional lattice and mean-field (infinite long-range connections)

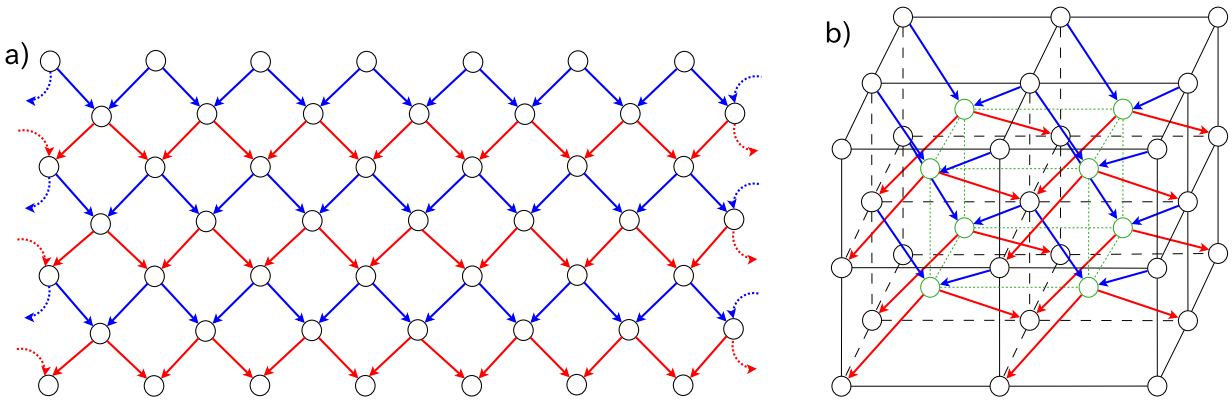

Figure 6.2: The "lattices" for the simulations in the flow optimization model. Each node is connected with four directed channels (links), two from the top and two from the bottom layer, both for the two- a) and three-dimensional b) simulations. We used in our simulations periodic boundary conditions.

---

case. For all the cases the current flows from top to bottom, see in Fig. 6.2. To perform our simulations for the mean-field case, we have considered the following: sites in the neighboring are connected uniformly at random, so each site is connected to two randomly chosen sites from the previous layer.

In our simulations we locally optimize the current flow. At each node, the current from two incoming channels are summed. This current J is then divided into the two outgoing currents j_1 and j_2, as shown in Fig. 6.1. If $J < I_c$, the current will flow through just one outgoing channel. On the other hand, if $J > I_c$, the current will flow through both outgoing channels. One time step consists in optimizing the current flow for the entire layer, so time corresponds to the N^{th} layer. Note that the total current $N \times \langle j \rangle$ is conserved, i.e., it is the same for every layer.

We start our simulations by injecting a total current $N \times \langle j \rangle$ at the first layer, when the costs of each channel are uniformly distributed in the interval $0 \leq e_i \leq 1$. The fraction of used channels $1 - B$ as function of time, i.e., the number of the current layer, is shown in Fig. 6.3, for the two dimensional simulations, using $N = 1000$, $\langle j \rangle = 10^{-4}$ and averaged over 100 samples.

In our simulations we have used two different initial configurations. In the first one we set the total input current equally divided between all channels. In the second one we put the total

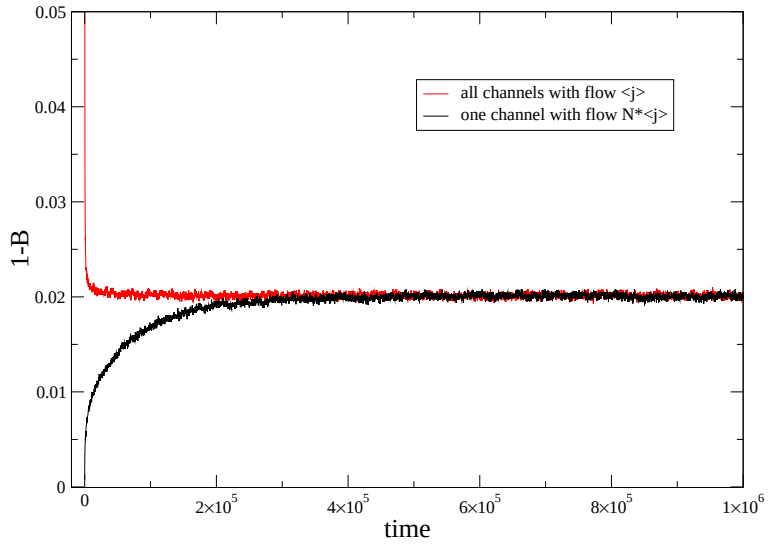

Figure 6.3: Two different initial configurations for the current flow in 2D. For the same amount of total current flow, in the first case (red line) the total current is equally divided for all channels. For the second case (black line), the total current is initially introduced in only one channel. For both cases the results are for 1000 channels, $\langle j \rangle = 10^{-4}$ and averaged over 100 samples. One can see that, despite having different relaxation times, both situations reach the same steady state with the same fraction of used channels.

current only in one channel. As one can see, the initial configuration is not important for the stationary regime, since after relaxation both configurations have the same result.

After the initial transient, the fraction of used channels $1 - B$ on the network stays constant. One can plot $(1 - B)$ at steady state as function of $\langle j \rangle$. Remarkably, this result does not depend on lattice (2D, 3D, or long-range connections), as one can see in Fig. 6.4. All the configurations show the same result, for a wide range of $\langle j \rangle$ in the small currents limit.

For the case of the high current limit, where $\langle j \rangle \to 1$, all channels on the network become used. In the small current limit, $\langle j \rangle \ll 1$, we observe that the fraction of used channels has the dependence $(1 - B) \sim 2j^{\frac{1}{2}}$.

From our simulations we obtained the distribution of the currents, $P(j)$. For large input currents, $\langle j \rangle \sim 1$, $P(j)$ follows a gaussian distribution, see in Fig. 6.5. The best fit with the gaussian distribution is obtained for the values of $\mu = 1.01$ and $\sigma^2 = 0.0872 \simeq \frac{1}{12}$. On the other

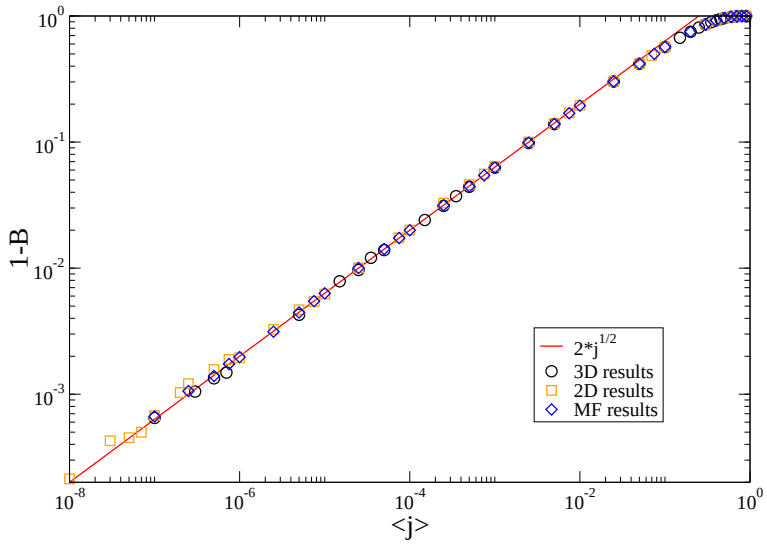

Figure 6.4: Fraction of used channels as function of $\langle j \rangle$ for mean-field, two- and three-dimensional results. One can see that 2D, 3D and mean-field networks provide the same stationary results, following the $2\langle j \rangle^{\frac{1}{2}}$ law in the limit of small current (red straight line).

---

hand, when we consider the limit of the small current flows, $\langle j \rangle \ll 1$, we found that the current distribution has an exponential dependence with $\langle j \rangle^{-\frac{1}{2}}$, as shown in Fig. 6.6.

Simulations were supported by a mean-field theory [171] which gives

$$1 - B = 2(\langle j \rangle)^{\frac{1}{2}}, \tag{6.5}$$

and

$$P(j) = 4e^{\frac{-2j}{\sqrt{\langle j \rangle}}} \tag{6.6}$$

for small $\langle j \rangle$, as it is shown in Fig 6.6. Our simulations demonstrate that these laws work also in 2D and 3D and for large $\langle j \rangle$, beyond the limits of the applicability of any MF theory.

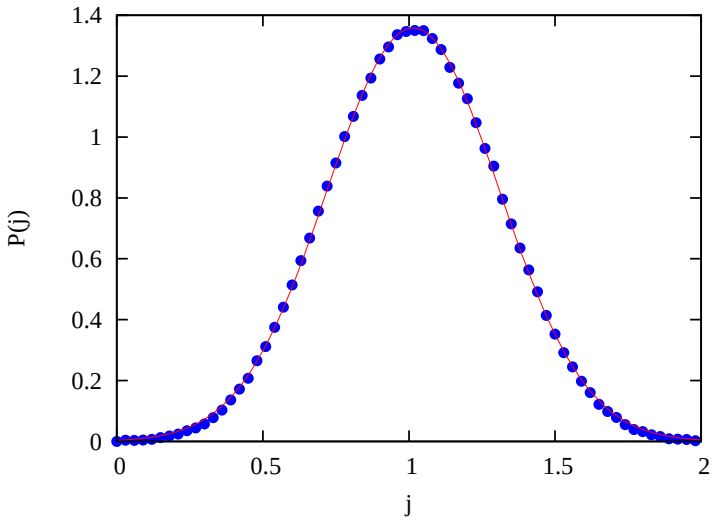

Figure 6.5: The current distribution for a channel in the limit of large input currents, in this case, $\langle j \rangle = 1$. The points are the result of our simulations and the red straight line is a gaussian fit with $\mu = 1.01$ (mean) and $\sigma^2 = 0.0872 \simeq \frac{1}{12}$ (variance).

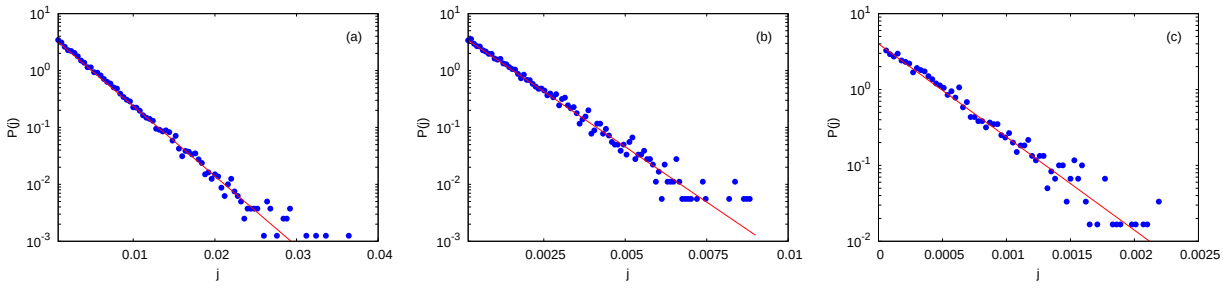

Figure 6.6: The current distribution in the limit of small current flows for different values of the $\langle j \rangle$. The straight line is the asymptotic value $P(j) = 4e^{\frac{-2j}{\sqrt{\langle j \rangle}}}$ and the points are the results from our simulations for $\langle j \rangle = 5 \times 10^{-5}$ (a), $\langle j \rangle = 5 \times 10^{-6}$ (b), and $\langle j \rangle = 5 \times 10^{-7}$ (c).

6.2 Emergence of Scale-free Architectures from Optimization Process

Numerous real-world networks have a power-law degree distribution. Preferential attachment is a standard mechanism producing power-laws in growing networks. Thanks to its simplicity this mechanism is realized in most of the models of scale-free network, but, unfortunately, it rather mimics scale-free networks and not explains them. Optimization based mechanisms have a much greater potential to explain the evolution of scale-free networks. We consider one of the simplest optimization based models generating power-law growing networks. Our model is defined as follows. At each time step, a new node is created and connected to *m* previous nodes in the network, which are selected to minimize the product $s^{\alpha}r$, where s is the birth time of the node and r is a random number drawn from some distribution. In the case of complete optimization, the networks grown from this model have a power law degree distribution with the exponent $\gamma = 1 + 1/\alpha$ for a wide range of the random number distributions. For partial optimization, including a finite fraction of nodes in a network, we observe an exponential degree distribution.

6.2.1 A simple model for optimization

A generic feature of numerous real-world networks, observed in many different real systems, as the Internet, scientific collaborations, WWW, protein and gene interaction networks, etc., is their scale-free organization. For all these examples, the number of nodes of degree q follows a power-law distribution, $P(q) \sim q^{-\gamma}$ with the exponent γ typically in the range $2 \leq \gamma \leq 3$. One of the most studied mechanisms producing such topology in networks is preferential attachment [11, 40, 172]. Optimization is an alternative mechanism explaining complex network architectures [92, 173, 174, 175, 176].

Although the idea of preferential attachment is simple and elegant, often the preferential attachment itself cannot be explained. Furthermore, standard preferential attachment models are often not realistic. It was shown recently that a refined optimization model, incorporating trade-off between popularity and similarity of nodes, can describe real-world network architectures

remarkably well [177]. In the present study we demonstrate that even within a very simple optimization based evolution model, essentially more simple than in Ref. [177], one can obtain a scale-free network having exponent γ in a wide range of values. This result is valid only for complete optimization, in which information about all nodes in the network is taken into account. For partial optimization, which accounts for a finite fraction of the network at each step, or even for a few randomly selected nodes, the degree distribution of a growing network has an exponential form.

6.2.2 Optimization based model for growing networks

Our model of a growing network is formulated as follows. At each time step we

- Create a new node which will be connected to *m* nodes in the network.
- Calculate for each node in the network the product $s^{\alpha}r_s$, where the label s is the birth time of the node, r_s is a random number taken from a distribution $p(r)$ and the exponent α is non-negative.
- Connect the new node to *m* nodes with minimal $s^{\alpha}r_s$.

In the case when $m \leq t$ we add only t connections for the new nodes. Here the random variable r actually plays the role of multiplicative noise.

Our simulations demonstrate that if the optimization process incorporates all existing nodes at each step (complete optimization), then the growing network exhibits a scale-free topology. In Fig. 6.7 we show the cumulative degree distribution of a network generated by the complete optimization model, in which α is set to 1 and $m = 1, 2, 5, 10$, after averaging over 100 samples. The random numbers are uniformly distributed and the probability density function is

$$p(r) = \begin{cases} 1 & \text{for } 0 < r < 1 \\ 0 & \text{otherwise.} \end{cases}$$

One can see that the exponent γ of the power-law node degree distribution in our model approaches 2 for any m. Introducing $\alpha < 1$ leads to $\gamma > 2$, as one can see in Fig 6.8, when arbitrary α are considered.

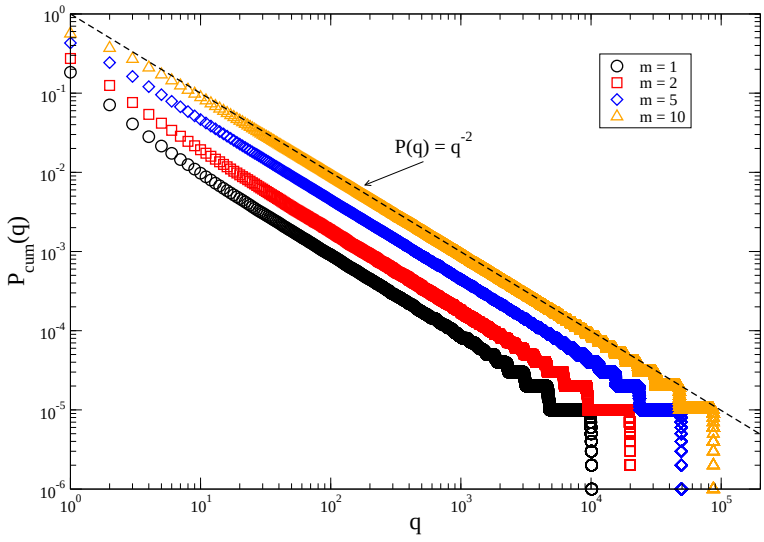

Figure 6.7: Cumulative degree distribution for a complete optimization process with various values of m, $\alpha = 1$, generating a network of 10^5 nodes, after averaging over 100 different samples. The distribution $p(r)$ is uniform, $p(0 < r < 1) = 1$ and $p(r > 1) = 0$. The resulting power law has exponent $\gamma = 2$ (dashed line).

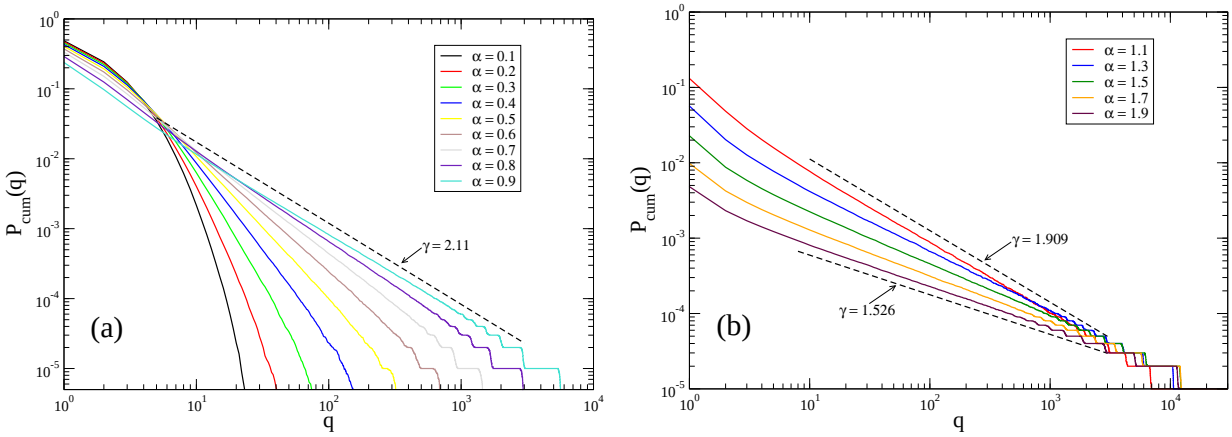

Figure 6.8: Cumulative degree distribution for a complete optimization and arbitrary α for a network of 10^5 nodes, after averaging over 50 different samples. Values of $\alpha < 1$ leads to $\gamma > 2$ (a), while $\alpha > 1$ leads to $\gamma < 2$ (b). The dashed lines correspond to exponents γ indicated in the picture.

6.2.3 Generation of power-law degree distributions

Let us derive the degree distribution for our model. Here we only present a simple estimate in the case of $\alpha = 1$, $m = 1$, and for a random number uniformly distributed from 0 to 1.

In the case of the uniform $p(r)$ defined above, the distribution of the product $\mathcal{P}(sr_s)$ is also uniform, namely

$$\mathcal{P}(\mathrm{sr}_s) = \begin{cases} \frac{1}{s} & \text{for } 0 < sr_s < s \\ 0 & \text{for } sr_s > 0. \end{cases} \tag{6.7}$$

Consequently, for small values of sr_s, we have $\mathcal{P}(sr_s) = 1/s$. This means that the probability that node s has the smallest product sr_s is proportional to $1/s$. Therefore, the mean degree $\langle q \rangle(s,t)$ of node s increases according to the following relation:

$$\frac{\partial \langle q \rangle(s,t)}{\partial t} \sim \frac{1}{s \ln t}, \tag{6.8}$$

where the factor $1/\ln t$ is due to normalization. So we have $\langle q \rangle(s) \sim 1/s$. In the continuum approximation which is applicable to scale-free networks, this corresponds to the degree distribution

$$P(q) = -\frac{1}{t}\Big(\frac{\partial q(s)}{\partial s}\Big)^{-1}\Big|_{s=s(q)\sim 1/q} \sim \frac{1}{q^2}, \tag{6.9}$$

where, as is usual in the continuous approximation, we set $\langle q \rangle(s,t) = q(s,t)$. This result agrees with our simulation, Fig. 6.7.

For arbitrary values of α, the distribution of the product $\mathcal{P}(s^\alpha r_s)$ in Eq. 6.7 is non-uniform and become $\mathcal{P}(s^\alpha r_s) \sim 1/s^\alpha$, which means that the probability that node s has the smallest product $s^\alpha r_s$ is now proportional to $1/s^\alpha$.

Thus, for arbitrary (but positive) α, we have the relation $\gamma = 1 + \frac{1}{\alpha}$. For the case when $0 < \alpha \leq 1$, assuming $p(r = 0) \neq 0$, one can obtain $\gamma \geq 2$ as indicated in Fig 6.8 (a). For $\alpha \geq 1$, the exponent $\gamma \leq 2$ as one can see in our results in Fig 6.8 (b) and the degree distribution is non-stationary.

For non-stationary degree distribution the initial and end parts of the distribution change in time. One can estimate how the number of nodes with only one connection, q_{min} evolves in time.

From the condition

$$\langle q \rangle = 1 = \int_1^t c(t) q q^{-\gamma} dq, \tag{6.10}$$

we have

$$c(t) \sim (2-\gamma) t^{(\gamma-2)}. \tag{6.11}$$

Due to normalization condition, $1 = \int_{q_{min(t)}}^{t} c(t) q^{-\gamma} dq$, one can estimate q_{min}, which leads to

$$q_{min} \sim t^{-(\frac{2-\gamma}{\gamma-1})}. \tag{6.12}$$

The end part of the distribution has a rapid decay, a cutoff. The cutoff has dependence with γ and t and we estimated from our data,

$$q_{cut}(\gamma, t) \sim C(\gamma) t \tag{6.13}$$

This constant, obtained from our simulations, is $C(\gamma) = 2.859 - 1.421\gamma$.

In the work [178], attachment to a node of the maximal degree selected from a random sample of n nodes was studied. The degree distributions of the resulting networks was found to be rapidly decaying in the range of degrees $q > n$. Inspired by these ideas we modify our model and consider a partial optimization process, in which at each step, the optimal node for attachment is selected from a finite fraction of the existing networks, namely from a uniformly randomly chosen fraction f of all nodes.

In Fig. 6.9 we show a linear-log plot of the cumulative degree distribution for the result of the partial optimization process, in which $f = 0.01$. One can see that for various values of m, the degree distribution decays exponentially. In Fig. 6.10 we show the cumulative degree distribution obtained for various values of f, where $f = 1$ corresponds to complete optimization resulting in the scale-free network having $\gamma = 2$, while $f = 0$ actually corresponds to the standard random recursive tree. Note that if at each time step, the optimization includes only a finite number of nodes, we arrive at the $f = 0$ case.

The well-known result for the random recursive graph [40] has an exponentially decaying

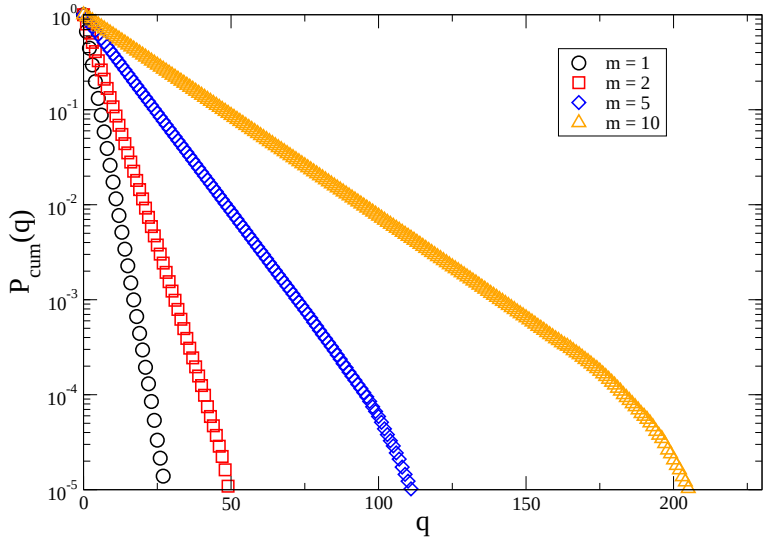

Figure 6.9: Linear-log plot of the cumulative degree distribution of the network of 10^5 nodes generated by a partial optimization process, $f = 0.01$, $m = 1, 2, 5, 10$, $\alpha = 1$.

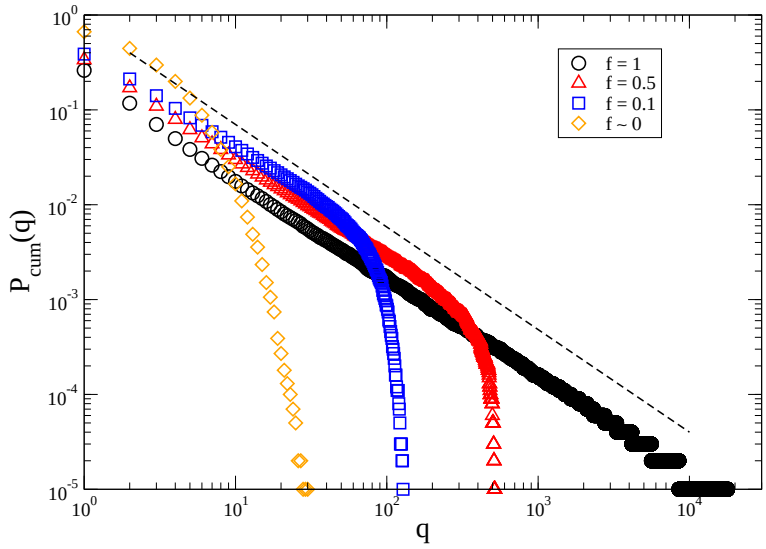

Figure 6.10: Log-log plot of the cumulative degree distribution of the network of 10^5 nodes generated by a partial optimization process, $f = 0, 0.1, 0.5, 1$, $m = 1$, $\alpha = 1$.

degree distribution in the form

$$P(q) = \frac{1}{m} e^{1-\frac{q}{m}}. \tag{6.14}$$

On the other hand, we find that considering the optimization process for a finite fraction of the network, $0 < f < 1$, produces an exponential cutoff of the power-law degree distribution as one can see in the Fig. 6.10.

6.3 Chapter conclusions

In the first part of this Chapter we discussed a flow optimization model, in which the current flows through a random network, actually a lattice, in which the randomness is due to random coefficients of a cost funcion defined at lattice bonds. We obtained the exponential current distribution for small and large currents limit, as well as the power-law dependence of the fraction of used channels with the mean input current $\langle j \rangle$. We found that if $\langle j \rangle$ is small, all the current flows through a tiny fraction of the channels, and that MF describes even 2D and 3D cases.

In the second part of this Chapter, we introduced an optmization based model for growing networks. We considered, maybe, the simplest example of the optimization driven evolution of complex networks. The resulting networks are scale-free if at each step, the optimization involves all existing nodes in a network. If the optimization is partial, i.e., it includes only a finite fraction of a network or a few nodes, the result is an exponential cut-off of a power-law degree distribution or even an exponential degree distribution. We suggest that the optimization driven evolution is a widespread mechanism generating complex networks architectures.

Chapter 7

Conclusions and Further Work

In this thesis we studied the interaction of agents on complex networks and their basic properties by means of computational simulations and statistical physics techniques. In the first Chapter we presented a brief historical introduction to complex network, followed by description of the basic properties of networks, in Chapter 2.

Chapter 3 provides the background and the related work of complex networks necessary to our investigation. Due to a large volume of work in this area, we restricted this Chapter to a few selected topics which are directly related to this present thesis.

In Chapter 4 we have studied an Ising spin model of opinions dynamics, namely a generalization of the Sznajd model. In our model, we included reputation, a mechanism that limits the capacity of persuasion of the agents. The reputation is a time-dependent score for each agent, which varies due to the dynamics of the model. The agents start with a random distribution of reputation values, and during the time evolution, the reputation of each agent may increase or decrease according to agent's capacity of persuasion. We studied in this Chapter two different situations: (i) the case where the reputations increase due to each persuaded individual, and (ii) the case where the reputations increase for persuasion and decrease if a group of agents fail to convince one of its neighbors. For both cases we observed a log-normal-like distribution of the relaxation times, i.e., the time needed to find all the agents at the end having the same opinion, but the relaxation times are greater for the second case. We have shown that the average relax-

ation times grow with the linear dimension of the lattice as $\tau \sim L^{5/2}$. The system undergoes a phase transition, identified by measurements of the fraction f of samples which show all spins up when the initial density of up spins d is varied. The model represents realistic situations of democracy, where our results show that the introduction of the reputation avoids full consensus even for large initial fraction of up spins.

In Chapter 5 we studied an evolving tree network model with interacting nodes embedded into a Euclidean space. In our model, the network grows through a branching process starting from a single root node and, at each time step, each existent node in the network can branch to produce up to two new daughter nodes at future generation. The new nodes are not allowed to grow closer than at distance a from a pre-existent node. Thus, our model generates a competition between species or individuals for resources, which can limit the density of nodes in the network and therefore the total population. Our model can demonstrate a transition from an explosive to gradual evolution accompanied by a dramatic change of the network structure. We have studied the time evolution of the network, which evolves in two different regimes. The initial regime is characterized by an exponentially fast grow, and the network is a small-world. After some crossover time t_x, this network becomes to grow much slowly, and, in this regime, the network has a large-world architecture. For the crossover time we obtained $t_x \sim \ln(1/a)$. We also embedded the network into a restricted area, as is natural for general evolution. This situation sets limits to growth and can result, for some cases, in complete extinction. Our results suggest that the dependency of the maximum number of nodes is $\overline{\mathrm{N}}_{max}(L, a) \sim L \cdot a^{-1}$, for all L.

Even these null models however are sufficient to demonstrate the transition from an explosive to gradual evolution accompanied by a dramatic change of the network structure. We believe that the significance of the network representation of evolutionary processes, e.g., the so-called "tree of life", is greater than simply being a convenient visualization. We suggest that through exploration of the structural organization of the empirical trees of life and their analogies on different stages of evolution will essentially improve our understanding of evolutionary processes.

In the first part of the Chapter 6 we studied a general transportation network in which current flows though the network's channels, with randomness introduced by the random cost function in the channels. The resulting distribution of currents optimizes the total cost function. We obtained

the current distribution for small and large currents limit, $P(j) = 4e^{\frac{-2j}{\sqrt{\langle j \rangle}}}$, and the fraction of empty channels as function of the mean input current, $1 - B = 2(\langle j \rangle)^{\frac{1}{2}}$.

Finally, in the last part of the Chapter 6 we studied a simple optimization based model for growing networks. It is well known that a basic characteristic present in many complex networks and observed in different real systems are their scale-free topology. One of the most studied mechanisms to produce power-law degree distribution is the preferential attachment mechanism. However, some models based on optimization process have a greater potential to explain the evolution of scale-free networks. In this Chapter we showed that networks grown by our simple model are scale-free networks (with $\gamma \geq 2$) if at each step, the optimization process involves all existing nodes in a network, corresponding to complete optimization. On the other hand, if the optimization process is partial, i.e., it includes only a finite fraction of a network or a few nodes, the result is an exponential cut-off of a power-law degree distribution or even an exponential degree distribution. One can see that the optimization driven evolution is a natural source of complex networks architectures.

Exploring some of the ideas presented in this PhD thesis, we foresee a number of generalizations and issues for future work of our resuls and models:

- In the social opinion model studied in Chapter 4, we can introduce inflexible contrarians, a fraction of agents which hold a strong opinion, that is they never change their opinion while they can influence others.

- Regarding the social opinion model, we can also study the effect of the authoritarianism, where an agent or a group of agents are "forced" to follow some predetermined agent's opinion. In this case we may have the opposite situation to the reputation, in which the capacity of persuasion of agents is not limited.

- We can study the introduction of reputation in others opinion models, namely the Voter model and the Majority rule model.

- In the evolving trees whose evolution is influenced by interaction among some of existing nodes which we studied in Chapter 5, we can introduce more than one species in the model

and study the model embedded into a non-Euclidean space.

- In evolving networks that we studied in Chapter 6, we can cite as an extention of our work the determination of the time of the expoential cutoff of the power-law degree distribution.

List of Publications

List of publications related to this thesis

In the following are listed the articles, communications and presentations related to this thesis.

- Journal Articles

  – N. Crokidakis and F. L. Forgerini, *"Consequence of reputation in the Sznajd consensus model"*, Physics Letters A **374**, 3380 (2010).
  Doi:10.1016/j.physleta.2010.06.036.

  – F. L. Forgerini, N. Crokidakis, S. N. Dorogovtsev, J. F. F. Mendes, *"Branching process for network growth with geometric restrictions"*, Int. J. Complex Systems in Science, vol. **1(2)** 141 (2011).
  http://www.ij-css.org/volume-01_02/ijcss01_02-141.pdf

  – N. Crokidakis and F. L. Forgerini, *"Competition of reputations in the 2D Sznajd model: spontaneous emergence of democratic states"*, Brazilian Journal of Physics **42**, 125 (2012).
  Doi:10.1007/s13538-011-0055-9

  – F. L. Forgerini, N. Crokidakis, S. N. Dorogovtsev, J. F. F. Mendes, *"Evolution of spatially embedded branching trees with interacting nodes"*, submitted to Physical Review E.
  Arxiv:1110.6108

  – F. L. Forgerini, S. N. Dorogovtsev and J. F. F. Mendes, *"Emergence of scale-free networks from optimization"*, accepted for publication in Journal of Physics: Conference Se-

ries.

- Oral Communications

  – F. L. Forgerini and N. Crokidakis, *Competition of reputations in the 2D Sznajd model: emergence and lack of consensus*, MAP/fis Conference, Porto - Portugal (2011).

  – F. L. Forgerini, S. N. Dorogovtsev and J. F. Mendes, *Emergence of scale-free networks from optimization*, International Conference on Mathematical Modeling in Physical Sciences, Budapest - Hungary (2012).

- Poster Communications

  – N. Crokidakis and F. L. Forgerini, *Efeitos de reputação na dinâmica de opiniões do modelo de Sznajd*, II Escola e Conferência em Modelagem Computacional, Volta Redonda/RJ - Brazil (2010).

  – F. L. Forgerini, N. Crokidakis, S. N. Dorogovtsev, J. F. F. Mendes, *Branching process for network growth with geometric restrictions*, International Conference Net-Works, Madrid - Spain (2011).

  – N. Crokidakis and F. L. Forgerini. *Consequence of reputation in the Sznajd sociophysics model: spontaneous emergence of democratic states*, In Encontro de Física, Foz do Iguaçu - Brazil (2011).

  – F. L. Forgerini and N. Crokidakis, *Competition among reputations in the 2D Sznajd model: emerge and lack of consensus*, i3N annual meeting, Quiaios - Portugal (2012).

Publications not related to this thesis

In the following are listed the articles and poster communications not related to this thesis.

- Journal Articles

  – F. L. Forgerini and W. Figueiredo, *"Thin-film growth by random deposition of linear polymers on a square lattice"*, Phys. Rev. E **81**, 051603 (2010). Doi:10.1103/PhysRevE.81.051603.

  – F. L. Forgerini and W. Figueiredo, *"Thin-film growth by random deposition of rod-like particles on a square lattice"*, Physica Status Solidi (c) **8**, N^o 11-12 3119 (2011). Doi:10.1002/pssc.201000692.

- Poster Communications

  – F. L. Forgerini and W. Figueiredo, *Thin film growth by random deposition of rod-like particles on a square lattice*, In 10th International Workshop on Non Cristalline Solids - IWNCS, Barcelona - Spain (2010).

Bibliography

[1] S. N. Dorogovtsev, *Lectures on Complex Networks.* Oxford University Press, Oxford (2010).

[2] P. Erdős and A. Rényi, On random graphs, *Publ. Math. Debrecen* **6**, 290 (1959).

[3] P. Erdős and A. Rényi, On the evolution of random graphs, *Publ. Math. Inst. Hung. Acad. Sci.* **5**, 17 (1960).

[4] S. Milgram, The small world problem, *Psychology Today* **2**, 60–67 (1967).

[5] M. E. J. Newman, A.-L. Barabási, and D. J. Watts, *The Structure and Dynamics of Networks*, Princeton University Press, Princeton (2006).

[6] S. N. Dorogovtsev and J. F. F. Mendes, *Evolution of Networks: From Biological Nets to the Internet and WWW*, Clarendon Press, Oxford (2002).

[7] D. J. de S. Price, Networks of Scientific Papers, *Science* **149**, 510 (1965).

[8] B. Bollobás, A probabilistic proof of an asymptotic formula for the number of labelled random graphs, *Eur. J. Comb.* **1**, 311 (1980).

[9] R. J. Baxter, *Exactly solved models in statistical mechanics*, Academic Press, London (1982).

[10] D. J. Watts and S. H. Strogatz, Collective dynamics of 'small-world' networks, *Nature* **393**, 440 (1998).

[11] A.-L. Barabási and R. Albert, Emergence of Scaling in Random Networks, *Science* **286**, 509 (1999).

[12] S. N. Dorogovtsev, J. F. F. Mendes, and A. N. Samukhin. Structure of growing networks with preferential linking. *Phys. Rev. Lett.* **85**, 4633 (2000).

[13] M. E. J. Newman, The Structure and Function of Complex Networks. *Proc. Natl. Acad. Sci. USA* **45**, 167–256 (2001).

[14] S. N. Dorogovtsev and J. F. F. Mendes, Evolution of networks, *Advances in Physics* **51**, 1079−1187 (2002).

[15] S. N. Dorogovtsev, A. V. Goltsev, and J. F. F. Mendes, Critical phenomena in complex networks, *Rev. Mod. Phys.* **80**, 1275−1335 (2008).

[16] R. Pastor-Satorras and A. Vespignani, Epidemic spreading in scale-free networks, *Phys. Rev. Lett.* **86**, 3200 (2001).

[17] S. N. Dorogovtsev, A. V. Goltsev, and J. F. F. Mendes, k-core organization of complex networks, *Phys. Rev. Lett.* **96**, 040601 (2006).

[18] A. V. Goltsev, S. N. Dorogovtsev, and J. F. F. Mendes, k-core (bootstrap) percolation on complex networks: Critical phenomena and nonlocal effects, *Phys. Rev. E,* **73**, 056101 (2006).

[19] M. E. J. Newman, Random graphs with clustering, *Phys. Rev. Lett.* **103**, 058701 (2009).

[20] M. E. J. Newman, *Networks: an introduction*, Oxford University Press, Oxford (2010).

[21] P. S. Bearman, J. Moody, and K. Stovel, Chains of Affection: The Structure of Adolescent Romantic and Sexual Networks, *American Journal of Sociology* **110**, 44 (2004).

[22] E. Spertus, M. Sahami, and O. Buyukkokten, Evaluating Similarity Measures: A Large-Scale Study in the Orkut Social Network, *Proceedings of the Eleventh ACM SIGKDD International Conference on Knowledge Discovery in Data Mining*, (2005).

[23] K. Lewis, J. Kaufman, M. Gonzalez, A. Wimmer, and N. Christakis, Tastes, ties, and time: a new social network dataset using Facebook.com, *Social Networks* **30**, 330 (2008).

[24] D. M. Boyd and N. B. Ellison, Social Network Sites: Definition, History, and Scholarship, *Journal of Computer-Mediated Communication* **13**, 210 (2007).

[25] S. K. Thompson and O. Frank, Model-based estimation with link-tracing sampling designs, *Survey Methodology* **26**, 87 (2000).

[26] E. Eisenberg and E. Y. Levanon, Preferential Attachment in the Protein Network Evolution, *Phys. Rev. Lett.* **91**, 138701 (2003).

[27] R. J. Allen, P. B. Warren, and P. Rein ten Wolde, Sampling Rare Switching Events in Biochemical Networks, *Phys. Rev. Lett.* **94**, 018104 (2005).

[28] A. M. Walczaka, A. Muglerb, and C. H. Wigginsc, A stochastic spectral analysis of transcriptional regulatory cascades, *Proc. Nat. Acad. Sci.* **106**, 6529 (2009).

[29] A.-L. Barabási, N. Gulbahce, and J. Loscalzo, Network medicine: a network-based approach to human disease, *Nature Reviews Genetics* **12**, 56 (2011).

[30] M. Droz and A. Pękalski, Coexistence in a predator-prey system, *Phys. Rev. E* **63**, 051909 (2001).

[31] J. Camacho, R. Guimerà, and L. A. N. Amaral, Robust Patterns in Food Web Structure, *Phys. Rev. Lett.* **88**, 228102 (2002).

[32] R. J. Williams, E. L. Berlow, J. A. Dunne, A.-L. Barabási, and N. D. Martinez, Two degrees of separation in complex food webs, *Proc. Nat. Acad. Sci.* **99**, 12913 (2002).

[33] J. M. Montoya and R. V. Solé, Small world patterns in food webs, *J. Theor. Biol.* **214**, 405 (2002).

[34] I. Yoon, R. J. Williams, E. Levine, S. Yoon, J.A. Dunne, and N. D. Martinez, Webs on the Web (WoW): 3D visualization of ecological networks on the WWW for collaborative

research and education, *Proceedings of the IS&T/SPIE Symposium on Electronic Imaging, Visualization and Data Analysis* **124**, (2004).

[35] J. G. White, E. Southgate, J. N. Thompson, and S. Brenner, The structure of the nervous system of the nematode *C. elegans*, *Phil. Trans. R. Soc. London* **314**, 1340 (1986).

[36] J. G. Oliveira, *Study of dynamical properties of complex networks*, PhD Thesis, University of Aveiro (2008).

[37] L. R. Varshney, B. L. Chen, E. Paniagua, D. H. Hall, D. B. Chklovskii. Structural Properties of the Caenorhabditis elegans Neuronal Network, *PLoS Comput. Biol.*, **7**, 2 (2011).

[38] V. M. Eguíluz, D. R. Chialvo, G. A. Cecchi, M. Baliki, and A. V. Apkarian, Scale-Free Brain Functional Networks, *Phys. Rev. Lett.* **94**, 018102 (2005).

[39] R. Ferrer i Cancho and R. V. Solé. The small-world of human language. *Proc. Royal Soc. London B* **268**, 2261 (2001).

[40] R. Albert and A.-L. Barabási, Statistical mechanics of complex networks, *Rev.Mod. Phys.* **74**, 47 (2002).

[41] D. Achlioptas, A. Clauset, D. Kempe, C. Moore, On the bias of traceroute sampling: Or, power-law degree distributions in regular graphs, *J. ACM* **56**, 21:1–21:28 (2009).

[42] M. Faloutsos, P. Faloutsos, and C. Faloutsos, On power-law relationships of the Internet topology, *SIGCOMM Comput. Commun. Rev.* **29**, 4 251–262 (1999).

[43] R. Pastor-Satorras, A. Vázquez, and A. Vespignani, Dynamical and Correlation Properties of the Internet, *Phys. Rev. Lett.* **87**, 258701 (2001).

[44] R. Cohen, K. Erez, D. ben-Avraham, and S. Havlin, Breakdown of the Internet under Intentional Attack, *Phys. Rev. Lett.* **86**, 3682 (2001).

[45] S. N. Dorogovtsev and J. F. F. Mendes, Comment on “Breakdown of the Internet under Intentional Attack”, *Phys. Rev. Lett.* **87**, 219801 (2001).

[46] A. E. Motter, Cascade Control and Defense in Complex Networks, *Phys. Rev. Lett.* **93**, 098701 (2004).

[47] L. A. N. Amaral, A. Scala, M. Barthélémy, and H. E. Stanley, Classes of small-world networks, *Proc. Nat. Acad. Sci.* 97, 11149 (2000).

[48] I. Dobson, B. A. Carreras, V. E. Lynch, and D. E. Newman, Complex systems analysis of series of blackouts: Cascading failure, critical points, and self-organization, CHAOS **7**, 026103 (2007).

[49] Qi Xuan, F. Du, and Tie-Jun Wu, Empirical analysis of Internet telephone network: From user ID to phone, *CHAOS* **19**, 023101 (2009).

[50] P. Sen, S. Dasgupta, A. Chatterjee, P. A. Sreeram, G. Mukherjee, and S. S. Manna, Small-world properties of the Indian railway network, textitPhys. Rev. E **67**, 036106, (2009).

[51] P. S. Dodds and D. H. Rothman, Geometry of river networks. I, Scaling, fluctuations, and deviations, *Phys. Rev. E* **63**, 016115, (2009).

[52] P. S. Dodds and D. H. Rothman, Geometry of river networks. II. Distributions of component size and number, *Phys. Rev. E* **63**, 016116, (2009).

[53] P. S. Dodds and D. H. Rothman, Geometry of river networks. III. Characterization of component connectivity, *Phys. Rev. E* **63**, 016117, (2009).

[54] R. Carvalho, L. Buzna, F. Bono, E. Gutiérrez, W. Just, and D. Arrowsmith, Robustness of trans-European gas networks, *Phys. Rev. E* **80**, 016106 (2009).

[55] V. Kalapala, V. Sanwalani, A. Clauset, and C. Moore, Scale invariance in road networks, *Phys. Rev. E* **73**, 026130 (2006)

[56] R. Cohen, K. Erez, D. ben-Avraham, and Shlomo Havlin, Resilience of the Internet to Random Breakdowns, *Phys. Rev. Lett.* **85**, 4626 (2000).

[57] S. Boccaletti, V. Latora, Y. Moreno, M. Chavez, D.-U. Hwang, Complex networks: Structure and dynamics, *Physics Reports* **424**, 175 (2006).

[58] W.B. Deng, W. Li, X. Cai, and Q. A. Wang, The exponential degree distribution in complex networks: Non-equilibrium network theory, numerical simulation and empirical data, *Physica A* **390**, 1481 (2011).

[59] R. Guimera, L. Danon, A. Diaz-Guilera, F. Giralt, and A. Arenas, Self-similar community structure in a network of human interactions, *Phys. Rev. E* **68**, 065103 (2003).

[60] R. Albert, I. Albert, and G.L. Nakarado, Structural vulnerability of the North American power grid, *Phys. Rev. E* **69**, 025103 (2004).

[61] M. E. J. Newman, Power laws, Pareto distributions and Zipf's law, *Contemporary Physics* **46**, 323 (2005).

[62] S. N. Dorogovtsev, A. L. Ferreira, A. V. Goltsev, and J. F. F. Mendes, Zero Pearson coefficient for strongly correlated growing trees, *Phys. Rev. E* **81**, 031135 (2010).

[63] L. da F. Costa, F. A. Rodrigues, G. Travieso, and P. R. Villas Boas. Characterization of complex networks: A survey of measurements. *Advances in Physics*, **56** 167, (2007).

[64] P. A. de Castro, *Rede Complexa e Criticalidade Auto-Organizada: Modelos e Aplicações*, PhD Thesis, University of São Paulo (2007).

[65] M. E. J. Newman, Assortative mixing in networks, *Phys. Rev. Lett.* **89**, 208701 (2002).

[66] R. Albert, H. Jeong, and A.-L. Barabási, Error and attack tolerance of complex networks. *Nature* **406**, 378 (2000).

[67] G. J. Baxter, S. N. Dorogovtsev, A. V. Goltsev, and J. F. F. Mendes, Bootstrap Percolation on Complex Networks, *Phys. Rev. E* **82**, 011103 (2010).

[68] A. Rapoport, Spread of information through a population with socio-structural bias I: Assumption of transitivity, *Bul. of Math. Bioph.* **15**, 523 (1953).

[69] P. S. Dodds, R. Muhamad, and D. J. Watts, An experimental study of search in global social networks, *Science* **301**, 827 (2003).

[70] R. Cohen and S. Havlin, Scale-Free Networks Are Ultrasmall, *Phys. Rev. Lett.* **90**, 058701 (2003).

[71] S.N. Dorogovtsev, J. F. F. Mendes, and A. N. Samukhin, Metric structure of random networks, *Nucl. Phys. B* **653**, 307 (2003).

[72] L. C. Freeman, A set of measures of centrality based on betweenness, *Sociometry* **40**, 35 (1977).

[73] S. Brin and L. Page, The anatomy of a large-scalehypertextual Web searchengine, *Computer Networks and ISDN Systems* **30**, 107 (1988).

[74] P. Erdős and A. Rényi, On the strenght of connectedness of a random graph, *Acta Mathematica Scientia Hungary*, **12**, 261 (1961).

[75] E. N. Gilbert, Random graphs, *Ann. Math. Statist.* **30**, 1141 (1959).

[76] E. A. Bender and E. R. Canfield, The asymptotic number of labelled graphs with a given degree sequence, *J. Combinatorial Teor. A*, **24**, 296 (1978).

[77] R. Albert and A.-L. Barabási, Topology of evolving networks: Local events and universality, *Phys. Rev. Lett.* **85**, 5234 (2000).

[78] S. N. Dorogovtsev and J. F. F. Mendes, Scaling behaviour of developing and decaying networks *Europhys. Lett.* **52**, 33 (2000).

[79] P. L. Krapivsky and S. Redner, A statistical physics perspective on Web growth, *Comput. Netw.* **39**, 261 (2002).

[80] H. Jeong, Z. Néda, and A.-L. Barabási, Measuring preferential attachment in evolving networks, *Europhys. Lett.* **61**, 567 (2003).

[81] A. G. McKendrick, Applications of mathematics to medical problems, *Proc. Edinburgh Math. Soc.* **44**, 98 (1926).

[82] W. O. Kermack and A. G. McKendrick, Contributions to the mathematical theory of epidemics, part 1, *Proc. Roy. Soc. London Ser. A* **115**, 700 (1927).

[83] H. W. Hethcote, The Mathematics of Infectious Diseases, *SIAM Review* **42**, 599 (2000).

[84] R. Pastor-Satorras and A. Vespignani. *Handbook of Graphs and Networks: From the Genome to the Internet.* Wiley-VCH, Berlin (2003).

[85] M. E. J. Newman, Spread of epidemic disease on networks, *Phys. Rev. E* **66**, 016128 (2002).

[86] M. E. J. Newman, I. Jensen, and R. M. Ziff, Percolation and epidemics in a two-dimensional small world. *Phys. Rev. E* **65**, 021904 (2002).

[87] T. Petermann, and P. De Los Rios, Role of clustering and gridlike ordering in epidemic spreading. *Phys. Rev. E* **69**, 066116 (2004).

[88] M. A. Serrano, and M. Boguñá, Percolation and Epidemic Thresholds in Clustered Networks. *Phys. Rev. Lett.* **97**, 088701 (2006).

[89] Z. Dezső and A.-L. Barabási, Halting viruses in scale-free networks, *Phys. Rev. E* **65**, 055103 (2002).

[90] R. Cohen, Shlomo Havlin, and D. ben-Avraham, Efficient Immunization Strategies for Computer Networks and Populations, *Phys. Rev. Lett.* **91**, 247901 (2003).

[91] A. Clauset, and M. E. J. Newman, and C. Moore, Finding community structure in very large networks, *Phys. Rev. E* **70**, 066111 (2004).

[92] G. Caldarelli, *Scale-Free Networks: complex webs in nature and technology*. Oxford University Press, New York (2007).

[93] M. Ostilli, and J. F. F. Mendes, Communication and correlation among communities, *Phys. Rev. E* **80**, 011142 (2009).

[94] S. Fortunato and C. Castellano, Community structure in graphs, in *Encyclopedia of Complexity and Systems Science*, edited by B. Meyers. Springer, Heildelberg, 2009.

[95] M. E. J. Newman and M. Girvan, *Phys. Rev. E* **69**, 026113 (2004).

[96] D. Liben-Nowell, J. Novak, R. Kumar, P. Raghavan, and A. Tomkins, Geograph routing in social networks. *Proc. Natl. Acad.* **102**, 11623 (2005).

[97] Y. Hu, Y. Wang, D. Li, S. Havlin, and Z. Di, Maximizing Entropy Yields Spatial Scaling in Social Networks, *arXiv:1002.1802* (2010).

[98] E. Agliari, R. Burioni, D. Cassi, and F. M. Neri, Efficiency of information spreading in a population of diffusing agents, *Phys. Rev. E* **73**, 046138 (2006).

[99] C. P. Herrero, Coordination sequences and information spreading in small-world networks, *Phys. Rev. E* **66**, 046126 (2002).

[100] J. Kleinberg and K. Ligett, Information-Sharing and Privacy in Social Networks, *arXiv:1003.0469* (2010).

[101] M. Kitsak, L. K. Gallos, S. Havlin, F. Liljeros, L. Muchnik, H. E. Stanley, and H. A. Makse, Identifying influential spreaders in complex networks, *Nature Physics* **6**, 888 (2010).

[102] C. Castellano, S. Fortunato, and V. Loreto, Statistical physics of social dynamics, *Rev. Mod. Phys.* **81**, 591 (2009).

[103] Y. Moreno, M. Nekovee, A. F. Pacheco, Dynamics of rumor spreading in complex networks, *Phys. Rev. E* **69**, 066130 (2004).

[104] D. H. Zanette, Critical behavior of propagation on small-world networks, *Phys. Rev. E* **64**, 050901(R) (2001).

[105] W. Weidlich, The statistical description of polarization phenomena in society, *Br. J. Math. Statist. Psychol.* **24**, 251 (1971).

[106] S. Galam, Y. Gefen, and Y. Shapir, A mean behavior model for the process of strike, *J. Math. Sociol.* **9**, 1 (1982).

[107] S. Galam and S. Moscovici, Towards a theory of collective phenomena: Consensus and attitude changes in groups, *Eur. J. Soc. Psychol.* **21** 49 (1991).

[108] S. Galam, Sociophysics: a review of Galam models, *Int. J. Mod. Phys. C* **19** 409 (2008).

[109] D. Stauffer, S. Moss de Oliveira, P. M. C. de Oliveira and J. S. Sá Martins, *Biology, Sociology, Geology by Computational Physicists* (Elsevier, Amsterdam, 2006).

[110] P. Clifford and A. Sudbury, A model for spatial conflict, *Biometrika* **60** 581 (1973).

[111] R. Holley and T. Liggett, Ergodic Theorems for Weakly Interacting Infinite Systems and the Voter Model, *Ann. Probab.* **3**, 643 (1975).

[112] T. Tomé and M. J. de Oliveira, *Dinâmica Estocástica e Irreversibilidade* (Edusp, São Paulo, 2001).

[113] S. Galam, Minority opinion spreading in random geometry, *Eur. Phys. J. B* **25**, 403 (2002).

[114] P. L. Krapivsky and S. Redner, Dynamics of Majority Rule in Two-State Interacting Spin Systems, *Phys. Rev. Lett.* **90**, 238701 (2003).

[115] Jae-Suk Yang, In-mook Kim, and W. Kwak, Existence of an upper critical dimension in the majority voter model, *Phys. Rev. E* **77**, 051122 (2008).

[116] K. Sznajd-Weron and J. Sznajd, Opinion evolution in closed community, *Int. J. Mod. Phys. C* **11**, 1157 (2000).

[117] D. Stauffer, A. O. Sousa, and S. Moss de Oliveira, Generalization to Square Lattice of Sznajd Sociophysics Model, *Int. J. Mod. Phys. C* **11**, 1239 (2000).

[118] I. Chang, Sznajd on triangular antiferromagnets, *J. Mod. Phys.* **12**, 1509 (2001).

[119] A. T. Bernardes, D. Stauffer, and J. Kertesz, Election results and the Sznajd model on Barabasi network, *Eur. Phys. J. B* **25**, 123 (2002).

[120] C. Schulze, Long-range interactions in Sznajd consensus model, *Physica A* **324**, 717 (2003).

[121] J. Bonnekoh, Monte Carlo Simulations of the Ising and the Sznajd model on growing Barabási-Albert Networks, *Int. J. Mod. Phys. C* **14**, 1231 (2003).

[122] K. Sznajd-Weron and J. Sznajd, Who is left, who is right?, *Physica A* **351**, 593 (2005).

[123] D. Stauffer, Better being third than second in a search for a majority opinion, *Adv. Comp. Sys.* **5**, 97 (2002).

[124] C. Schulze, Advertising in the Sznajd Marketing Model, *Int. J. Mod. Phys. C* **14**, 95 (2003).

[125] D. Stauffer, Monte Carlo simulations of Sznajd models, *J. Artif. Soc. Soc. Simul.* **5**, 1 (2001).

[126] K. Sznajd-Weron, Sznajd model and its applications, *Acta Phys. Pol. B* **36**, 2537 (2005).

[127] F. Slanina and H. Lavicka, Analytical results for the Sznajd model of opinion formation, *Eur. Phys. J. B* **35**, 279 (2003).

[128] K. Sznajd-Weron, Controlling simple dynamics by a disagreement function, *Phys. Rev. E* **66**, 046131 (2002).

[129] K. Sznajd-Weron, Dynamical model of Ising spins, *Phys. Rev. E* **70**, 037104 (2004).

[130] K. Sznajd-Weron, Mean-field results for the two-component model, *Phys. Rev. E* **71**, 046110 (2005).

[131] A. A. Moreira, J. S. Andrade Jr., and D. Stauffer, Sznajd social model on square lattice with correlated percolation, *Int. J. Mod. Phys. C* **12**, 39 (2001).

[132] E. Brigatti, Consequence of reputation in an open-ended naming game, *Phys. Rev. E* **78**, 046108 (2008).

[133] J.J. Schneider, The influence of contrarians and opportunists on the stability of a democracy in the Sznajd model, *Int. J. Mod. Phys. C* **15**, 659 (2004).

[134] A. O. Sousa, T. Yu-Song, and M. Ausloos, Effects of agents' mobility on opinion spreading in Sznajd model, *Eur. Phys. J. B* **66**, 115 (2008).

[135] N. Crokidakis and F. L. Forgerini, Consequence of reputation in the Sznajd consensus model, *Phys. Lett. A* **374**, 3380 (2010).

[136] N. Crokidakis and F. L. Forgerini, Competition Among Reputations in the 2D Sznajd Model: Spontaneous Emergence of Democratic States, *Braz. J. Phys.* **42**, 125 (2012).

[137] V. Sood, M. Mathieu, A. Shreim, P. Grassberger, and M. Paczuski, Interacting Branching Process as a Simple Model of Innovation, *Phys. Rev. Lett.* **105**, 178701 (2010).

[138] A. Fujikawa *et al.*, Cross-cultural patterns of marriage and inheritance: A phylogenetic approach, *Ethol. Sociobiol.* **17**, 87 (1996).

[139] V. Schwämmle and P. M. C. de Oliveira, A simple branching model that reproduces language family and language population distributions, *Physica A* **388**, 2874 (2009).

[140] S. N. Dorogovtsev and J. F. F. Mendes, Language as an evolving word web, *Proc. R. Soc. Lond. B* **268**, 2603 (2001).

[141] E. V. Koonin, The Biological Big Bang model for the major transitions in evolution, *Biology Direct.* vol. 2, **21** (2007).

[142] B. M. E. Moret, L. Nakhleh, T. Warnow, C. R. Linder, A. Tholse, A. Padolina, J. Sun, and R. Timme, Phylogenetic Networks: Modeling, Reconstructibility, and Accuracy, *IEEE ACM Trans. Comput. Biol. Bioinf.* **1**, 13 (2004).

[143] D. H. Huson and D. Bryant, Application of Phylogenetic Networks in Evolutionary Studies, *Mol. Biol. Evol.* **23(2)**, 254–267 (2006).

[144] M. J. Alava and K. B. Lauritsen, Branching process, in *Encyclopedia of Complexity and Systems Science*, edited by B. Meyers. Springer, Heildelberg, 2009.

[145] G. Cowlishaw and R. Mace, Cross-cultural patterns of marriage and inheritance: a phylogenetic approach, *Ethol. Sociobiol.* **17**, 87 (1996).

[146] R. D. Gray and Q. D. Atkinson, Language-tree divergence times support the Anatolian theory of Indo-European origin, *Nature* **426**, 435 (2003).

[147] D. G. Kendall, Branching processes since 1873, *J. London Math. Soc.* **s1-41**, 385-406 (1966).

[148] J. Dall and M. Christensen, Random geometric graphs, *Phys. Rev. E* **66**, 016121 (2002).

[149] J. Kleinberg, Navigation in a Small World, *Nature* **406**, 845 (2000).

[150] S. Carmi, S. Carter, J. Sun, and D. ben-Avraham, Asymptotic behavior of the Kleinberg model, *Phys. Rev. Lett.* **102**, 238702 (2009).

[151] C. C. Cartozo and P. De Los Rios, Extended navigability of small world networks: exact results and new insights, *Phys. Rev. Lett.* **102**, 238703 (2009).

[152] M. Boguñá and D. Krioukov, Navigating ultrasmall worlds in ultrashort time, *Phys. Rev. Lett.* **102**, 058701 (2009).

[153] D. Krioukov, F. Papadopoulos, M. Kitsak, A. Vahdat, and M. Boguñá, Hyperbolic Geometry of Complex Networks, *Phys. Rev. E* **82**, 036106 (2010).

[154] S. N. Dorogovtsev, P. L. Krapivsky, and J. F. F. Mendes, Transition from small to large world in growing networks, *EPL* **81**, 30004 (2008).

[155] J. L. Cardy and P. Grassberger, Epidemic models and percolation, *J. Phys. A: Math. Gen.* **18**, 267 (1985).

[156] K. Sznajd-Weron and R. Weron, A new model of mass extinctions, *Physica A* **293**, 559 (2001).

[157] M. D. Raup, Biological extinction in earth history, *Science* **231**, 4745 (1986).

[158] H. Takayasu and A. Y. Tretyakov, Extinction, survival, and dynamical phase transition of branching annihilating random walk, *Phys. Rev. Lett.* **68**, 3060 (1992).

[159] I. Jensen, Critical exponents for branching annihilating random walks with an even number of offspring, *Phys. Rev. E* **50** 3623 (1994).

[160] B. W. Roberts and M. E. J. Newman, A model for evolution and extinction, *J. Theor. Biol.* **180**, 39 (1996).

[161] P. Sibani, M. R. Schmidt, and P. Alstrøm, Fitness Optimization and Decay of Extinction Rate Through Biological Evolution, *Phys. Rev. Lett.* **75**, 2055 (1995).

[162] D. Helbing, Traffic and related self-driven many-particle systems, *Rev. Mod. Phys.* **73**, 1067 (2001).

[163] S. Valverde and R. V. Solé, Self-organized critical traffic in parallel computer networks, *Physica A* **289**, 595 (2001).

[164] M. Takayasu, H. Takayasu, and T. Sato, Critical behaviors and $1/f$ noise in information traffic, *Physica A* **233**, 824 (1996).

[165] M. Takayasu, H. Takayasu, and K. Fukuda, Dynamic phase transition observed in the Internet traffic flow, *Physica A* **277**, 248 (2000)

[166] D. De Martino, L. Dall'Astra, G. Bianconi, and M. Marsili, Congestion phenomena on complex networks, *Phys. Rev. E* **79**, 015101(R) (2009).

[167] D. De Martino, L. Dall'Astra, G. Bianconi, and M. Marsili, A minimal model for congestion phenomena on complex networks, *J. Stat. Mech* **P08023** (2009).

[168] Yu-hua Xue, J. Wang, L. Li, D. He, and B. Hu, Optimizing transport efficiency on scale-free networks through assortative or dissortative topology, *Phys. Rev. E* **81**, 037101 (2010).

[169] A. L. Pastore y Piontti, L. A. Braunstein, and P. A. Macri, Jamming in complex networks with degree correlation, *Phys. Lett. A* **374**, 4658 (2010).

[170] Han-Xin Yang, Wen-Xu Wang, Yan-Bo Xie, Ying-Cheng Lai, and B. Wang, Transportation dynamics on networks of mobile agents, *Phys. Rev. E* **83**, 016102 (2011).

[171] R. A. da Costa, *Study of Complex Networks: Application to Social and Communications Networks*, PhD Thesis under submission, University of Aveiro.

[172] P. L. Krapivsky, S. Redner, and F. Leyvraz, Connectivity of Growing Random Networks, *Phys. Rev. Lett.* **85**, 4629 (2000).

[173] A. Fabrikant, E. Koutsoupias, and C. H. Papadimitriou, Heuristically Optimized Trade-offs: A New Paradigm for Power Laws in the Internet, *Lect. Notes Comp. Sci.* **5632**, 110 (2002).

[174] R. M. D'Souza, C. Borgs, J. T. Chayes, N. Berger, and R. D. Kleinberg, Emergence of tempered preferential attachment from optimization, *Proc. Natl. Acad. Sci. USA* **104**, 6112 (2007).

[175] S. N. Dorogovtsev, J. F. F. Mendes, and A. Samukhin, Size-dependent degree distribution of a scale-free growing network, *Phys. Rev.* E **63** 062101 (2001).

[176] R. Ferrer i Cancho and R. V. Solé *Optimization in complex networks* in Statistical Mechanics of Complex Networks, R. Pastor-Satorras, M. Rubi, and A. Diaz-Guilera eds., Springer, Berlin, 2003, pp. 114-125.

[177] F. Papadopoulos, M. Kitsak, M. A. Serrano, M. Bogũńa, and D. Krioukov, Popularity versus Similarity in Growing Networks, arXiv:1106.0286.

[178] R. M. D'Souza, P. L. Krapivsky, and C. Moore, The power of choice in network growth, *Eur. Phys. J.* B **59**, 535 (2007).